National Library of Canada
Acquisitions and Bibliographic Services Branch
395 Wellington Street
Ottawa, Ontario
K1A 0N4

Bibliotnèque nationale du Canada
Direction des acquisitions et des services bibliographiques
395, rue Wellington
Ottawa (Ontario)
K1A 0N4

Your file Votre référence

Our file Notre référence

NOTICE

The quality of this microform is heavily dependent upon the quality of the original thesis submitted for microfilming. Every effort has been made to ensure the highest quality of reproduction possible.

If pages are missing, contact the university which granted the degree.

Some pages may have indistinct print especially if the original pages were typed with a poor typewriter ribbon or if the university sent us an inferior photocopy.

AVIS

La qualité de cette microforme dépend grandement de la qualité de la thèse soumise au microfilmage. Nous avons tout fait pour assurer une qualité supérieure de reproduction.

S'il manque des pages, veuillez communiquer avec l'université qui a conféré le grade.

La qualité d'impression de certaines pages peut laisser à désirer, surtout si les pages originales ont été dactylographiées à l'aide d'un ruban usé ou si l'université nous a fait parvenir une photocopie de qualité inférieure.

Canada

Numerical Modeling of Passive Earth Pressure for Normally and Over Consolidated Sands

Riad Diab

A Thesis In
The Department of Civil Engineering

Presented in Partial Fulfillment of the Requirements
for the Degree of Master of Applied Science at
Concordia University
Montreal, Quebec, Canada

July 1994

ISBN 0-315-97669-1

ABSTRACT

Numerical Modeling of Passive Earth Pressure for Normally and Over Consolidated Sands

Riad Diab
Concordia University, 1994

Previous experimental and analytical investigations on passive earth pressure showed that the current available theories did not take into consideration the effect of the critical state soil mechanics parameters. They also ignored the effect of the stress history of the soil represented by the Over Consolidation Ratio (OCR) on the passive earth pressure coefficient (Kp). This may lead to an overestimation or underestimation of the evaluation of Kp and accordingly to an uneconomical or unsafe design respectively.

The present thesis is oriented to study the effect of the above mentioned parameters on the value of passive earth pressure developed behind a vertical rigid wall translating horizontally into a Normally or Over Consolidated horizontal cohesionless backfill.

A numerical model of a translating wall was developed using the finite element technique and the program CRISP which was developed at Cambridge University. The deduced stress distribution and failure mechanism in the soil mass were examined against the available theories and good agreement was achieved.

The results, for Normally Consolidated soil, were presented in form of parametric study to determine the effect of each of the critical state parameters on the value of Kp. These results were compared with the existing theories on passive earth pressure and it was found that the theoretical value of Kp obtained by Coulomb and by Shields produced intermediate values inside the range of Kp obtained by the critical state theory.

For Over Consolidated soil, the results showed that the soil stress history had a very significant effect on the passive earth pressure, as the value of Kp increases considerably due to an increase of OCR. Based on this fact an empirical relationship was proposed to relate Kp to the OCR.

ACKNOWLEDGEMENTS

I would like to express my sincerest gratitude to professor, Dr. A. M. Hanna, for his guidance, encouragement and support that he provided me. I am honored to carry out the present investigation study under his direct supervision.

I wish to thank Dr. H. Keira for the valuable discussion during the preparation of this thesis.

TABLE OF CONTENTS

LIST OF SYMBOLS

SYMBOL	REPRESENTS
CSL	Critical State Line.
ESP	Effective Stress Path.
E_c	Young's modulus of concrete.
E_s	Young's modulus of slip element.
E	Young's modulus of soil.
e	Void ratio of soil.
ecs	Critical state void ratio.
H	Height of the wall.
H_r	Soil height located at some horizontal distance from the wall at which no vertical shear exists.
k	Slope of the swelling line.
K_o	Coefficient of earth pressure at-rest.
Knc	Coefficient of earth pressure at-rest under normally consolidated state.
Kp	Coefficient of passive earth pressure.
Kpnc	Coefficient of passive earth pressure for normally consolidated soil.
M	Frictional constant of soil.
N	Value of v when P' = 1 on the NCL.
NCL	Normal Consolidation Line.
OCR	Over Consolidation Ratio.
Pp	Total passive earth pressure.
Pr	Passive Rankine force.
P'	Mean normal effective stress.

P'_c	Size of current yield locus.
q	Deviator stress.
SSBS	Stable State Boundary Surface.
v	Specific volume of the soil.
v_k	Value of v when P' = 1 on the swelling line.
v_λ	Specific volume at reference section.
W	Weight of a slice of the soil mass.
γ	Unit weight of soil.
γ_c	Unit weight of concrete.
ϕ	Angle of shearing resistance.
τ	Shear stress.
δ	Angle of wall-soil friction.
α	Angle between the horizontal and the failure surface for each slice of the soil mass.
α_w	Angle between the horizontal and the failure surface at the wall.
μ	Poisson ratio of soil.
μ_c	Poisson ratio of concrete.
μ_s	Poisson ratio of slip element.
λ	Slope of the critical state line in P':v space.
σ_1	Major principal effective stress.
σ_3	Minor principal effective stress.
σ_f	Effective stress at failure.
σ_y	Effective vertical stress.
σ_x	Effective horizontal stress.
Γ	Value of v when P' = 1 on the CSL.
η	Stress ratio.

LIST OF TABLES

LIST OF FIGURES

CHAPTER 1
INTRODUCTION

1.1 Preface

In the construction and design of many structures, the determination of earth pressure, to which these structures are subjected, is required. Among these structures are retaining walls, sheet piles, temporary sheathings for supporting vertical cuts in soils and earth anchors. The prediction of lateral earth pressure to which the above types of structures are subjected has been among the most important problems in geotechnical engineering. The development of active lateral earth pressure in particular has received a considerable amount of attention. This is due to the fact that the majority of these retaining structures are made to support active earth pressure. However, design of many geotechnical structures requires the evaluation of passive lateral earth pressures. In the literature, several theoretical and experimental studies are reported to investigate the magnitude and distribution of passive earth pressure behind a retaining wall. Most of these studies considered the shear strength of the soil (the cohesion c and the angle of shearing resistance ϕ) as the only parameters affecting the values of earth pressure and further, none of them took into consideration effect of the stress history of the soil represented by the Over Consolidation Ratio (OCR). Furthermore, no attempts were made to analyze the problem and to estimate the value of passive earth pressure using the parameters of the theories of critical state soil mechanics which reflect realistically and with a great degree of precision the behavior of soils.

1.2 Research objectives

The objectives of this research program are:

a. To conduct and report a literature review on passive earth pressure and over consolidation ratio for sand.

b. To develop a numerical model, using finite element technique, of a vertical rigid wall translating horizontally into a mass of homogeneous dry sand of horizontal surface.

c. To compare the theoretical values produced by the numerical model with those obtained from the available theories.

d. To conduct a parametric study on passive earth pressure developed behind the above described wall, where the soil is represented by the critical state soil mechanics parameters.

e. To study the effect of degree of over consolidation on the coefficient of passive earth pressure K_p.

f. To develop some design charts to be used by practicing engineers for estimating the value of K_p in case of homogeneous normally consolidated sand.

1.3 Scope of the thesis

A review of the classical theories for passive earth pressure for homogenous normally consolidated soil is given in chapter 2. Chapter 3 describes the formulation of the finite element model proposed for the problem and a brief review on the critical state theory. The results and the analysis are discussed in chapter 4. Finally, the conclusion and the recommendations are presented in chapter 5.

CHAPTER 2
LITERATURE REVIEW

2.1 General

Earth pressure problems have intrigued and challenged engineers for a very long time and they still occupy a place of high importance in the field of soil mechanics.

Over three hundred years ago, failure of retaining wall was not perceived as a geotechnical problem, but mostly due to the structure. these walls were therefore reinforced many times more than needed, resulting in uneconomical structures such as walls 10 feet to 20 feet wide.

Later on, with the development of the instrumentation in geotechnical engineering and powerful computers, researchers started to examine the problem from the theoretical and experimental point of view, data was gathered and exchanged, and experience began to play a role in solving the problem.

2.2 Historical development

The first recorded results of experimental work on lateral earth pressure were those of the French researcher Belidore in 1729, who concluded that the surface of rupture behind a retaining wall was on a slope of 1:1 . That was later modified by Mayniel, in 1808, to a slope of 2:4.

In 1758, Gauthey succeeded in measuring the earth pressures at five different depths showing that the pressure was increasing with depth.

In 1776, Coulomb was the first to suggest a mathematical solution for the calculation of earth pressure, taking into consideration the wall-soil friction angle, he assumed that the failure surface was plane and that the friction forces were distributed uniformly along this rupture surface. He gave his equation of total passive earth pressure, which is being used so far, as follows:

$$P_p = \frac{1}{2}\gamma H^2 K_p \qquad (2\text{-}1)$$

where $$K_p = \frac{1}{\cos\delta}\left\{\frac{1}{\left(\frac{1}{\cos\phi}\right) - \sqrt{\tan^2\phi + \tan\phi\,\tan\delta}}\right\}^2 \qquad (2\text{-}2)$$

and P_p is the total passive earth pressure

γ is the unit weight of the soil

H is the height of the wall

K_p is the coefficient of passive earth pressure

δ is the angle of wall-soil friction

ϕ is the angle of shearing resistance

In 1857, Rankine found a mathematical solution using an entirely different approach from that of coulomb. He assumed that the whole earth mass is in a state of plastic equilibrium and he showed that the two systems of straight parallel lines, intersecting at angles of $90^o \pm \phi$ formed the rupture lines. He used the condition of failure defined by Mohr-Coulomb criterion of the soil to give his famous equation for smooth retaining wall ($\delta = 0$) as follows:

$$K_p = \tan^2(45^o + \frac{\phi}{2}) \qquad (2\text{-}3)$$

In 1906, in Germany, Muller-Breslau, found that the point of application of the resultant of active and passive earth pressure was somewhere between 0.33 and 0.36 of the height of the wall, for the case of no surcharge existing above the ground surface.

In 1920, Terzaghi adopted a method for predicting the passive earth pressure assuming that the failure surface consists of two parts: logarithmic spiral and straight line. He recorded some measurements of horizontal and vertical force components of passive earth pressure and reported that passive pressure coefficients K_p were obtained to be

greater than 10 for dense sand after a small wall displacement and about 2 for loose sand at a wall displacement equal to 15% of the wall height.

In 1924, Franzius determined experimentally the effects of wall friction on passive resistance and concluded that the observed values of passive earth pressure of rough walls were at least twice the values for smooth walls.

Caquot and Kerisel, in 1948, derived solutions for passive pressure acting on the face of a wall showing that the magnitude of the wall friction angle δ depends on the type of wall movement.

An extensive study of rupture surfaces under different types of wall movements was made by Hansen in 1953. His findings indicated differences in the shape and size of the rupture wedges under different wall movements and with different wall friction.

Rowe and Peaker (1965) have used elaborated equipment which allowed the control of the wall direction to measure passive earth pressure in the laboratory . They directed their research to study the relationship between the average mobilized angle of shearing resistance ϕ_m along the failure plane and the deduced average coefficient of earth pressure K_{pm}. They concluded that the slip line emerged at the sand surface at a stage which did not necessarily coincide with the achievement of K_{pmax} but at a stage which generally lay in the vicinity of the peak value of ϕ_{max}. They also found that the distribution of pressure on a horizontally translating wall was essentially linear at each stage of deformation up to failure.

Brooker and Ireland, in 1965, were the first to conduct an extensive study on the effect of soil stress history on earth pressure. Their experimental results indicated that the stress history governs the value of the coefficient of lateral earth pressure in at-rest state (Ko), and they concluded that an increase in the OCR leads to an increase in (Ko).

Later in 1966, Schmidt plotted Ko against over consolidation ratio OCR using logarithmic axes for both. He found a linear relationship and he gave a simple expression relating Ko to OCR as follows:

$$K_0 = K_{nc}.OCR^b \qquad (2\text{-}4)$$

where Knc is the coefficient of lateral earth pressure at rest under normally consolidation state. The value of the parameter b was found to be between 0.3 and 0.55 depending on the plasticity index of the soil (PI).

In 1969 , Narain , Saran and Nandakumaran investigated experimentally the determination of the rupture surface and the pressures behind a wall subjected to: translation or rotation about the bottom or the top in case of loose and dense sand. They concluded that the magnitude of passive pressure and the displacement required to cause its maximum are the highest when the wall is rotated about its bottom and the lowest when the wall is rotated about its top. They also reported that in case of translation Kpmax occurs when the displacement is about 8.5% of the height of the wall in case of loose sand and about 6.5% in case of dense sand. The distribution of passive pressure along the height of the wall is a triangular one only in the case of horizontal translation of the wall while it is a parabolic one in the case of wall rotation. The rupture surface for all types of wall movements were curved .

James and Bransby (1970) studied the distribution of normal and shear stresses on wall rotating about its toe into mass of dry sand, they showed that the earth pressure reaches first its peak value near the top of the wall where the rupture surfaces were first observed and no rupture surface below the mid height of the wall was observed. When a wall is rotated about its top there is a single rupture surfaces extended from the toe of the wall up to the sand surface. They also confirmed the observation made by Narain et al concerning the non linear distribution of the normal stress on the rotating wall at any stage of the test. Finally they showed that the locally mobilized angle of sand-wall friction δ varies from a value close to the angle of shearing resistance ϕ of the soil at the top of the wall to almost zero at the bottom of the wall.

In 1971, Clough and Duncan were the first to develop procedure for representing the interface between a structure and the adjacent soil in a finite element analysis of soil

structure interaction. However, the study was directed to investigate the active earth pressure of the sand behind a rigid wall. Two dimensional linear strain quadrilateral elements were employed to represent the backfill. The sand behavior was described in terms of bulk elastic modulus(K) and elastic shear modulus (G)

In 1972 and later in 1973 Shields and Tolunay followed Terzaghi's suggestion of failure surface composed of a logarithmic spiral and a straight line. They computed values of passive earth pressure coefficient Kp using a simplified method of slices similar to that of Bishop for slope stability analysis and they proposed the following equation :

$$K_p = \frac{P_r + \Sigma[W \tan(\alpha + \phi)]}{1 - \tan\delta \tan(\alpha_w + \phi)} \frac{2}{\gamma H^2} \qquad (2\text{-}5)$$

where

$$P_r = \frac{1}{2}\gamma H_r^2 \tan^2(45^\circ + \frac{\phi}{2})$$

where Pr is passive Rankine force acting on soil height H_r located at some horizontal distance from the wall, beyond which no vertical shear, caused by the wall roughness, exists.

δ is the wall friction angle

α_w is the angle between the horizontal and the failure surface at the wall.

α is the angle between the horizontal and the failure surface for each slice.

W is the weight of the slice .

H is the height of the wall.

Ghahramani and Sabzevari (1974) presented an analytical formulation for estimating the passive earth pressure of a retaining wall rotated about its toe into a dry loose and dense sands. They concluded that the distribution of the normal as well as the shear stresses acting on the wall are not linear. Furthermore the stresses decrease towards the toe but the decrease is not as much as the experimental results obtained by James and Bransby (1970) indicate. Their theory predicted also a peak value for the normal force as

the wall progressively rotates into dense and medium sand and the peak occurred at about 4 degrees wall rotation.

In 1976, Bellotti, Formigoni and Jamiolkowski conducted an experimental investigation to study the effect of OCR on (Ko). Their results were in good agreement with the relationship proposed by Schmidt. Also they proposed a value of 0.42 to the non dimensional exponent b.

Wroth (1975) proposed an alternative relationship between Ko, Knc and OCR to that of Schmidt. This relationship was as follow:

$$K_0 = OCR.K_{nc} - \frac{\mu}{1-\mu}(OCR-1) \qquad (2\text{-}6)$$

where μ is the Poisson ratio of the soil.

Wroth stated that this relation is only valid for lightly over consolidated soil (OCR up to 5) and a range of μ between 0.254 and 0.37i.

Meyerhof, in 1976, modified the experimental relationship found by Schmidt to the following form:

$$K_0 = K_{nc}.OCR^{0.5} \qquad (2\text{-}7)$$

In 1987, Bang and Kim described an analytical solution to predict the transition of the passive earth pressure from the at-rest state to an initial-passive to the full passive state of a vertical rigid retaining wall rotating about its toe or top into a dry sand. They used the condition of failure defined by Mohr-Coulomb criterion and equilibrium condition to obtain the necessary equations for solution. The results from the proposed method of analysis were compared with the experimental results reported by Narain et al. and the comparison showed to be generally in good agreement.

2.3 Discussion

All the previous analytical and experimental studies related to the calculation of passive earth pressure are based on the assumption that the shear strength parameter of

the soil (ϕ) and the wall friction angle (δ) are the only variables affecting K_p . These studies have been helpful for understanding the mechanism of failure of the soil mass behind the wall for all kinds of wall movements. However none of them analyzed the problem using the theories of the critical state soil mechanics. It is believed that some discrepancy between existing theories will vanish, to a great extent, when the critical state soil mechanics parameters are taken into consideration for predicting the value of passive earth pressure coefficient (Kp). Also no attempts were made to study the effect of the in-situ stress condition or the degree of over consolidation on Kp.

The purpose of the present thesis is to present a parametric study, based on finite element analysis, of passive earth pressure behind a vertical rigid wall translating horizontally into a mass of homogeneous normally consolidated or over consolidated soil. The soil is represented by the critical state soil mechanics parameters.

CHAPTER 3
NUMERICAL MODELING

3.1 General

The finite element method is a powerful technique to solve varieties of science and engineering problems. It has become very popular in recent years in the field of geotechnical engineering to provide solution to problems including foundations, dams and earth retaining structures.

The following steps are usually taken in developing solutions by means of the finite element technique:

a. Establish the governing equation and boundary conditions for the given problem, then the appropriate finite element solution algorithm can be obtained.

b. Divide region under investigation into a number of elements.

c. Select interpolation function based on the number of points within the elements, to define the displacement field.

d. Determine element properties: Each element makes a contribution to the overall region which is a function of element geometry, material properties, number of nodal points, and other variables.

e. Element properties should be assembled to form a set of algebraic equations for the nodal values of the physical variables.

f. Many standard techniques are available to give a solution of global equations whether the global equations are linear or non-linear.

g. Verification of solution: two conditions must be satisfied in the theory of finite element analysis, these are:

1) The forces acting on the elements must be in equilibrium

2) The displacements of each element as a result of the applied forces must be consistent with the physical properties of the material as well as the specified boundary conditions.

3.2 Mesh Geometry and Element type

The choice of element and mesh design has to reflect a compromise between an acceptable degree of accuracy and computing costs. The finite element mesh that was used in the analysis, immediately after excavation of the soil in front of the wall as explained in section 3-9, is shown in figure 3-1. This mesh has smaller elements in the regions near the wall where rapidly varying stress/strain are expected.

Figures 3-2 and 3-3 represent the finite element mesh at the in-situ stage (before any loading). These figures show that the soil and the wall were modeled by 272 eight nod[illegible]d Linear Strain Quadrilateral (LSQ) element, this type of element is recommended by Britto and Gun (1981) to be used for plane strain and drained analysis. The total number of corner nodes was 306.

3.3 Boundary Conditions

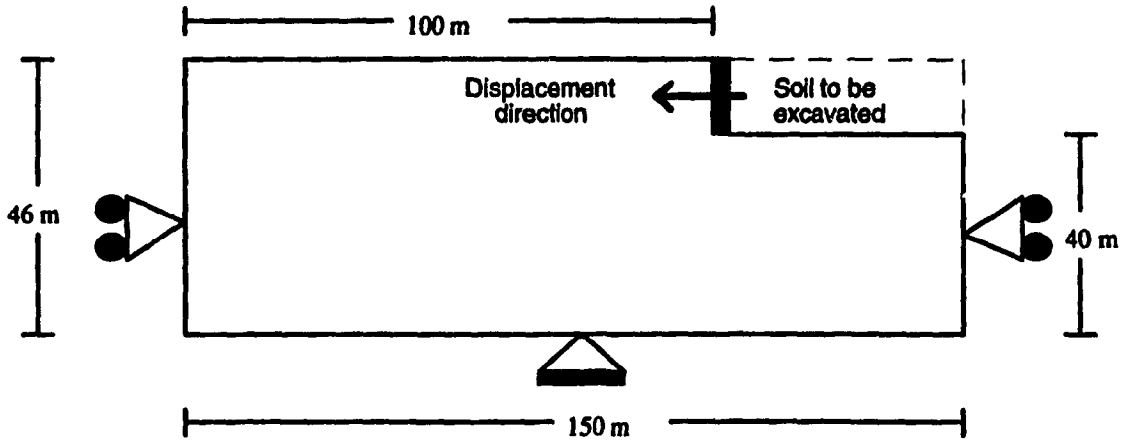

The outer boundary should be placed as far away as possible from the region

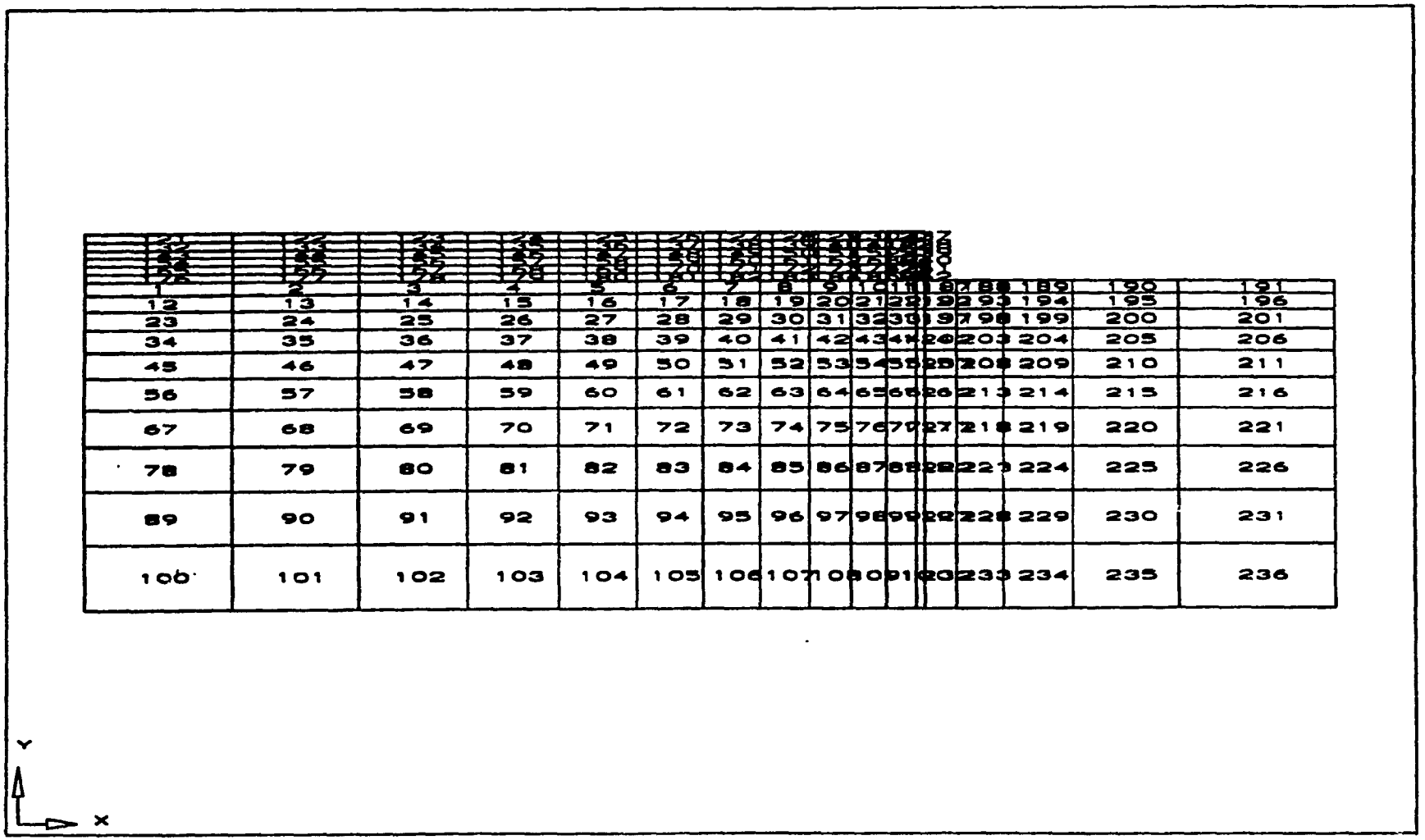

Figure (3-1): Finite element mesh immediately after excavation of the soil in front of the wall

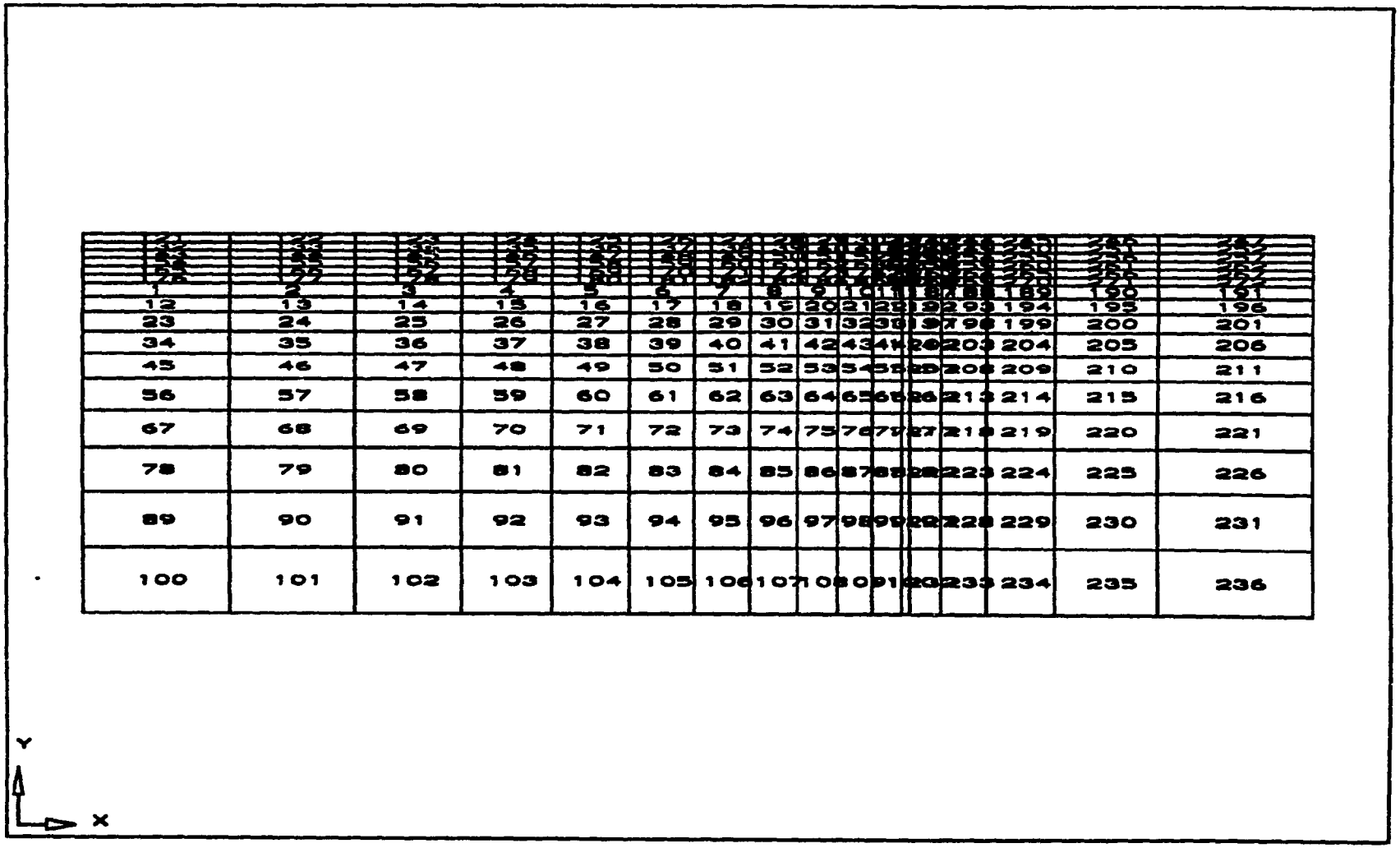

Figure (3-2): Finite element mesh before loading showing the number of elements

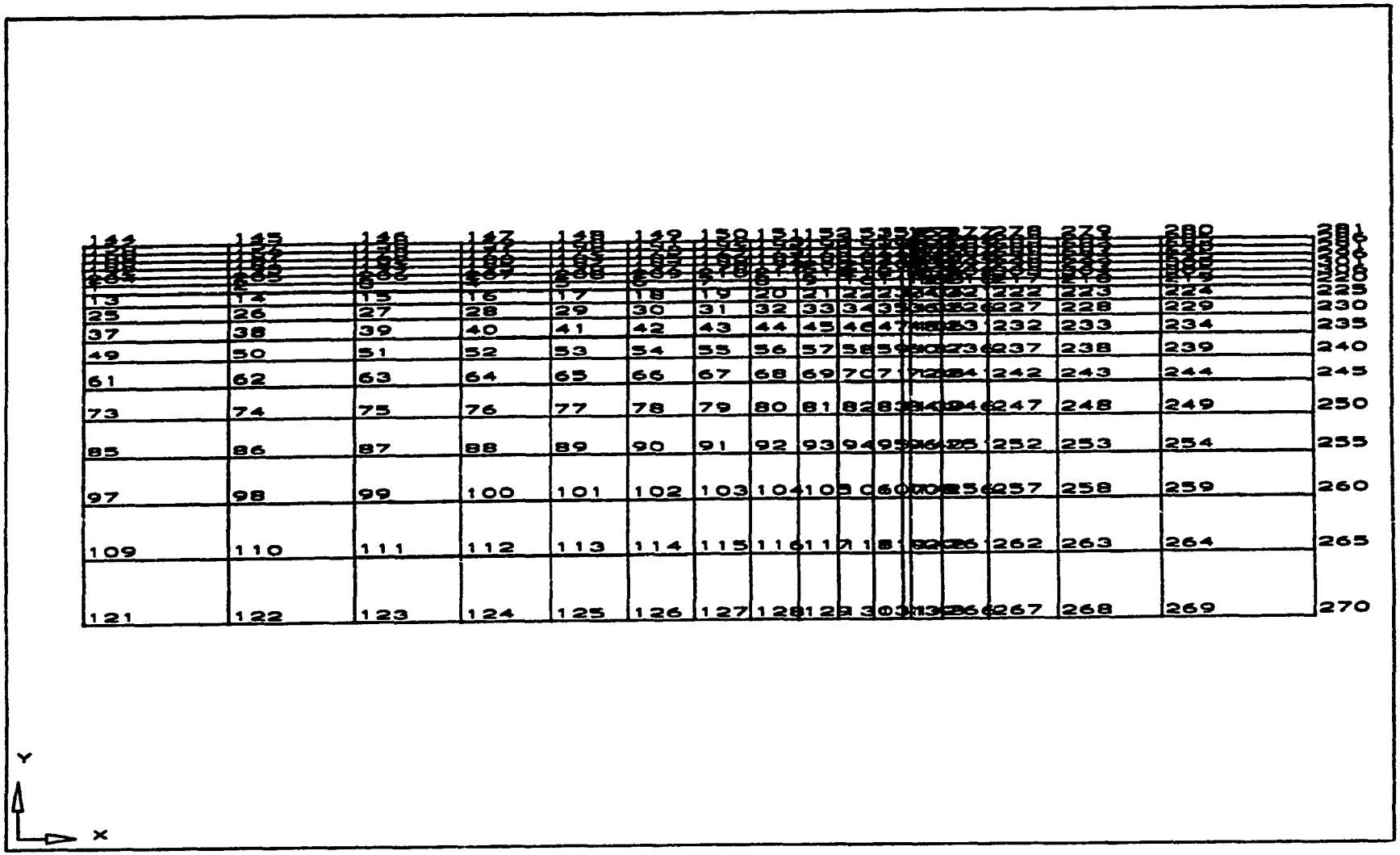

Figure (3-3): Finite element mesh before loading showing the number of nodes

subjected to the largest change in the loading in order that no influence to the results will be reported.

The height of the wall, as shown in the above figure, was chosen to be 6 m. The locations of the outer boundaries were determined as follows: 100 m away from the wall, in the direction of loading, and 50 m in the opposite direction, the total height of the studied mesh was 46 m. These dimensions were sufficient to eliminate any effect of boundary.

The Boundary conditions of the mesh were specified as follows: the outer vertical boundaries (left and right sides) are restrained in the (x) direction. This means that these boundaries are only free to move in the vertical (y) direction, the base of the mesh is assumed to be rough and hence is restrained in both (x) and (y) directions which simulate the field condition.

3.4 Wall and slip element model

Three material zones were assigned to the mesh representing: the wall, the soil and the slip element. Each zone associates all the elements in it with a particular set of material properties. The concrete wall was considered to be a linear elastic model having the following characteristics :

E_c (Young's modulus) $= 11{,}000{,}000\ KN/m^2$

μ_c (Poison ratio) $= 0.11$

γ_c (unit weight) $= 23\ KN/m^3$

The width of the wall was 0.5 m.

A slip (or interface) element was used in the analysis in order to simulate the interface between the soil and the wall.

The following properties were assigned to this element:

δ (the angle of wall-soil friction) $= 2\phi / 3$

μ_s (Poison's ratio) $= \mu$ of soil

E_S (Young's modulus)	= 65,000 KN/m^2	for	$\phi = 45^o$
	= 50,000 KN/m^2	for	$\phi = 40^o$
	= 35,000 KN/m^2	for	$\phi = 35^o$
	= 20,000 KN/m^2	for	$\phi = 30^o$
t (the thickness of the slip element)	= 10 cm		

3.5 Soil model

The soil was represented by the critical state soil mechanics parameters, it was considered as a Modified Cam Clay model.

The Modified Cam Clay parameters are: the slope of the Critical State Line (CSL) λ, the slope of the swelling line k, the critical state void ratio ecs and Poisson's ratio μ. A brief review of the theory of critical state and a definition of the above mentioned parameters will be presented in the next section

3.5.1 Theoretical background on critical state soil mechanics

The theory of soil behavior known as critical state soil mechanics were developed from the application of the theory of plasticity to soil mechanics.

Three parameters, P' (the mean normal effective pressure), q (the deviator stress) and v (the specific volume) describe the state of a sample of soil during a triaxial test. The parameters are defined as :

$$P' = \frac{\sigma_1 + 2\sigma_3}{3} \qquad (3\text{-}1)$$

$$q = \sigma_1 - \sigma_3 \qquad (3\text{-}2)$$

$$v = 1 + e \qquad (3\text{-}3)$$

where σ_1 : the major principal effective stress

σ_3 : the minor principal effective stress

e : the void ratio of the soil

The instantaneous state of a soil sample during a triaxial test can be represented by a point in a three dimensional space with axes P', v and q and the line connecting these points is called Effective Stress Path (ESP). From the theory of plasticity, it is concluded that the ESP for a soil reaches a yield surface and moves on this surface until it reaches a final destination at which failure occur, this final destination is called the critical state.

Figure 3-4 shows the ESP for family of drained test in q-P' and v-P' space during a standard triaxial test.

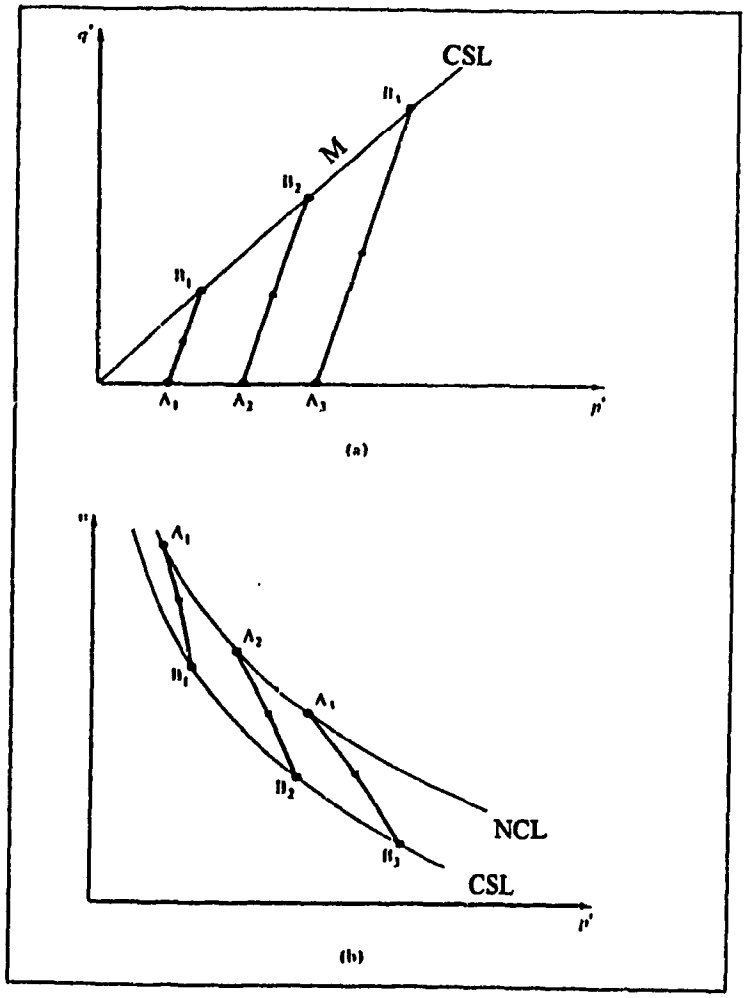

Figure (3-4): Effective Stress Path for a family of drained test in q-P' and v-P' spaces.

All samples fail at values of q,P' and v which define a straight line in q-P' space through the origin and a curved line in v-P' space . This single and unique line of failure

points of both spaces is defined as the critical state line. Its crucial property is that failure occurs once the stress states of the samples reach the line, irrespective of the stress path followed by the samples on their way to the critical state line.

3.5.1.1 Critical state line equations

In a standard drained triaxial test, the sample is subjected to:

i) isotropic compression pressure: during this part of the test the sample follows a stress paths in (P',v) plots, which is called the Normal Consolidation Line (NCL), as shown in figure 3-5a. Its state may be moved to the left of the (NCL) by unloading along a swelling line, but it is not possible to move the state of the soil to the right of the NCL. In critical state theory the virgin compression, swelling and recompression lines are assumed to be straight line in (ln(P'), v) plots with slope $-\lambda$ and -k respectively as shown in figure 3-5b .

The equation of the isotropic virgin compression line is:

$$v = N - \lambda \ln P' \qquad (3\text{-}4)$$

where N is a constant for a particular soil. It is the value of v when $\ln P' = 0$ or $P' = 1 kN/m^2$

The equation of the swelling or recompression line is

$$v = v_k - k \ln P' \qquad (3\text{-}5)$$

The value of v_k depends upon which k line the soil is on, but it stays constant while the soil is moving up or down the same line.

ii) Increase of the axial stress: during this part, the ESP approaches the Critical State Line (CSL) (figure 3-4) at which failure occurs. As for NCL, the CSL, in (ln(P',v) plot, is assumed to be a straight line lying on the right of the NCL and parallel to it. The CSL has the 2 following equations corresponding to its location in P'-q space and P'-v space respectively:

$$q = MP' \qquad (3\text{-}6)$$

$$v = \Gamma - \lambda \ln P' \qquad (3\text{-}7)$$

where M is the slope of CSL in q-P' space.

Γ is the value of v corresponding to $P' = 1 kN/m^2$ on the CSL.

Thus Γ locates the CSL in v-lnP' plane in the same way that N locates the Normal Compression Line. Equations (3-6) and (3-7) together define the position of the CSL in q-P'-v space. M and Γ, like N, λ and k are regarded as soil constants.

Figure 3-6 shows the critical state line in a three dimensional q-P'-v space, the normal isotropic compression line is shown in the q=0 plane.

3.5.1.2 Elastic and plastic deformation of soil

The distinction between elastic and plastic deformation is best illustrated by the behavior during isotropic compression. If the soil is unloaded from B (figure 3-5b) it moves along the swelling line BV_{k1}, if it is reloaded from V_{k1}, the soil retraces path V_{k1} to B, after which additional compression occur as the sample moves down the normal consolidation line to C. Similarly, if the sample is unloaded from C, it moves back along the swelling or k line to V_{k2}. The strain is elastic along any swelling or k lines such as $V_{k1}B$ and $V_{k2}C$, and is plastic along the Normal Consolidation Line.

3.5.1.3 Yield surface

When a triaxial test is conducted on a sample of soil, the stress state of the sample can follow undetermined number of stress paths depending on two factors: The type of test (drained or undrained) and the variation of the principal major and minor stresses. Each stress path consists of 2 parts: elastic one, when the behaviour of the soil is elastic and plastic one, when the soil is yielding. These 2 parts are separated by a point called the yield point.

The yield curve is defined as the link of yield points, in P'-q plot, for all possible stress paths for samples having the same initial stress state.

Figure 3-7 shows the stress path for lightly Over Consolidated sample in both P'-q and P'-v spaces. During the initial part of the test, before the ESP intersects the current yield locus at B, the soil behavior is elastic. After point B the soil is yielding and each stress state on BF is associated with a new (enlarged) yield locus. Finally the soil fails when the ESP intersects the CSL at point F.

Figure 3-8 shows different yield curves, each one is associated with a particular initial stress state, a set of all yield curves, in P'-q-v space, forms a yield surface.

Clearly this surface is considered as a Stable State Boundary Surface (SSBS) with the Critical State Line lying on it, when the stress state of the sample is inside this surface, its behavior is elastic, when the stress path moves on the surface, its behavior is plastic and the stress state cannot lie outside the surface.

3.5.1.4 Cam clay model

Cam Clay is the name given to an elasto-plastic model of soil behavior. Thus Cam Clay is not a real soil. However, the Cam Clay equations developed at Cambridge University can describe many real soils if appropriate material parameters are chosen.

This theory was developed for Normally Consolidated and lightly Over Consolidated soil.

The Cam Clay State Boundary Surface equation as developed by research team at Cambridge University is as follows:

$$q = \frac{MP'}{\lambda - k}(\Gamma + \lambda - k - v - \lambda \ln P') \qquad (3\text{-}8)$$

Figure 3-9 shows this equation in P'-q-v space

The state boundary surface intersects the v-P' plane along the normal consolidation line where q=o and v=N-λlnP' (NCL). Hence, from equation (3-8):

$$N = \Gamma + \lambda - k \qquad (3\text{-}9)$$

Equation (3-8) can also be written as :

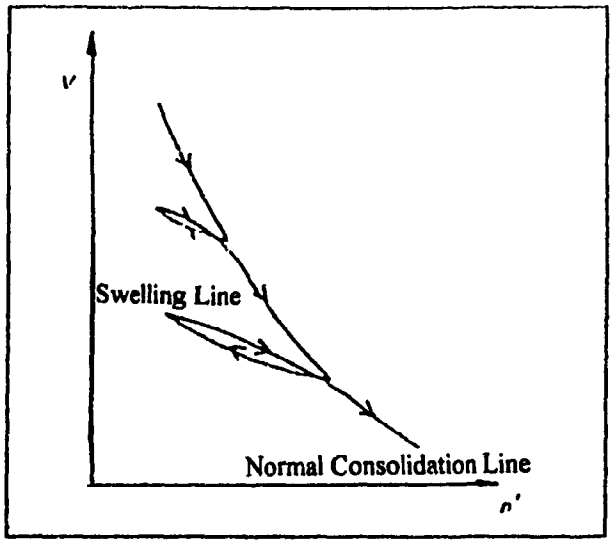

Figure (3-5a): Normal Consolidation Line and swelling line in v-P' space.

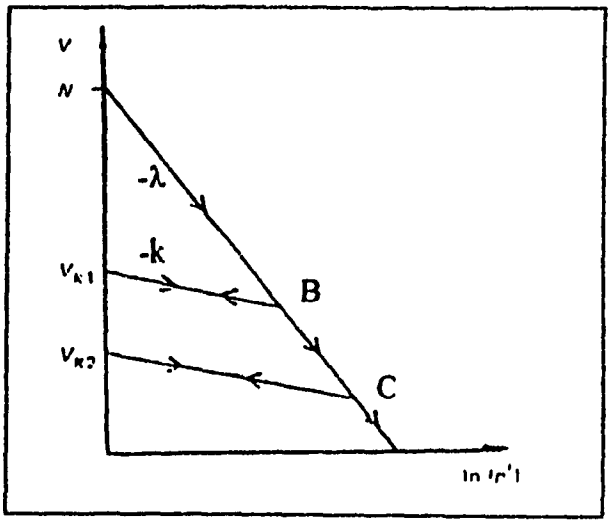

Figure (3-5b): Normal Consolidation Line and Swelling Line in v-ln(P') space.

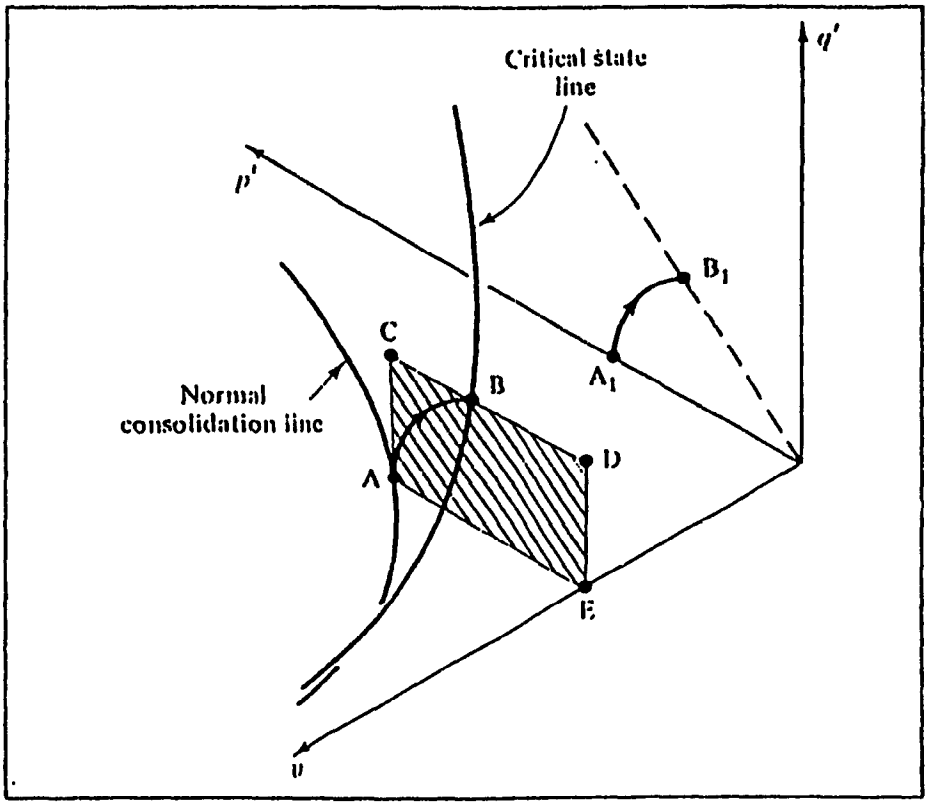

Figure (3-6): Critical State Line and Normal Consolidation Line in three dimensional q-P'-v space.

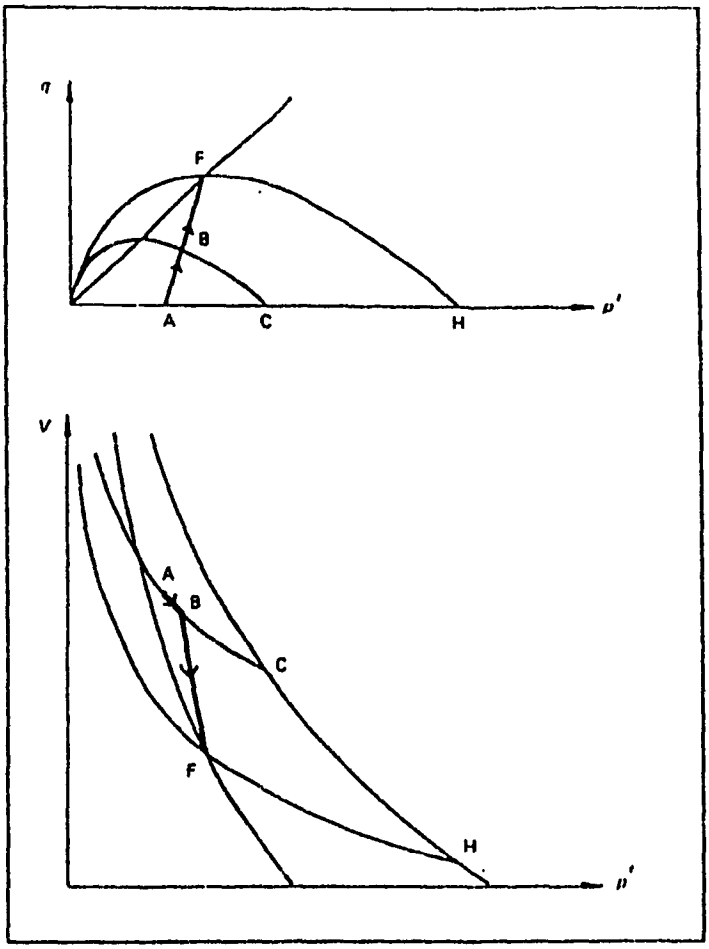

Figure (3-7): Stress path for lightly over consolidated sample in both q-P' and v-P' spaces.

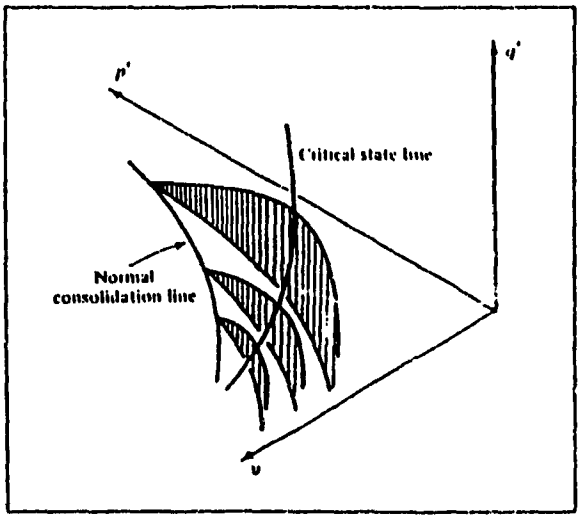

Figure (3-8): Yield curves in q-P'-v space

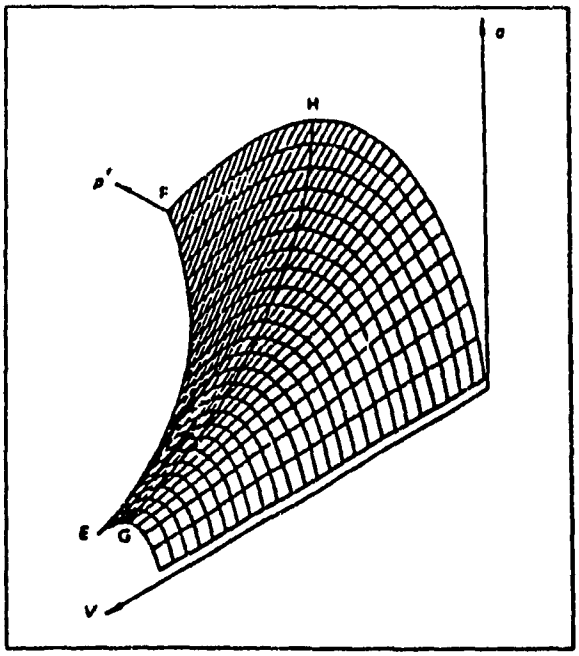

Figure (3-9): Cam clay Stable State Boundary Surface in q-P'-v space.

$$v_\lambda = \Gamma + (\lambda - k)(1 - \eta/M) \qquad (3\text{-}10)$$

where η is the stress ratio.

v_λ is defined as a specific volume at reference section.

Elastic straining underneath the SSBS corresponds tc movement along a k-line, with a corresponding change in v. Thus when an elastic sample is brought to the point of yield it must simultaneously lie on both the k-line and the SSBS. Therefore the intersection of the SSBS with the k-line equation gives the current yield surface :

$$q = MP'\ln(P'_c/P') \qquad (3\text{-}11)$$

where P'_c is the size of the current yield locus. This point lies on the isotropic normal consolidation line.

It is of interest to note that when q=0, P'_c=P'. Thus, for an over consolidated soil, P'c=P'max when no deviator stress exists (q=0).

3.5.1.5 Modified Cam clay model

Modified Cam Clay model modifies essentially the shape of the yield locus in the original Cam Clay model, to be an elliptical one. So the equation of the SSBS will change to:

$$v_\lambda = \Gamma + (\lambda - k)[\ln(2) - \ln(1 + (\eta / M)^2] \qquad (3\text{-}12)$$

The equation of the isotropic NCL is the same as for Cam Clay

$$v = N - \lambda\ln(P')$$

but $$N = \Gamma + (\lambda - k)\ln 2 \qquad (3\text{-}13)$$

and the current yield locus will be given by :

$$q^2 + M^2 P'^2 = M^2 P' P_c' \qquad (3\text{-}14)$$

3.5.1.6 Summary of parameters used in (Modified) Cam clay model

The critical state soil parameters can all be determined from the normal range of laboratory tests that are performed on a soil. These parameters are :

a. The frictional constant M

M is the slope of the CSL in q-P' space. Triaxial tests on isotropically consolidated samples can be used to obtain the frictional constant M. A number of tests need to be carried out with different consolidation pressures, for each test, P' and q have to be determined. The frictional constant M and the angle of shearing resistance ϕ are related with the following equation (see figure 3-4):

$$M = \frac{6\sin\varnothing}{3-\sin\varnothing} \qquad (3\text{-}15)$$

b. Slope of the normal consolidation line λ and swelling line k

These parameters can be obtained from odometer test or from triaxial tests on sample either isotropically or with K_o normally consolidated. λ is the slope of NCL or CSL in (ln(P'),v) or (ln(P'),e) plot. k is the slope of the swelling line in the same plot.

c. Critical state void ratio ecs

ecs is defined as the void ratio on the critical state line for a P'=1 or lnP'=0. This parameter determines the location of the CSL in v-lnP' space. ecs is obtained from:

$$ecs = \Gamma - 1 \qquad (3\text{-}16)$$

d. Poison's ratio μ

Poisson's ratio may be evaluated from the ratio of the lateral strain to axial strain during a triaxial compression test with axial loading. This parameter is needed to calculate the terms of the D matrix for (modified) Cam Clay under the yield locus when the behavior of the soil is elastic.

e. Size of the initial yield locus P'_c

Knowing the stress history of the ground, one can calculate P'_{max} and q_{max} as follows:

$$P'_{max} = (2.\sigma'_{x_{max}} + \sigma'_{y_{max}}) / 3$$
$$q_{max} = \sigma'_{y_{max}} - \sigma'_{x_{max}} \qquad (3\text{-}17)$$

where

$$\sigma'_{y_{max}} = OCR.\sigma'_{y}$$
$$\sigma'_{x_{max}} = K_{nc}.\sigma'_{y_{max}} \qquad (3\text{-}18)$$

where k_{nc} is defined in section 3.6.

Substituting these values in the expression for the Cam Clay (or modified Cam Clay) yield locus (equations 3-11 and 3-14), we obtain P_c' value for any point as :

For Cam Clay :

$$P_c' = P'_{max} * e^{(q_{max} / MP'_{max})} \qquad (3\text{-}19)$$

For modified Cam Clay:

$$P_c' = (q_{max} / M)^2 / P'_{max} + P'_{max} \qquad (3\text{-}20)$$

It is obvious that in case of normally consolidated soil $P'_{max}=P'$ and $q_{max}=q$.

3.6 In-situ stage

In this stage, the mesh covers the whole area including the region of soil in front of the wall which is going to be excavated (figure 3-1). Since the soil is subjected, at this stage, only to its self-weight, the in situ-stresses are specified at the bottom and the top of the mesh as follows :

$$\sigma_y' = \gamma y$$
$$\sigma_x' = \sigma_z' = K_0 \sigma_y' \qquad (3\text{-}21)$$
$$\tau_{xy} = 0$$

P'_c is calculated from equation (3-20), in cases of normally and over consolidated soil.

σ'_y and σ'_x are the normal and the horizontal effective stresses respectively

y = 0 at the top of the mesh and y = 46 m. at the bottom

K_0 is the coefficient of earth pressure at-rest.

This coefficient was calculated, in case of normally consolidated soil, from the experimental relation of Jaky (1944):

$$K_0 = 1 - \sin(\phi) \qquad (3\text{-}22)$$

In the case of over consolidated soil, the experimental relationship found by Schmidt (1966) and modified by Meyerhof (1976) case was used:

$$K_0 = K_{nc} \cdot \sqrt{OCR} \qquad (3\text{-}23)$$

where

k_{nc} is the coefficient of earth pressure at-rest under normally consolidated state.

τ_{xy} is the shear stress

3.7 Program CRISP

The finite element program which was used in the present investigation was CRISP (CRItical State Program) version 1990. This program was written and developed by a Geotechnical Group in Cambridge starting in 1975. The program allows several types of analysis: drained, undrained, consolidation analysis for three or two dimensional plane strain or axisymmetric solid bodies. The soil models which can be used are : anisotripic elastic, unhomogeneous elastic, critical state soil models and elastic perfectly plastic model. Finally, several types of elements can be used like: linear strain triangle (LST), cubic strain triangle (CuST), linear strain quadrilateral (LSQ) and the 20-node brick element.

The program consists of "geometry program" and "main program", the input data which must be supplied to the program are:

1. Information describing the finite element mesh, the number of super elements, the coordinates and number of super nodes, number of divisions of each side of the super

elements etc. . Based on this information, the program generates the node and element numbering system.

2. Material properties associated with each super element.

3. In-situ stress and boundary conditions of the region under investigation.

3.8 Variables considered

The Critical State Soil Mechanics parameters were isolated in order to determine their effects on the value of Kp. Table (3-1) summarizes the range of physical and mechanical characteristics of the sand employed in the present investigation.

Table (3-1): Summary of the range of physical and mechanical characteristics of the sand in the present investigation.

Angle of friction resistance, ϕ (degrees)	30 to 45
Slope of the Critical State Line, λ	0.1 to 0.3
Slope of the swelling line, k	0.00125 to 0.01
Critical State void ratio, ecs	0.5 to 3
Poisson's ratio, μ	0.2 to 0.4
Unit weight of soil, γ (KN/m^3)	17 to 21.5
Over Consolidation Ratio, OCR	1 to 4

The range of the Critical State soil parameters: λ, k and ecs used in the present investigation were taken from Atkinson (An Introduction to The Mechanics of Soils and Foundation Through Critical State Soil Mechanics, 1993). The unit weight of the soil γ was constant for each value of ϕ. Finally the theoretical range of Poisson's ratio μ was taken from 0.2 to 0.4 for each value of ϕ.

3-9 Loading increment

The entire loading was divided into 11 increments. These increments are grouped into 2 increments blocks:

a. Block increment 1 consists of only one increment which is the excavation of the soil in front of the wall and, at the same time, replace it by an equivalent triangular loading. This loading takes a value of $k_o \gamma h$ at the bottom of the wall and 0 at the top.

During this increment block, the soil is in at-rest state.

b. Block increment 2 is divided into 10 increments of equal load. This number of increment loading was sufficient to give a good accuracy to the results. This load consists of pushing the wall horizontally toward the soil by means of imposing a constant (x) displacement along the height of the wall. The total imposed displacement was 0.7 m, which means that each displacement increment was 0.07 m.

During this increment block, the soil is in passive state.

Several trials were made in order to examine the soil reaction against the displacement of the wall and it was found that the distribution of passive pressure along the height of the wall was triangular. The plot of distribution of passive pressure against the height of the wall is given in chapter 4. Readings of the stress created at the bottom of the wall (at 5.88 m depth) for each increment were taken and the wall displacement versus pressure for each trial analysis were plotted.

Figures 3-10 and 3-11 show typical wall displacement versus pressure curve in case of loose and dense sand, respectively.

The determination of the failure stress (σ_f) was made by plotting two tangent lines on the two portions of the load-pressure curve (as shown in the same figures). Their intersection was considered as the stress at which general failure occurs. So the coefficient of passive earth pressure k_p was calculated as follows:

$$k_p = \frac{\sigma_f}{\gamma h} \qquad (3\text{-}24)$$

where σ_f is the stress at the bottom of the wall at failure (KN/m^2)

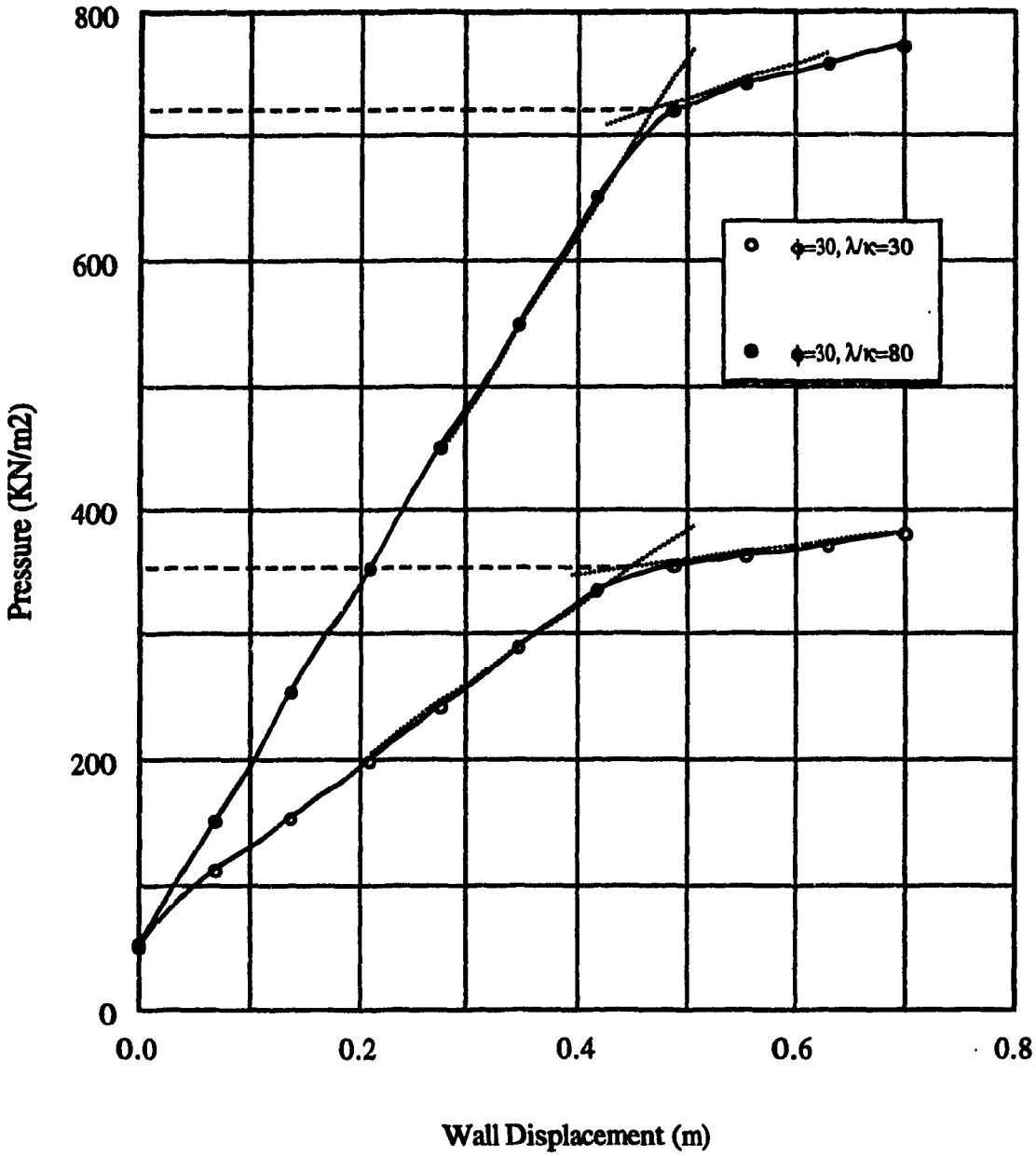

Figure (3-10): Typical wall displacement versus pressure for loose sand at a depth of 5.88 m on the wall

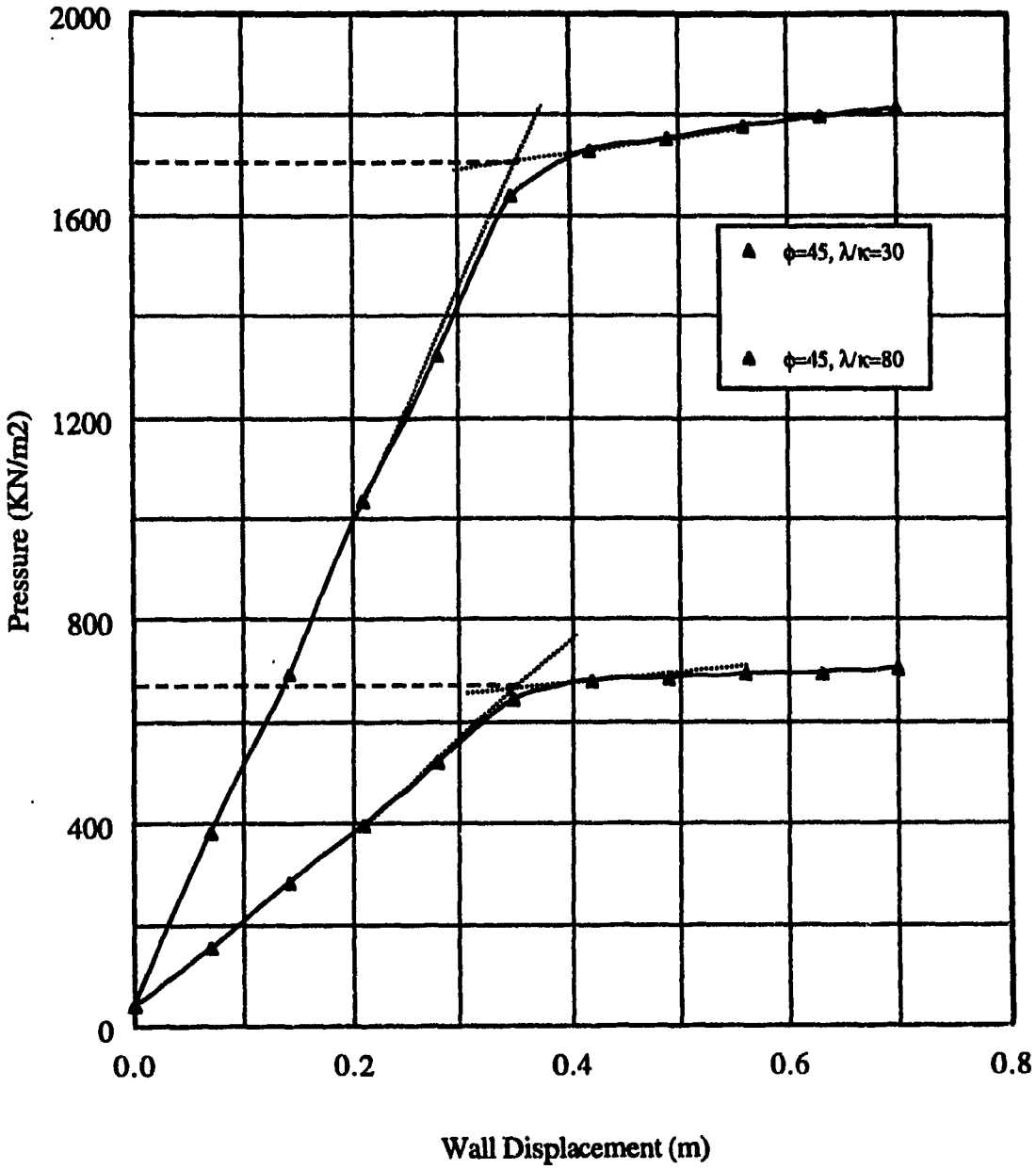

Figure (3-11): Typical wall displacement versus pressure for dense sand at a depth of 5.88 m on the wall

CHAPTER 4
RESULTS AND ANALYSIS

4.1 General

In this investigation, 384 trial analyses were conducted using the numerical model described in chapter three to examine the parameters affecting the value of the coefficient of passive earth pressure (Kp). 288 trials were conducted on normally consolidated sand while 96 analysis were conducted to examine the effect the Over Consolidation Ratio (OCR) on (Kp). The distribution of passive earth pressure behind the wall was also examined.

The testing program was divided into 5 groups, 4 groups for the case of Normally Consolidated sands corresponding to ϕ = 30, 35, 40 and 45 degrees each of them is divided into 2 series: series 1 concerns the case when λ/k=80 and series 2 is for λ/k=30. The last group is for the case of Over Consolidated sand, this group is divided into: series 1 when OCR = 2 and series 2 when OCR = 4.

The design parameters which are believed to have a direct effect on the value of the coefficient of passive earth pressure (Kp) were isolated and examined in order to determine their effects on (Kp) values.

Table 4-1 to 4-8 present the test results for Normally Consolidated sand. Table 4-9 and 4-10 present the test results for the case of Over Consolidated sand.

4.2 Passive pressure distribution behind the wall and rupture surface

Several trial analyses were made in order to examine the distribution of the passive earth pressure behind a vertical rigid wall. Reading of the stress at 6 different depths (0.88, 1.88, 2.88, 3.88, 4.88 and 5.88 m.) close to the wall were taken at various stage of wall displacement. This distribution was found to be approximately linear at every stage of wall displacement starting from a value of 0 at the top of the wall and reaching a

Table (4-1): Test Results: Passive Earth Pressure Coefficients for Normally Consolidated Soil

Group 1	Series 1
Angle of shearing resistance, ϕ = 30°	λ/k = 80
Unit weight γ (kN/m^3) = 17	
OCR = 1	

Test No.	Slope of the CSL, λ	Critical State Void Ratio, e_{cs}	Slope of the Swelling Line, k	Poisson Ratio, μ	Coefficient of Passive Earth Pressure, K_p
1	0.1	0.5	0.00125	0.2	7.63
2				0.3	6.68
3				0.4	5.83
4		1	0.00125	0.2	10.60
5				0.3	8.70
6				0.4	7.10
7		2	0.00125	0.2	18.96
8				0.3	14.60
9				0.4	11.28
10		3	0.00125	0.2	37.10
11				0.3	24.90
12				0.4	16.53
13	0.2	0.5	0.00025	0.2	5.24
14				0.3	4.85
15				0.4	4.51
16		1	0.00025	0.2	7.20
17				0.3	6.20
18				0.4	5.50
19		2	0.00025	0.2	14.40
20				0.3	11.00
21				0.4	8.10
22		3	0.00025	0.2	26.90
23				0.3	18.10
24				0.4	12.10
25	0.3	0.5	0.00375	0.2	3.77
26				0.3	3.16
27				0.4	2.66
28		1	0.00125	0.2	5.30
29				0.3	4.10
30				0.4	3.30
31		2	0.00375	0.2	10.00
32				0.3	7.35
33				0.4	5.02
34		3	0.00375	0.2	19.30
35				0.3	12.20
36				0.4	7.77

Table (4-2): Test Results: Passive Earth Pressure Coefficients for Normally Consolidated Soil

Group I	Series II
Angle of shearing resistance, ϕ = 30°	λ/k = 30
Unit weight γ (kN/m^3) = 17	
OCR = 1	

Test No.	Slope of the CSL, λ	Critical State Void Ratio, e_{cs}	Slope of the Swelling Line, k	Poisson Ratio, μ	Coefficient of Passive Earth Pressure K_p
1	0.1	0.5	0.00333	0.2	3.05
2				0.3	2.57
3				0.4	2.23
4		1	0.00333	0.2	4.00
5				0.3	3.40
6				0.4	2.83
7		2	0.00333	0.2	6.90
8				0.3	5.50
9				0.4	4.32
10		3	0.00333	0.2	11.90
11				0.3	9.18
12				0.4	7.00
13	0.2	0.5	0.00667	0.2	2.39
14				0.3	2.06
15				0.4	1.77
16		1	0.00667	0.2	3.15
17				0.3	2.64
18				0.4	2.25
19		2	0.00667	0.2	5.60
20				0.3	4.50
21				0.4	3.55
22		3	0.00667	0.2	9.70
23				0.3	7.30
24				0.4	5.75
25	0.3	0.5	0.01667	0.2	1.84
26				0.3	1.57
27				0.4	1.33
28		1	0	0.2	2.45
29				0.3	2.08
30				0.4	1.73
31		2	0.01	0.2	4.36
32				0.3	3.50
33				0.4	2.74
34		3	0.01	0.2	7.68
35				0.3	6.04
36				0.4	4.67

Table (4-3): Test Results: Passive Earth Pressure Coefficients for Normaliy Consolidated Soil

Group II	Series 1
Angle of shearing resistance, ϕ = 35°	λ/κ = 80
Unit weight γ (kN/m^3) = 18.5	
OCR = 1	

Test No.	Slope of the CSL, λ	Critical State void ratio, ecs	Slope of the Swelling Line, κ	Poisson Ratio, μ	Coefficient of Passive Earth Pressure, K_p
1	0.1	0.5	0.00125	0.2	11.71
2				0.3	9.15
3				0.4	7.05
4		1	0.00125	0.2	15.50
5				0.3	11.95
6				0.4	8.60
7		2	0.00125	0.2	27.90
8				0.3	18.80
9				0.4	12.67
10		3	0.00125	0.2	48.60
11				0.3	32.00
12				0.4	18.87
13	0.2	0.5	0.00025	0.2	8.37
14				0.3	6.62
15				0.4	5.05
16		1	0.00025	0.2	10.80
17				0.3	8.41
18				0.4	6.20
19		2	0.00025	0.2	19.90
20				0.3	14.10
21				0.4	9.27
22		3	0.00025	0.2	35.50
23				0.3	22.60
24				0.4	14.02
25	0.3	0.5	0.00375	0.2	5.41
26				0.3	4.33
27				0.4	3.34
28		1	0.00375	0.2	7.27
29				0.3	5.59
30				0.4	4.14
31		2	0.00375	0.2	14.00
32				0.3	9.34
33				0.4	6.25
34		3	0.00375	0.2	25.00
35				0.3	15.60
36				0.4	9.64

Table (4-4): Test Results: Passive Earth Pressure Coefficients for Normally Consolidated Soil

Group II	Series II
Angle of shearing resistance, ϕ = 35°	M_c = 30
Unit weight γ (kN/m^3) = 18.5	
OCR = 1	

Test No.	Slope of the CSL, λ	Critical State Void Ratio, e_{cs}	Slope of the Swelling Line, κ	Poisson Ratio, μ	Coefficient of Passive Earth Pressure, K_p
1	0.1	0.5	0.00125	0.2	3.73
2				0.3	3.15
3				0.4	2.66
4		1	0.00125	0.2	4.80
5				0.3	4.10
6				0.4	3.36
7		2	0.00125	0.2	8.20
8				0.3	6.51
9				0.4	5.01
10		3	0.00125	0.2	14.20
11				0.3	11.10
12				0.4	8.10
13	0.2	0.5	0.00025	0.2	2.96
14				0.3	2.52
15				0.4	2.16
16		1	0.00025	0.2	3.89
17				0.3	3.21
18				0.4	2.73
19		2	0.00025	0.2	6.59
20				0.3	5.30
21				0.4	4.13
22		3	0.00025	0.2	11.45
23				0.3	8.60
24				0.4	6.67
25	0.3	0.5	0.00375	0.2	2.17
26				0.3	1.93
27				0.4	1.7
28		1	0.00375	0.2	2.87
29				0.3	2.49
30				0.4	2.15
31		2	0.00375	0.2	5.00
32				0.3	4.16
33				0.4	3.28
34		3	0.00375	0.2	8.77
35				0.3	6.90
36				0.4	5.32

Table (4-5): Test Results: Passive Earth Pressure Coefficients for Normally Consolidated Soil

Group III	Series I
Angle of shearing resistance, ϕ = 40°	λ/κ = 80
Unit weight γ (kN/m^3) = 20	
OCR = 1	

Test No.	Slope of the CSL, λ	Critical State Void Ratio, e_{cs}	Slope of the Swelling Line, κ	Poisson Ratio, μ	Coefficient of Passive Earth Pressure, K_p
1	0.1	0.5	0.00125	0.2	16.16
2				0.3	11.64
3				0.4	7.97
4		1	0.00125	0.2	21.20
5				0.3	14.90
6				0.4	9.80
7		2	0.00125	0.2	36.20
8				0.3	23.60
9				0.4	14.32
10		3	0.00125	0.2	62.40
11				0.3	38.90
12				0.4	21.80
13	0.2	0.5	0.00025	0.2	11.48
14				0.3	8.52
15				0.4	5.71
16		1	0.00025	0.2	14.90
17				0.3	10.90
18				0.4	6.90
19		2	0.00025	0.2	26.80
20				0.3	17.70
21				0.4	11.13
22		3	0.00025	0.2	44.60
23				0.3	29.10
24				0.4	15.91
25	0.3	0.5	0.00375	0.2	6.85
26				0.3	5.41
27				0.4	4.09
28		1	0.00375	0.2	9.10
29				0.3	7.10
30				0.4	5.08
31		2	0.00375	0.2	17.90
32				0.3	11.70
33				0.4	7.65
34		3	0.00375	0.2	30.90
35				0.3	19.40
36				0.4	11.90

Table (4-6): Test Results: Passive Earth Pressure Coefficients for Normally Consolidated Soil

Group III	Series II
Angle of shearing resistance, ϕ = 40°	λ/κ = 30
Unit weight γ (kN/m^3) = 20.5	
OCR = 1	

Test No.	Slope of the CSL, λ	Critical State Void Ratio, e_{cs}	Slope of the Swelling Line, κ	Poisson Ratio, μ	Coefficient of Passive Earth Pressure, K_p
1	0.1	0.5	0.00333	0.2	4.55
2				0.3	3.75
3				0.4	3.12
4		1	0.00333	0.2	5.80
5				0.3	4.76
6				0.4	3.86
7		2	0.00333	0.2	10.10
8				0.3	7.91
9				0.4	5.93
10		3	0.00333	0.2	16.20
11				0.3	12.30
12				0.4	9.08
13	0.2	0.5	0.00667	0.2	3.66
14				0.3	3.06
15				0.4	2.54
16		1	0.00667	0.2	4.70
17				0.3	3.90
18				0.4	3.15
19		2	0.00667	0.2	8.20
20				0.3	6.31
21				0.4	4.93
22		3	0.00667	0.2	13.40
23				0.3	10.05
24				0.4	7.55
25	0.3	0.5	0.01667	0.2	2.54
26				0.3	2.24
27				0.4	2.00
28		1	0.01667	0.2	3.30
29				0.3	2.90
30				0.4	2.50
31		2	0.01667	0.2	6.12
32				0.3	4.83
33				0.4	3.89
34		3	0.01667	0.2	10.10
35				0.3	8.10
36				0.4	6.09

Table (4-7): Test Results: Passive Earth Pressure Coefficients for Normally Consolidated Soil

Group IV	Series I
Angle of shearing resistance, ϕ = 45°	λ/κ = 80
Unit weight γ (kN/m^3) = 21.5	
OCR = 1	

Test No.	Slope of the CSL, λ	Critical State Void Ratio, e_{cs}	Slope of the Swelling Line, κ	Poisson Ratio, μ	Coefficient of Passive Earth Pressure, K_p
1	0.1	0.5	0.00125	0.2	20.87
2				0.3	14.33
3				0.4	8.88
4		1	0.00125	0.2	27.50
5				0.3	18.30
6				0.4	11.10
7		2	0.00125	0.2	45.10
8				0.3	28.10
9				0.4	16.00
10		3	0.00125	0.2	79.20
11				0.3	47.90
12				0.4	25.40
13	0.2	0.5	0.00025	0.2	14.70
14				0.3	10.43
15				0.4	6.43
16		1	0.00025	0.2	19.10
17				0.3	13.40
18				0.4	7.90
19		2	0.00025	0.2	33.10
20				0.3	21.60
21				0.4	12.20
22		3	0.00025	0.2	57.10
23				0.3	35.80
24				0.4	18.95
25	0.3	0.5	0.00375	0.2	8.83
26				0.3	6.77
27				0.4	4.92
28		1	0.00375	0.2	11.80
29				0.3	8.70
30				0.4	6.05
31		2	0.00375	0.2	21.60
32				0.3	13.80
33				0.4	9.50
34		3	0.00375	0.2	38.40
35				0.3	23.20
36				0.4	14.60

Table (4-8): Test Results: Passive Earth Pressure Coefficients for Normally Consolidated Soil

Group IV	Series II
Angle of shearing resistance, ϕ = 45°	λ/κ = 30
Unit weight γ (kN/m^3) = 21.5	
OCR = 1	

Test No.	Slope of the CSL, λ	Critical State Void Ratio, e_{cs}	Slope of the Swelling Line, κ	Poisson Ratio, μ	Coefficient of Passive Earth Pressure, K_p
1	0.1	0.5	0.00333	0.2	5.51
2				0.3	4.54
3				0.4	3.75
4		1	0.00333	0.2	7.03
5				0.3	5.66
6				0.4	4.40
7		2	0.00333	0.2	11.74
8				0.3	9.10
9				0.4	6.80
10		3	0.00667	0.2	19.00
11				0.3	14.50
12				0.4	10.26
13	0.2	0.5	0.00667	0.2	4.38
14				0.3	3.62
15				0.4	2.90
16		1	0.00667	0.2	5.67
17				0.3	4.58
18				0.4	3.60
19		2	0.00667	0.2	9.50
20				0.3	7.48
21				0.4	5.60
22		3	0.00667	0.2	15.90
23				0.3	11.90
24				0.4	8.60
25	0.3	0.5	0.001667	0.2	3.10
26				0.3	2.61
27				0.4	2.36
28		1	0.01667	0.2	4.07
29				0.3	3.40
30				0.4	2.93
31		2	0.01667	0.2	6.95
32				0.3	5.50
33				0.4	4.45
34		3	0.01667	0.2	12.45
35				0.3	9.40
36				0.4	6.98

Table (4-9): Test Results: Passive Earth Pressure Coefficients for Over Consolidated Soil

Group V	Series 1
	OCR = 2

Test No.	Angle of Shearing Resistance, ϕ^o	Unit Weight, γ (kN/m^3)	Slope of the CSL, λ	Critical State Void Ratio, e_{cs}	Slope of the Swelling Line, k	Poisson Ratio, μ	Coefficient of Passive Earth Pressure, K_p
1	30	17	0.1	0.5	0.00125	0.2	11.46
2					0.00333	0.2	4.53
3				1	0.00125	0.3	14.10
4					0.00333	0.3	5.81
5			0.2	1	0.0025	0.2	10.74
6					0.0067	0.2	4.67
7				2	0.0025	0.4	14.10
8					0.0067	0.4	6.73
9			0.3	2	0.00375	0.3	11.89
10					0.01	0.3	5.89
11				3	0.00375	0.4	13.96
12					0.01	0.4	8.12
13	35	18.5	0.1	0.5	0.00125	0.2	18.79
14					0.00333	0.2	6.23
15				1	0.00125	0.3	20.21
16					0.00333	0.3	6.98
17			0.2	1	0.0025	0.2	16.96
18					0.00667	0.2	6.41
19				2	0.0025	0.4	16.79
20					0.00667	0.4	7.05
21			0.3	2	0.00375	0.3	16.71
22					0.01	0.3	7.67
23				3	0.00375	0.4	18.46
24					0.01	0.4	9.91

Continue Table (4-9):

Group V	Series I
	OCR = 2

Test No.	Angle of Shearing Resistance, ϕ^0	Unit Weight, γ (kN/m^3)	Slope of the CSL, λ	Critical State Void Ratio, ecs	Slope of the Swelling Line, κ	Poisson Ratio, μ	Coefficient of Passive Earth Pressure, K_p
25	40	20	0.1	0.5	0.00125	0.2	27.64
26					0.00333	0.2	7.87
27				1	0.00125	0.3	26.47
28					0.00333	0.3	9.41
29			0.2	1	0.0025	0.2	27.13
30					0.0067	0.2	7.63
31				2	0.0025	0.4	21.50
32					0.0067	0.4	9.67
33			0.3	2	0.00375	0.3	22.42
34					0.01	0.3	9.31
35				3	0.00375	0.4	23.71
36					0.01	0.4	12.23
37	45	21.5	0.1	0.5	0.00125	0.2	40.26
38					0.00333	0.2	9.30
39				1	0.00125	0.3	35.10
40					0.00333	0.3	12.31
41			0.2	1	0.0025	0.2	36.45
42					0.00667	0.2	10.24
43				2	0.0025	0.4	23.38
44					0.00667	0.4	11.87
45			0.3	2	0.00375	0.3	28.41
46					0.01	0.3	10.60
47				3	0.00375	0.4	30.14
48					0.01	0.4	14.84

Table (4-10): Test Results: Passive Earth Pressure Coefficients for Over Consolidated Soil

Group V	Series II
	OCR = 4

Test No.	Angle of Shearing Resistance, ϕ^0	Unit Weight, γ (kN/m^3)	Slope of the CSL, λ	Critical State Void Ratio, ecs	Slope of the Swelling Line, k	Poisson Ratio, μ	Coefficient of Passive Earth Pressure, K_p
1	30	17	0.1	0.5	0.00125	0.2	16.87
2					0.00333	0.2	6.46
3				1	0.00125	0.3	20.78
4					0.00333	0.3	7.78
5			0.2	1	0.0025	0.2	15.32
6					0.0067	0.2	6.83
7				2	0.0025	0.4	19.97
8					0.0067	0.4	9.13
9			0.3	2	0.00375	0.3	17.61
10					0.01	0.3	8.21
11				3	0.00375	0.4	18.62
12					0.01	0.4	11.72
13	35	18.5	0.1	0.5	0.00125	0.2	30.21
14					0.00333	0.2	9.27
15				1	0.00125	0.3	31.16
16					0.00333	0.3	11.19
17			0.2	1	0.0025	0.2	28.33
18					0.00567	0.2	9.85
19				2	0.0025	0.4	25.21
20					0.00667	0.4	11.48
21			0.3	2	0.00375	0.3	24.56
22					0.01	0.3	10.87
23				3	0.00375	0.4	27.18
24					0.01	0.4	15.63

Continue table (4-10):

Group V	Series I
	OCR = 4

Test No.	Angle of Shearing Resistance, ϕ^o	Unit Weight, γ (kN/m^3)	Slope of the CSL, λ	Critical State Void Ratio, e_{cs}	Slope of the Swelling Line, k	Poisson Ratio, μ	Coefficient of Passive Earth Pressure, K_p
25	40	20	0.1	0.5	0.00125	0.2	46.87
26					0.00333	0.2	12.28
27				1	0.00125	0.3	45.94
28					0.00333	0.3	14.32
29			0.2	1	0.0025	0.2	42.86
30					0.0067	0.2	14.60
31				2	0.0025	0.4	35.19
32					0.0067	0.4	15.62
33			0.3	2	0.00375	0.3	34.53
34					0.01	0.3	15.16
35				3	0.00375	0.4	36.11
36					0.01	0.4	18.11
37	45	21.5	0.1	0.5	0.00125	0.2	66.51
38					0.00333	0.2	17.13
39				1	0.00125	0.3	63.06
40					0.00333	0.3	18.26
41			0.2	1	0.0025	0.2	65.91
42					0.00667	0.2	17.84
43				2	0.0025	0.4	43.20
44					0.00667	0.4	20.21
45			0.3	2	0.00375	0.3	44.93
46					0.01	0.3	19.21
47				3	0.00375	0.4	51.27
48					0.01	0.4	25.25

maximum value at the bottom. Figure 4-1 shows typical pressure distribution on the wall at different stage of wall movement corresponding to wall displacement equal to: 0, 0.14, 0.28 and 0.42m. It is of interest to note that when the displacement is equal to 0 (the first line in figure 4-1), the soil is in at-rest state.

Also, several trials analysis were conducted to examine the variation of pressure, at different depths on the wall, with wall displacement. It was found that the pressure, at all depths, increases with increased wall displacements and the maximum pressures at all points are reached simultaneously. Figure 4-2 shows a typical pressure variation, at three different depths on the wall (1.88, 3.88 and 5.88 m) with wall displacements

From the typical wall displacement versus pressure for loose and dense sand (figure 3-1 and 3-2), it can be seen that failure occurred at wall displacement of about 0.45m in case of loose sand and 0.37m in case of dense sand which represent 7.5% and 6.2% of the height of the wall respectively. These values were, generally, not affected by the other critical state soil mechanics parameters.

The rupture surface was found to be curved, starting from the toe of the wall, going down under the foundation level and then up to reach the sand surface, this is shown in the deformed mesh figures (figure 4-3 and 4-4) where the deformation scale was taken equal to 8 in order to exaggerate the view of the deformation. These figures represent a typical deformed mesh in case of loose and dense sands at the end of increment number 8 for loose sand and increment number 7 for dense sand (immediately after failure occurs) where the wall displacement is equal to 0.49 and 0.42 m respectively. It can be seen from these figures that the rupture wedge for dense sand is larger than that for loose sand.

Figures 4-5 and 4-6 represent the directions of the displacement vectors, at a scale also equal to 8, at the end of increment number 8 and 7 for loose and dense sand respectively. They, clearly, show the upward movement of the soil near the wall and the downward movement of the soil under the foundation level due to the displacement of the wall.

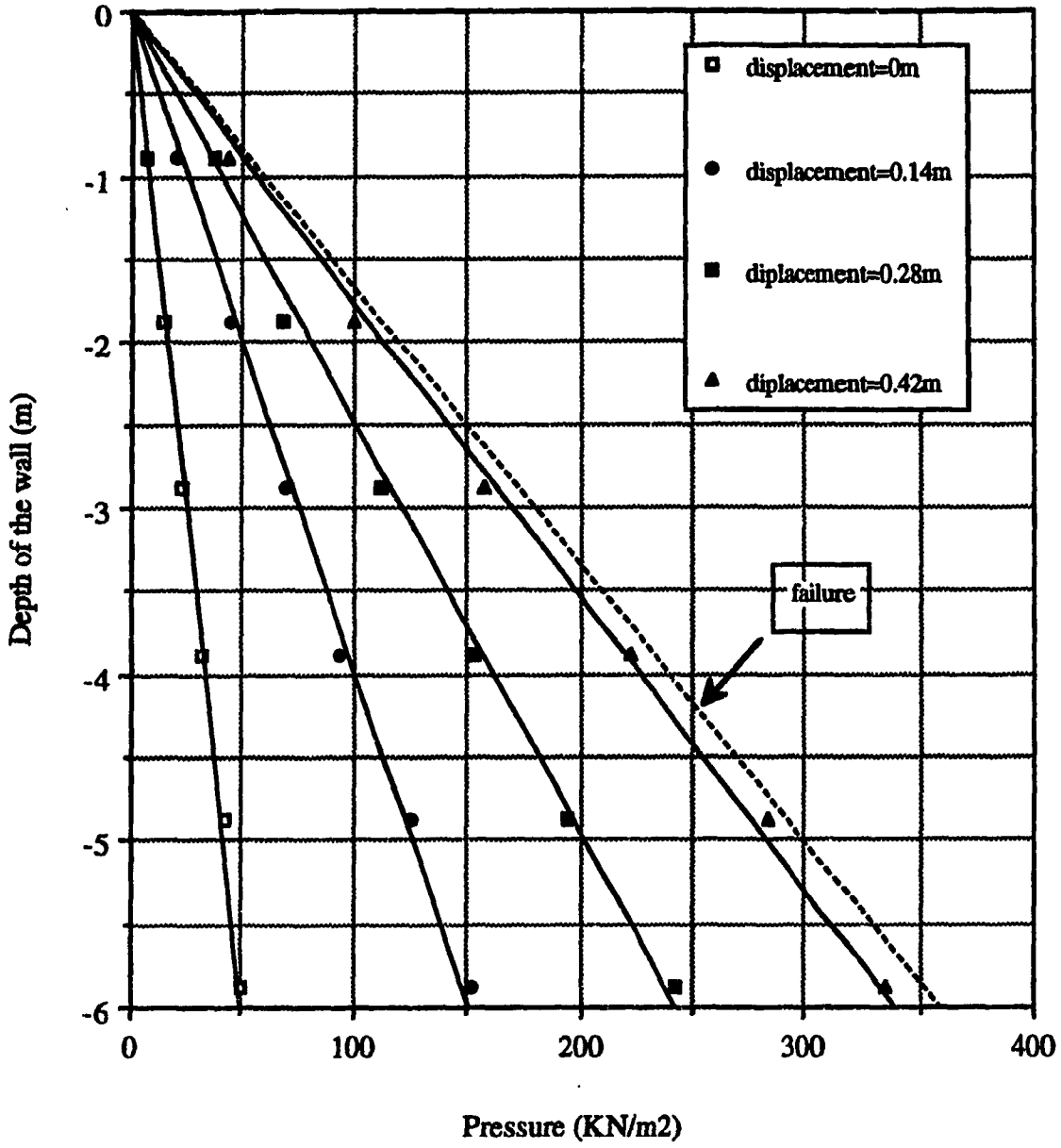

Figure (4-1): Typical pressure distribution on wall at different stages of wall movement

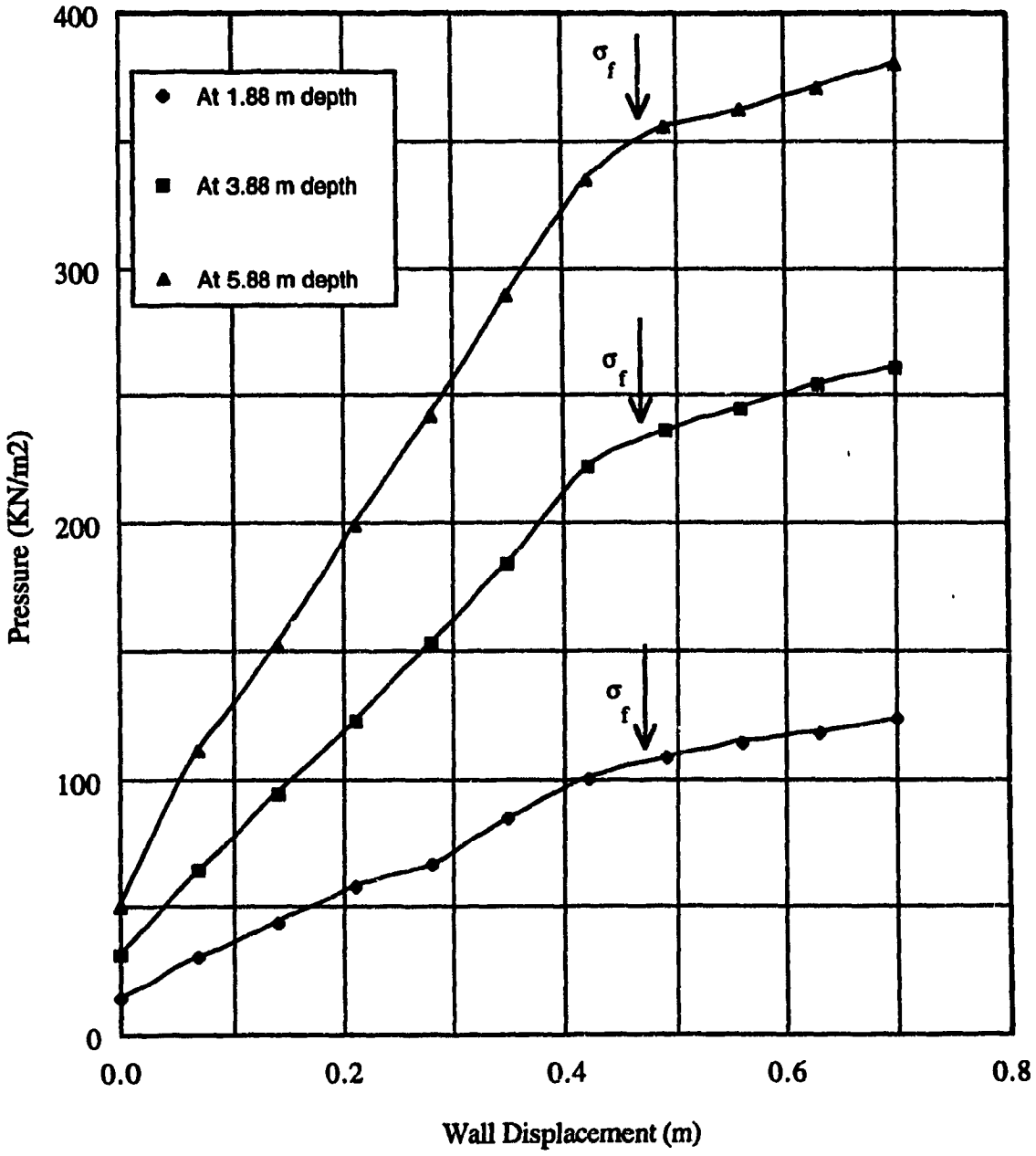

Figure (4-2): Typical wall displacement versus pressure curve at different depth on the wall

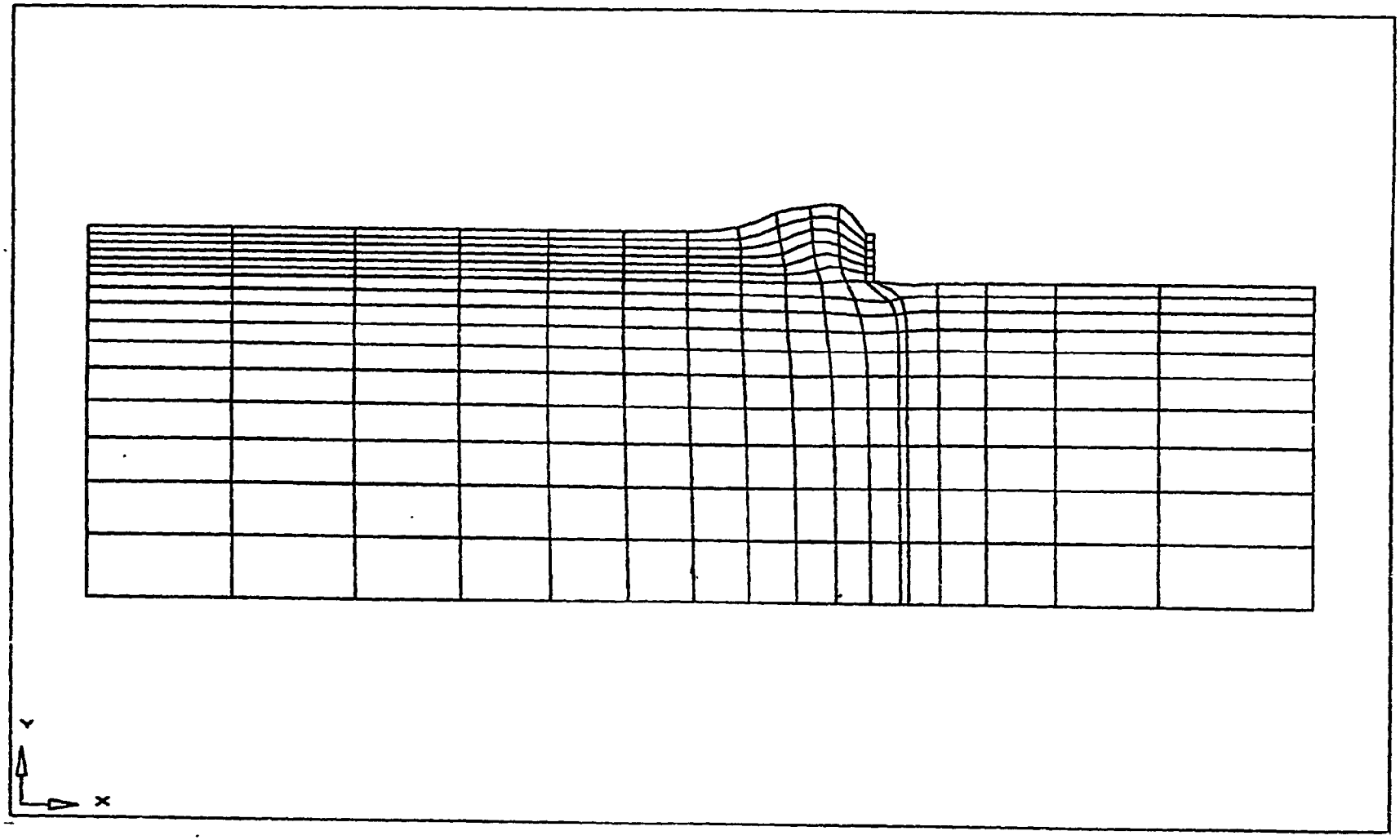

Figure (4-3): Finite element deformed mesh immediately after failure for loose sand.
(The deformation scale is equal to 8)

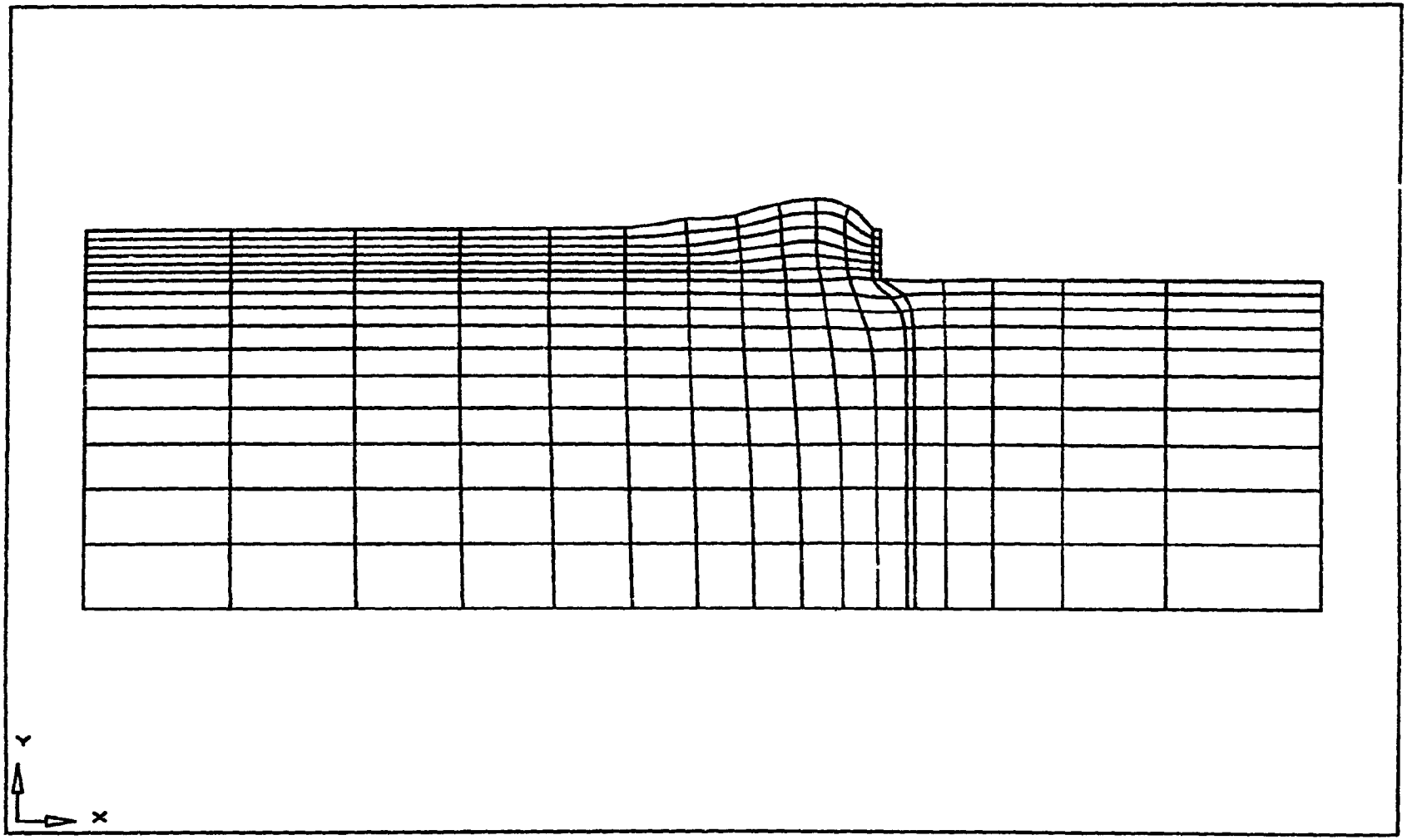

Figure (4-4): Finite element deformed mesh immediately after failure for dense sand.
(The deformation scale is equal to 8)

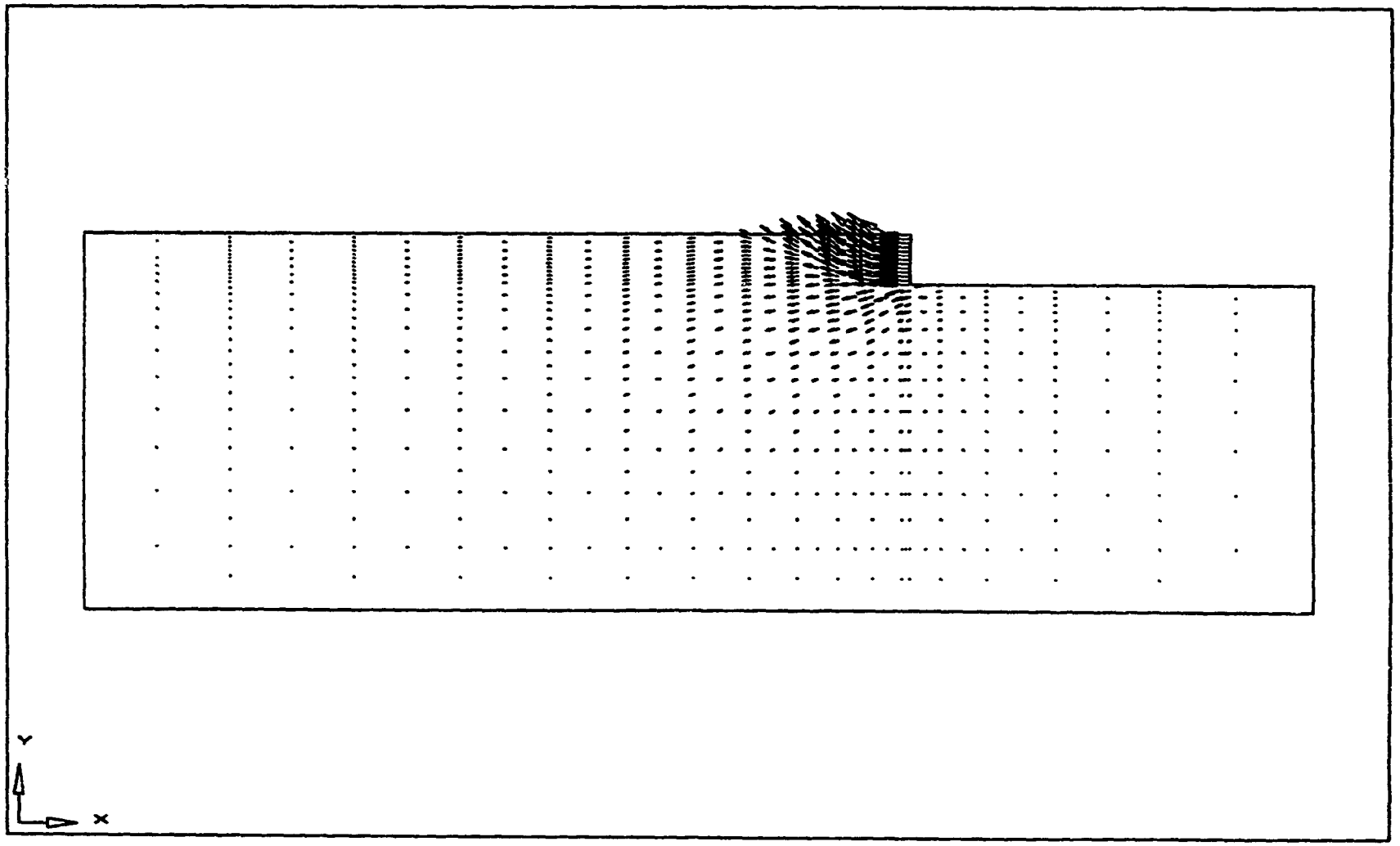

Figure (4-5): Direction of displacement vector, at 0.49m wall displacement, for loose sand at a scale equal to 8.

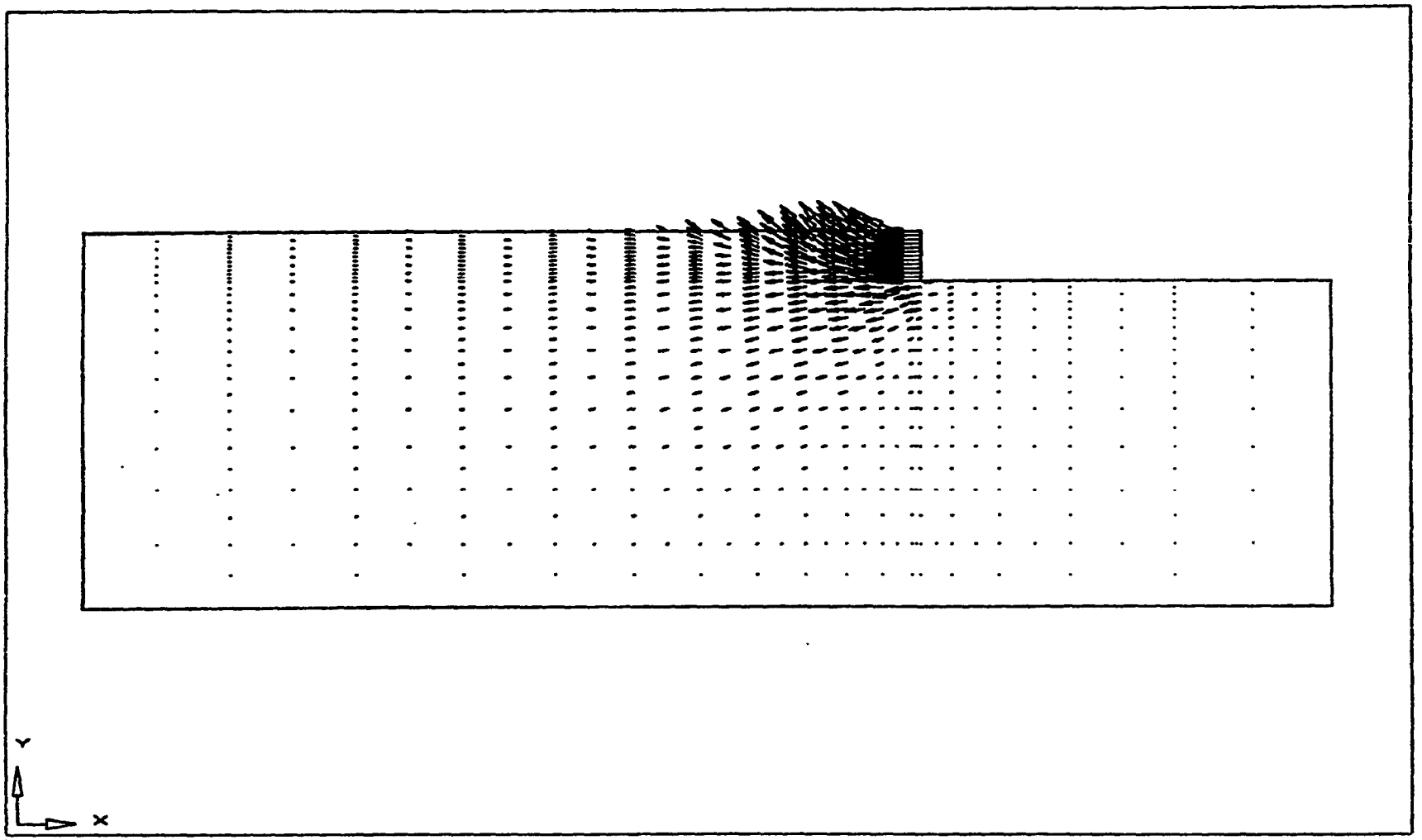

Figure (4-6): Direction of displacement vector, at 0.42m wall displacement, for dense sand at a scale equal to 8.

All the above mentioned observations are in good agreement with the conclusions made by Rowe and Peaker (1965) and by Narain et al (1969) concerning the passive pressure distribution behind a wall translating horizontally into a mass of dry sand, as described in chapter 2.

4.3 Passive earth pressure for normally consolidated sand

The results of analyses, for normally consolidated sand, are presented in form of a parametric study. The parameters that affect the value of Kp were isolated in order to determine their effects. These parameters are: the angle of shearing resistance ϕ, the slope of the CSL λ, the slope of the swelling line k, the critical state void ratio ecs and Poisson's ratio μ.

4.3.1 Effect of the critical state void ratio, ecs

The variation of Kp versus ecs for each value of λ, ϕ and μ is presented in figures 4-7 to 4-14. These figures show that the value of Kp increases considerably due to an increase of the critical state void ratio ecs. This increase is due to the fact that when ecs is large, the CSL is located far away from the e axis in P' versus e plot and when ecs is small, the CSL is located, for the same λ, near the e axis in the same plot. Thus the stress needed to cause failure is greater in case of large ecs. Thus the value of Kp will be greater (see figure 3-5b).

It is of interest to note that the increase of Kp due to an increase of ecs is more significant for a large values of ecs.

4.3.2 Effect of the elastic parameters k and μ

The slope of the swelling line k and Poisson's ratio μ are the elastic parameters of the soil. A soil having a higher interlocked particles has small values of k and/or μ which

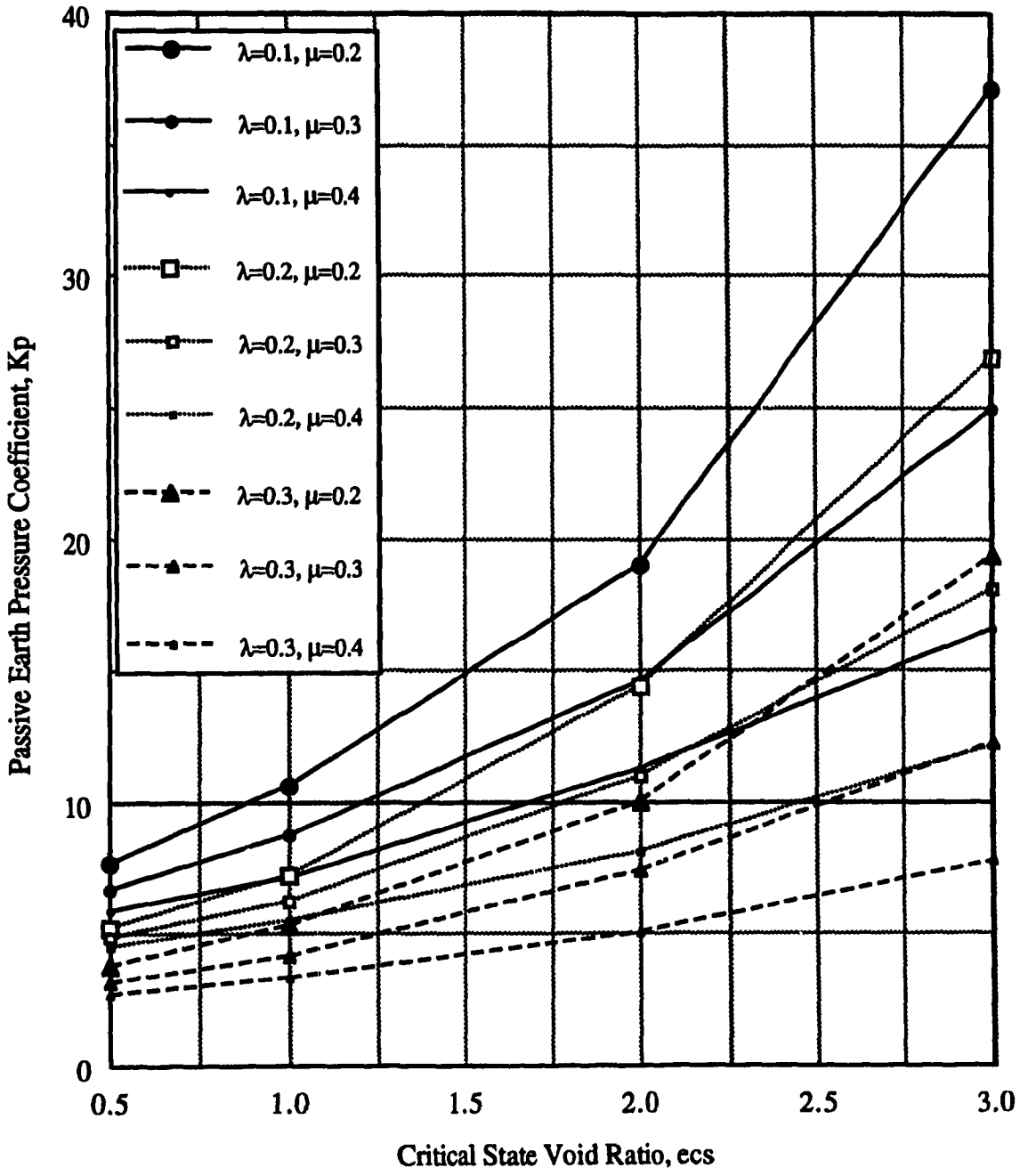

Figure (4-7): Kp versus ecs for $\phi = 30^0$ and $\lambda/k=80$

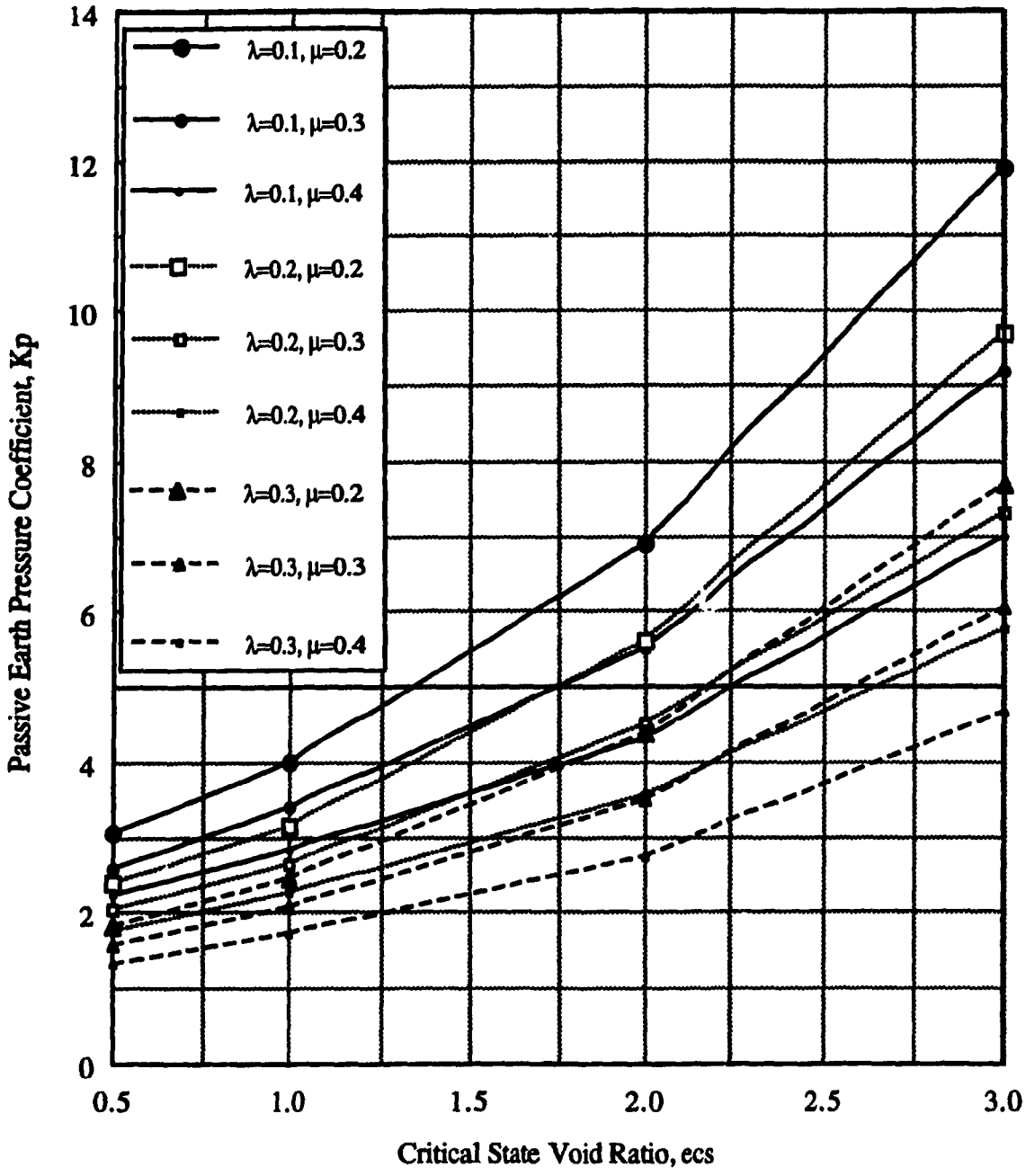

Figure (4-8): Kp versus ecs for $\phi = 30^0$ and $\lambda/k=30$

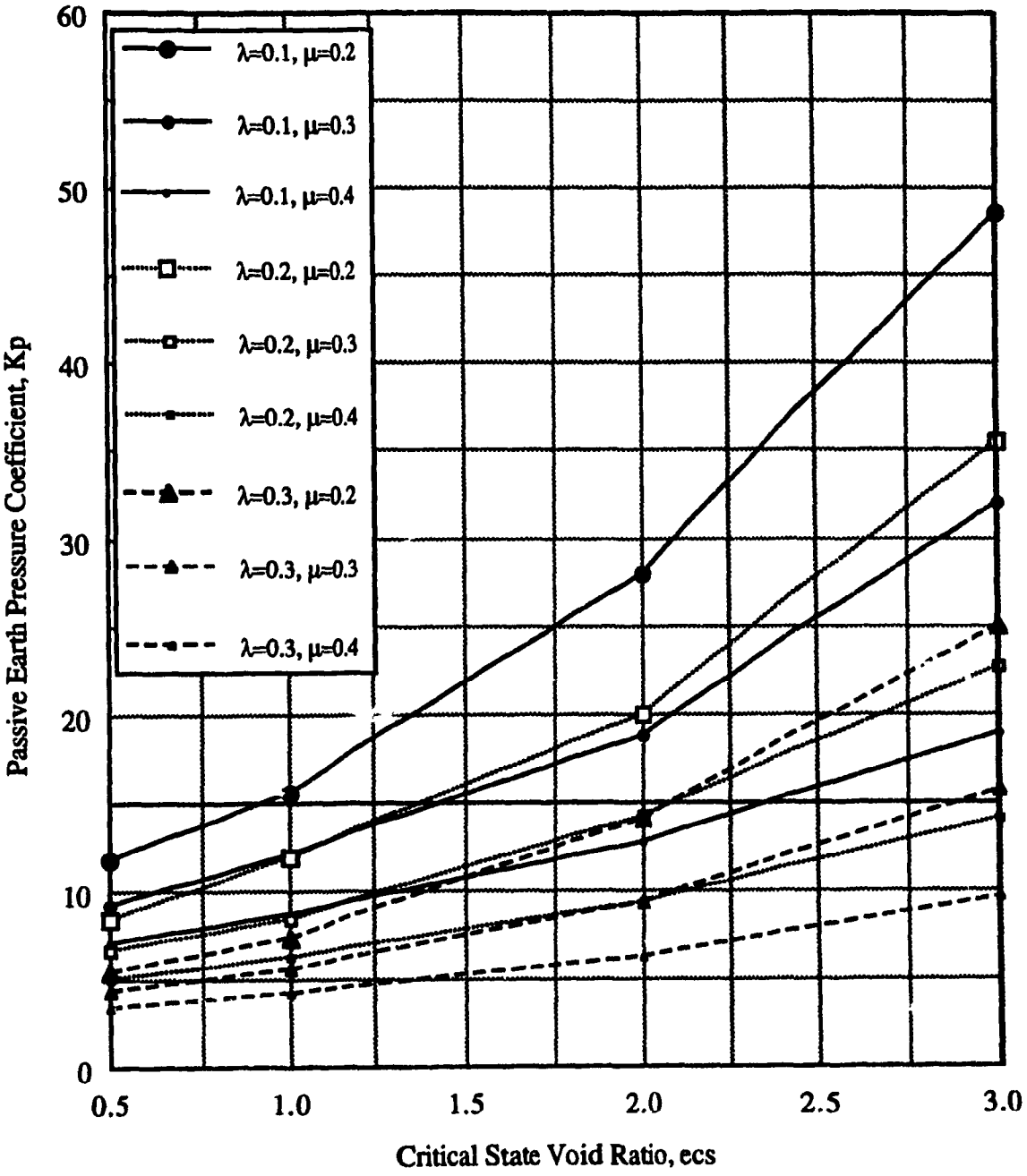

Figure (4-9): Kp versus ecs for $\phi = 35^{o}$ and $\lambda/k=80$

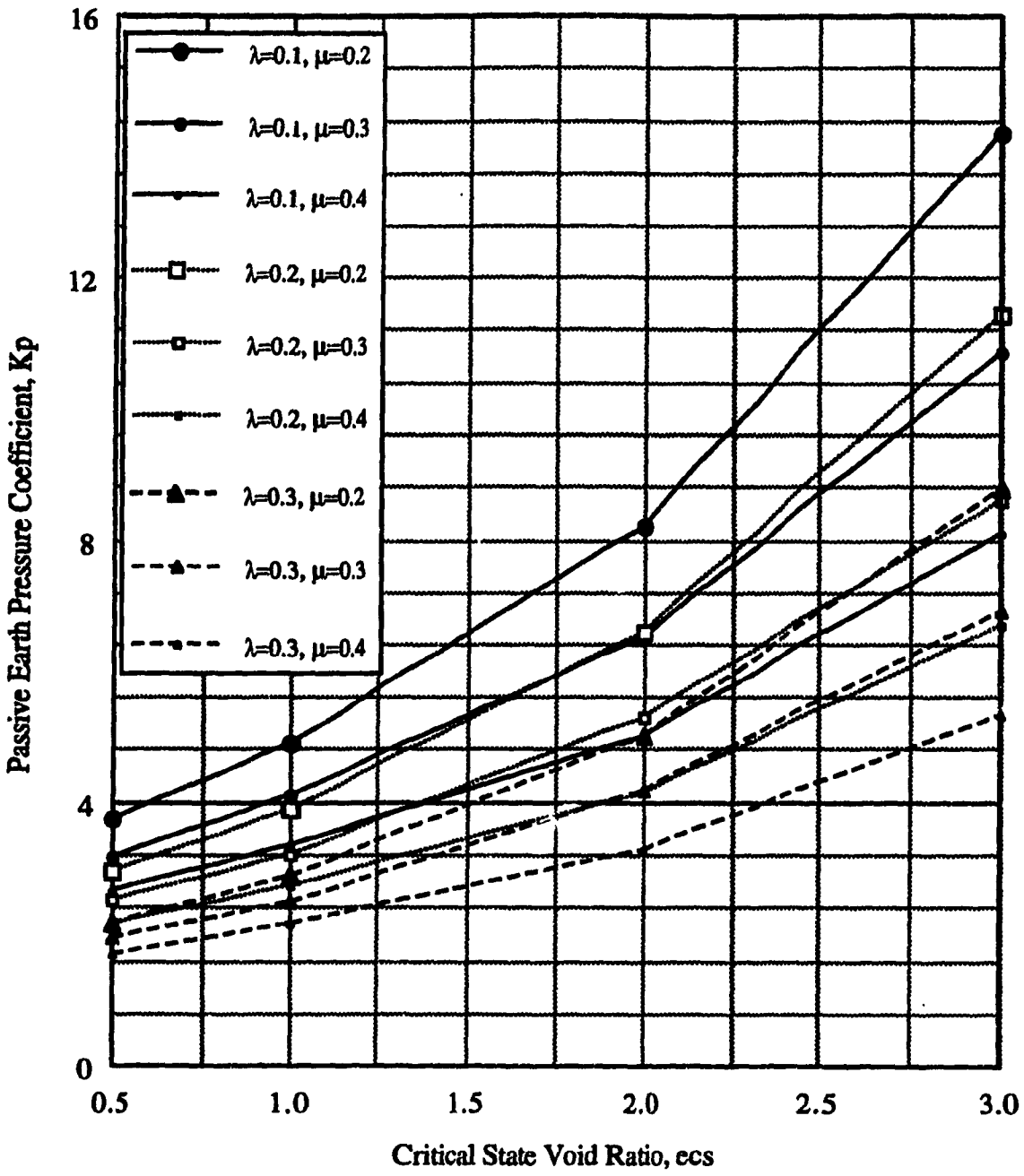

Figure (4-10): Kp versus ecs for $\phi = 35^0$ and $\lambda/k=30$

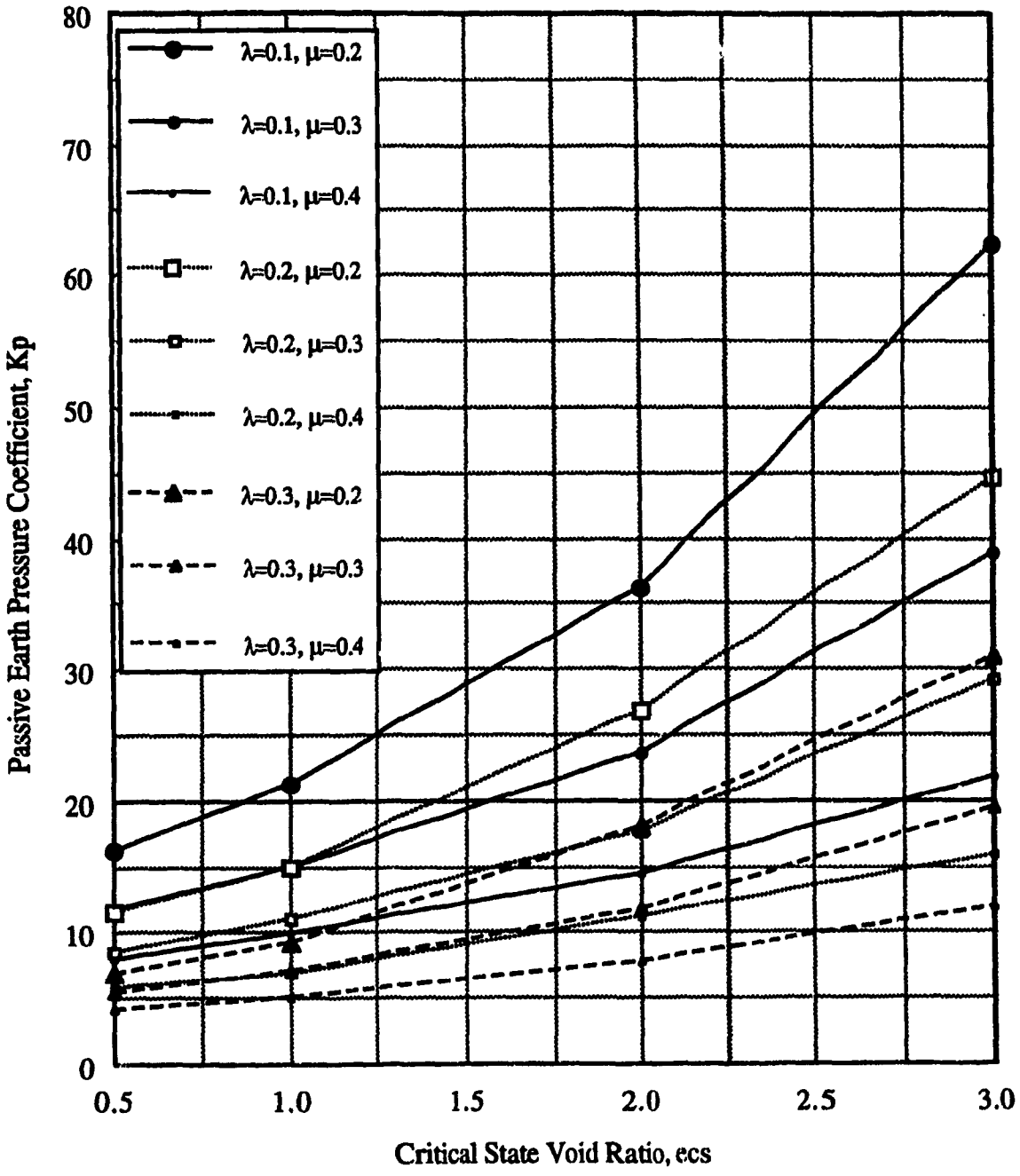

Figure (4-11): Kp versus ecs for $\phi = 40^{o}$ and $\lambda/k=80$

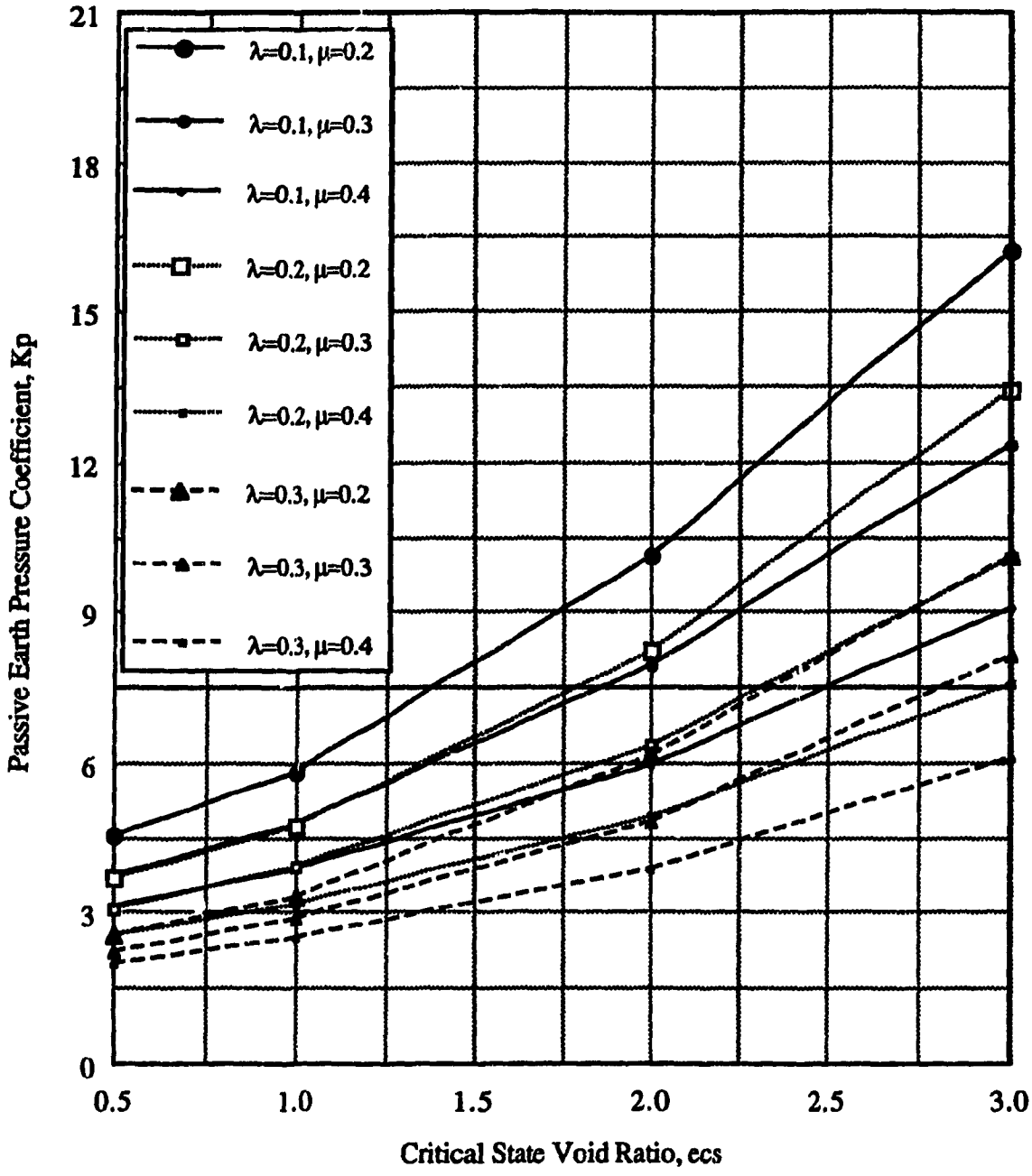

Figure (4-12): Kp versus ecs for $\phi = 40^{o}$ and $\lambda/k=30$

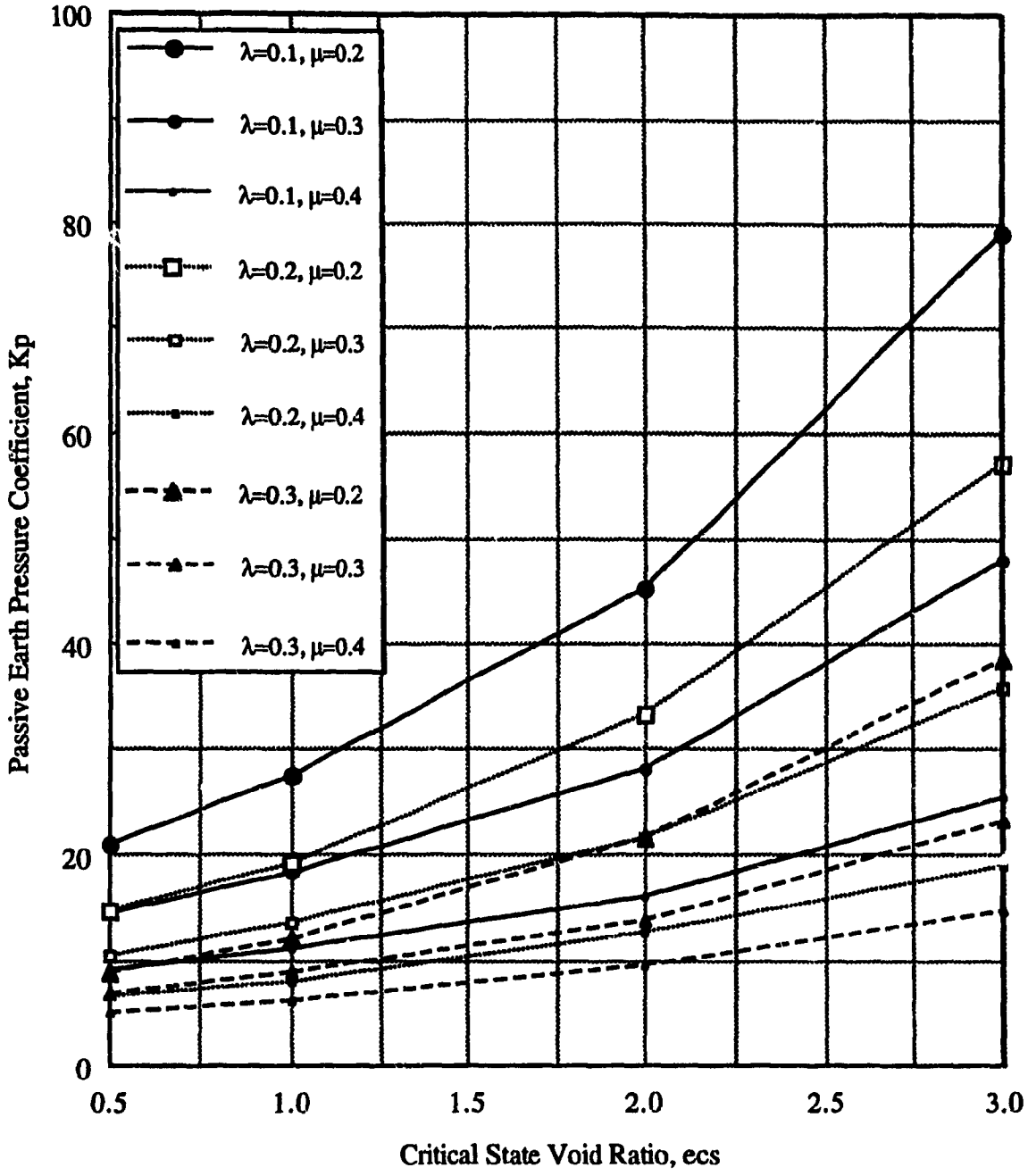

Figure (4-13): Kp versus ecs for $\phi = 45^0$ and $\lambda/k=80$

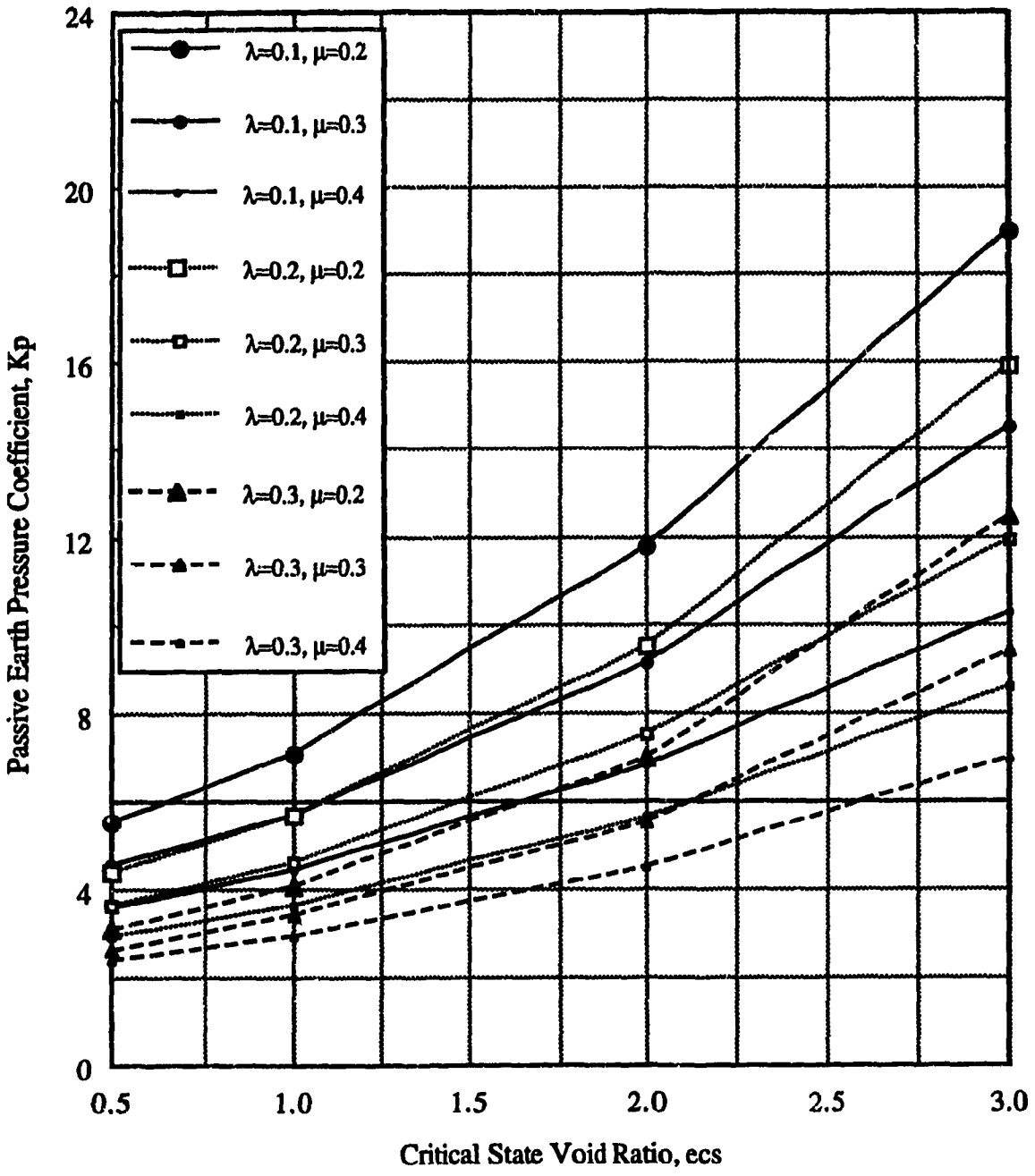

Figure (4-14): Kp versus ecs for $\phi = 45^{o}$ and $\lambda/k=30$

means that this soil is more rigid than that having large values of k and/or μ. As expected, the test results show that the smaller the elastic parameters, the greater the coefficient of passive earth pressure, Kp.

When μ decreases by an amount of 0.1, the value of Kp increases approximately from about 15% for $\phi = 30^o$ and $\lambda/k = 30$ to about 70% for $\phi = 45^o$ and $\lambda/k = 80$. From figures 4-7 to 4-14, it can be seen that the variation of Kp with μ could be considered as a linear one in all cases. λ and ecs have a little or no effect on this variation.

The increase of Kp due to a decrease of k is a little more significant, this increase is affected essentially by the value of μ. Kp increases, when the ratio λ/k increases from 30 to 80, from 2.5 to 4 times for a value of μ equal to 0.2 and it increases, for the same variation of λ/k, from 2 to 3 times for μ equal to 0.4.

ϕ and ecs have a little effect on this variation.

4.3.3 Effect of the slope of the CSL, λ

The calculated value of Kp increases with a decrease of λ. This can be explained by the fact that the smaller the value of λ, the smaller the initial void ratio. It is of interest to note that λ is also the slope of the NCL which is parallel to the CSL (chap 3). When the soil is isotropically consolidated to a given stress P1 and then to a given larger stress P2, if the change in the specific volume is small, λ is small and the initial void ratio is small which implies that the value of Kp is large. If the change in v is large, λ is large, the initial void ratio is large and then the value of Kp is small.

The variation of Kp versus λ for each value of ecs, ϕ and μ are presented in figures 4-15 to 4-22. It can be seen from these figures that Kp varies approximately linearly with the slope of the Critical State Line, λ.

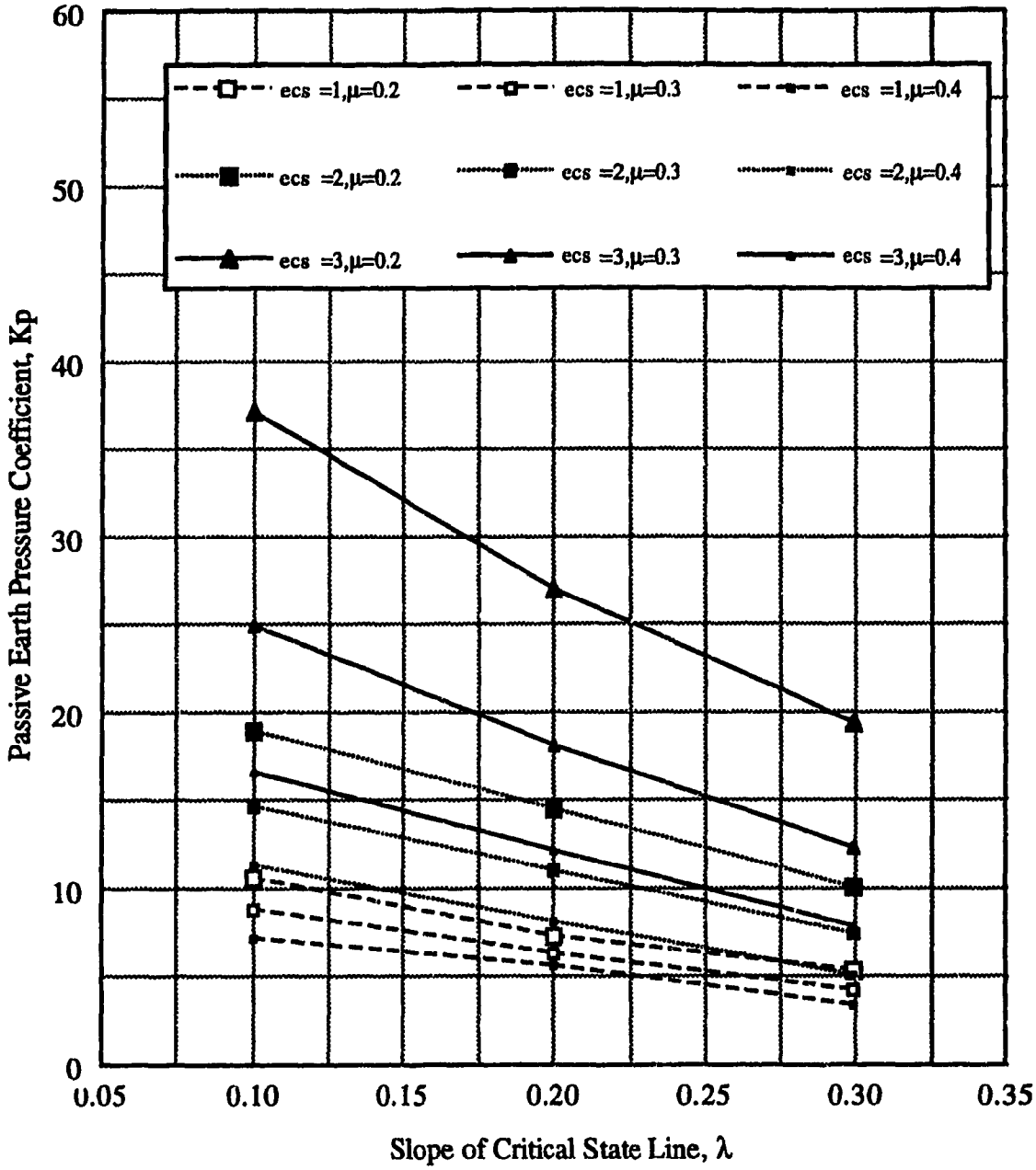

Figure (4-15): Kp versus λ for $\phi = 30^0$ and $\lambda/k = 80$

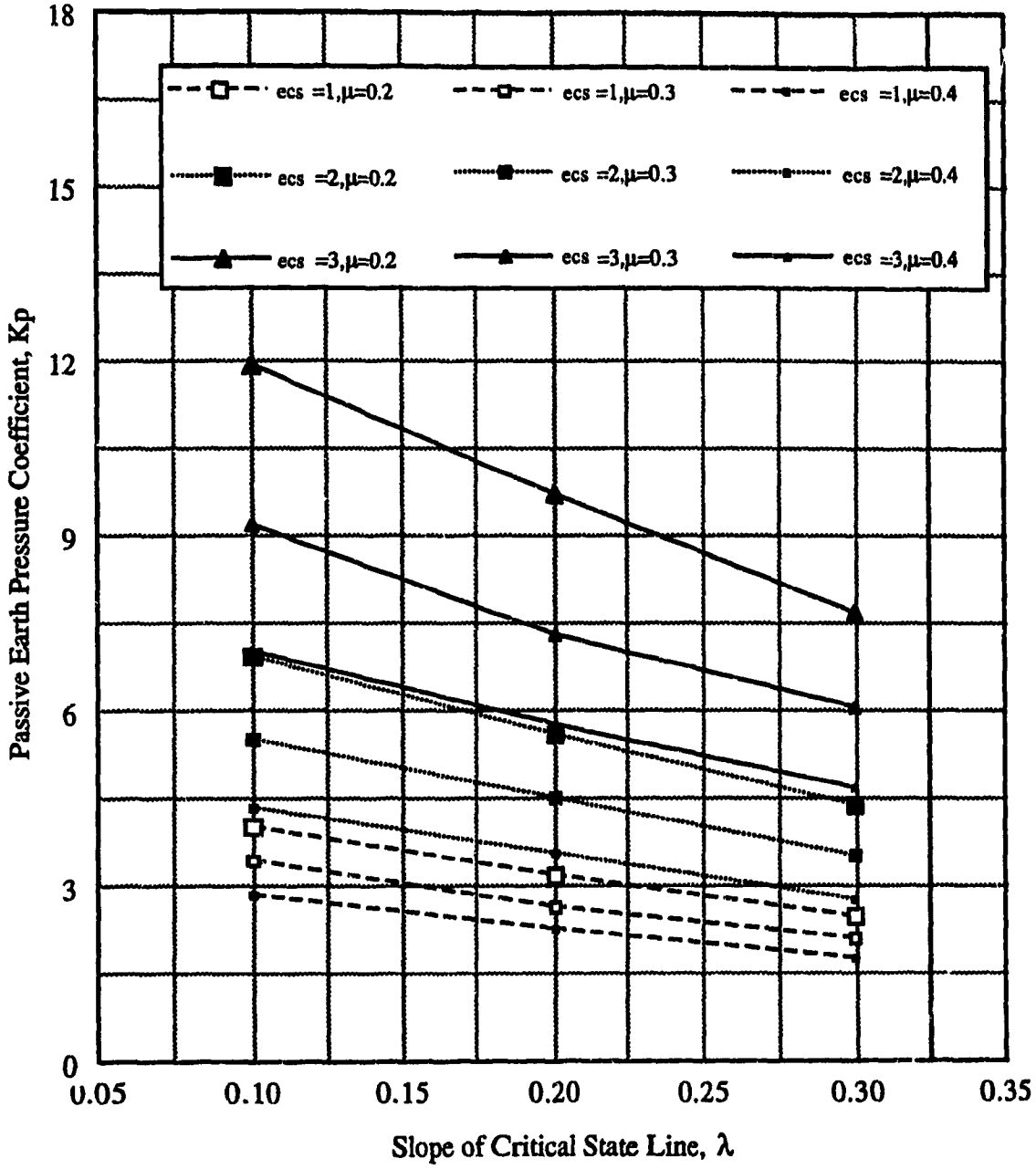

Figure (4-16): Kp versus λ for $\phi = 30^{o}$ and $\lambda/k = 30$

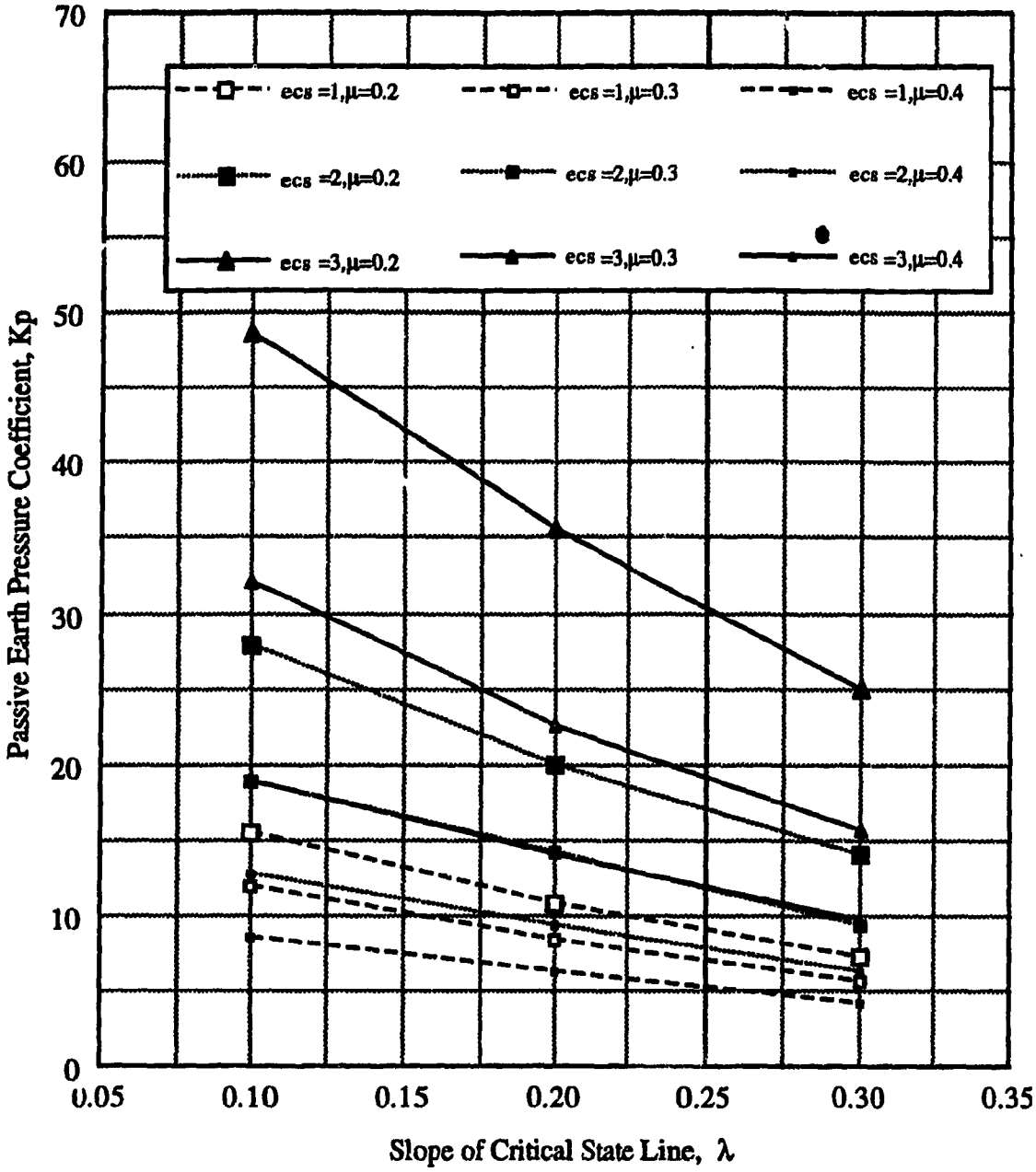

Figure (4-17): Kp versus λ for $\phi = 35^0$ and $\lambda/k = 80$

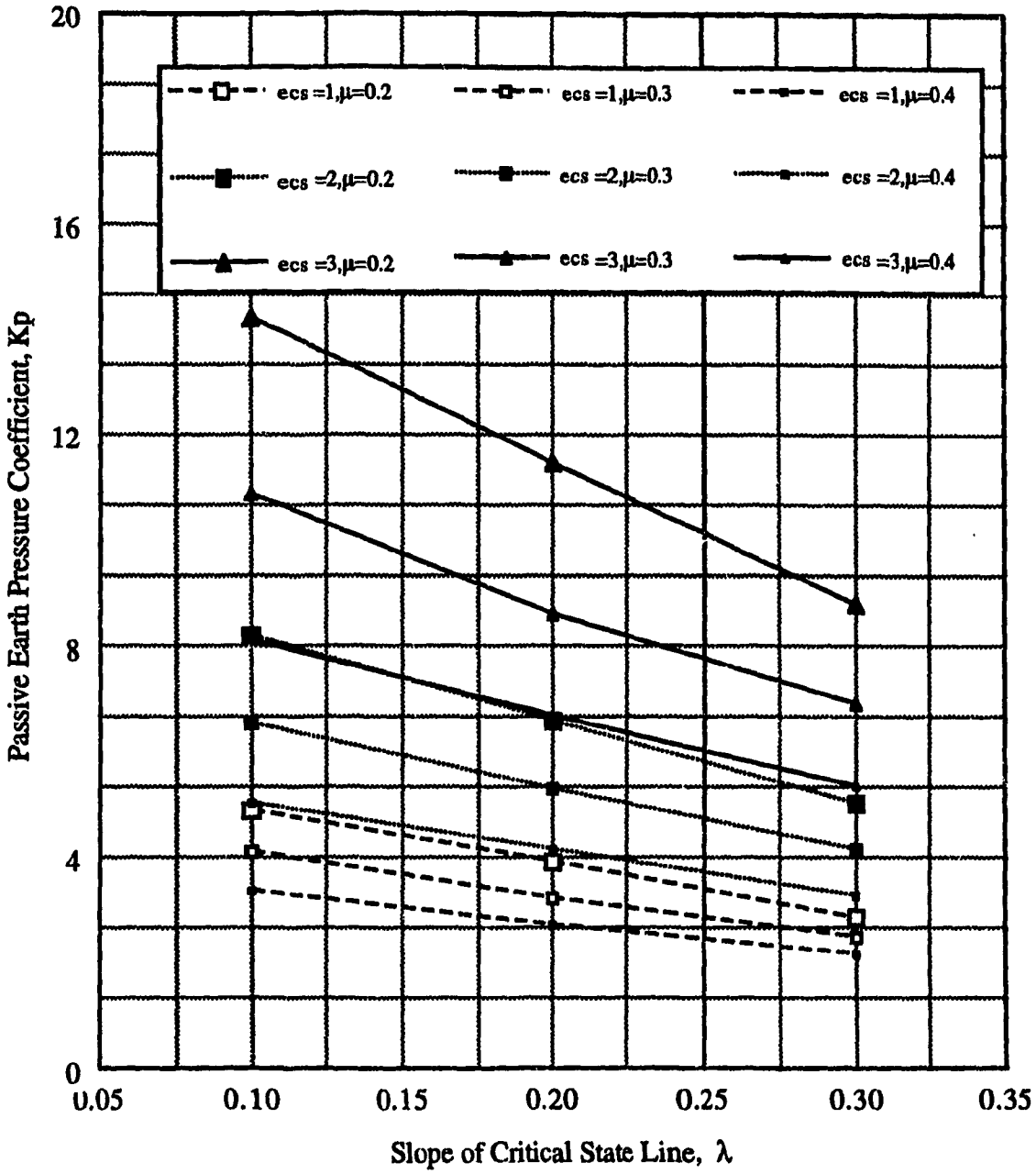

Figure (4-18): Kp versus λ for $\phi = 35^{o}$ and $\lambda/k = 30$

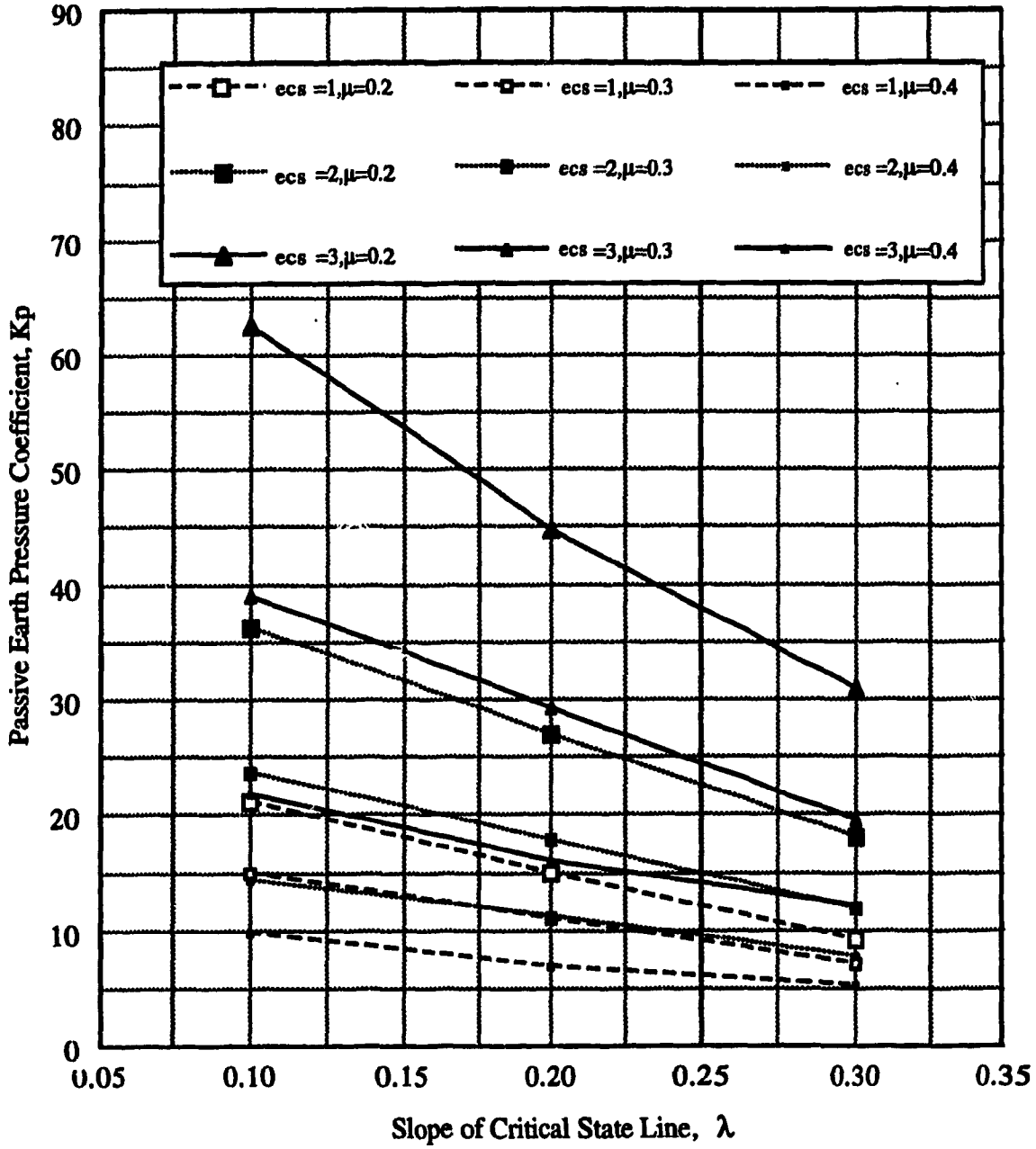

Figure (4-19): Kp versus λ for $\phi = 40^0$ and $\lambda/k = 80$

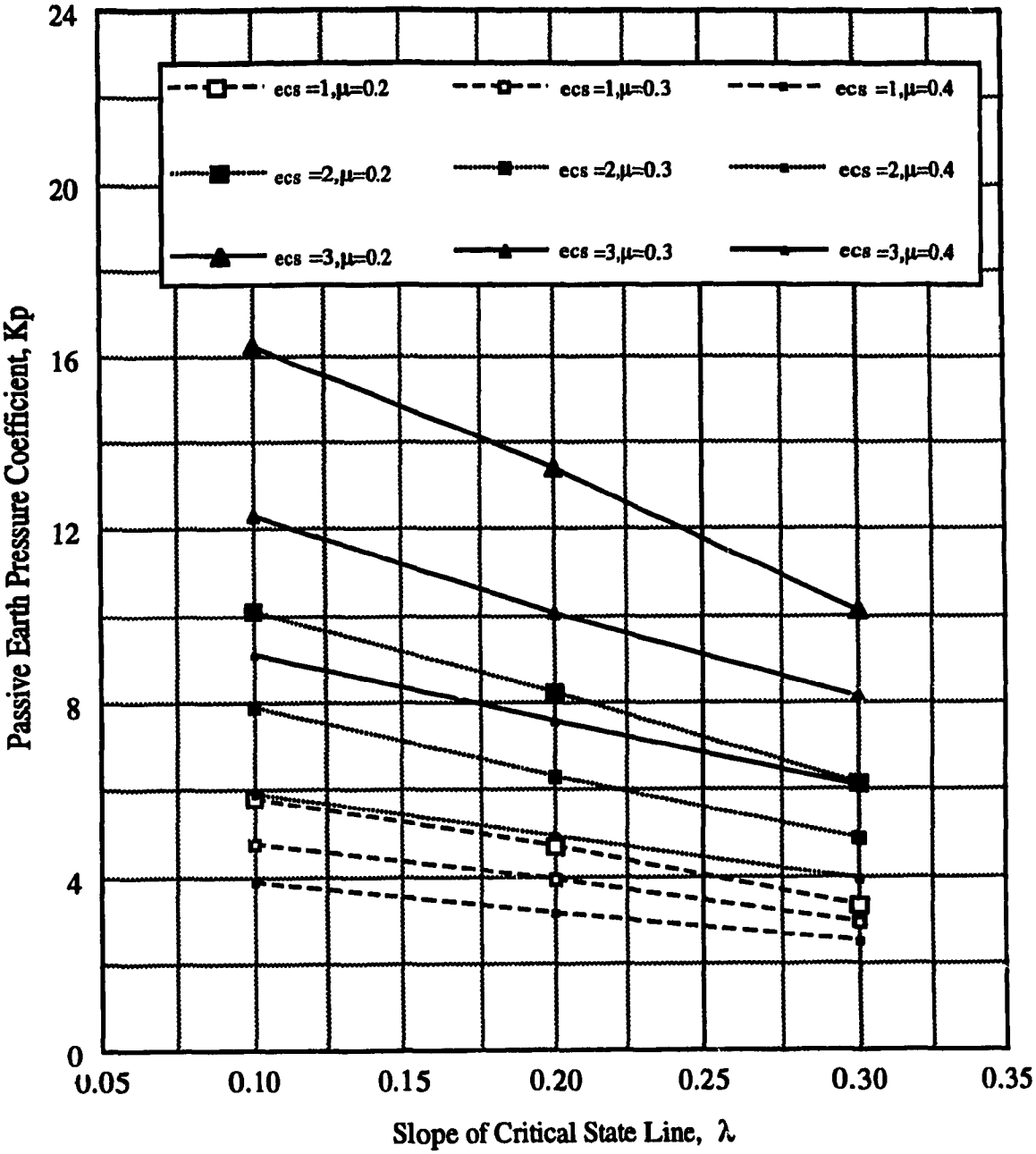

Figure (4-20): Kp versus λ for $\phi = 40^o$ and $\lambda/k = 30$

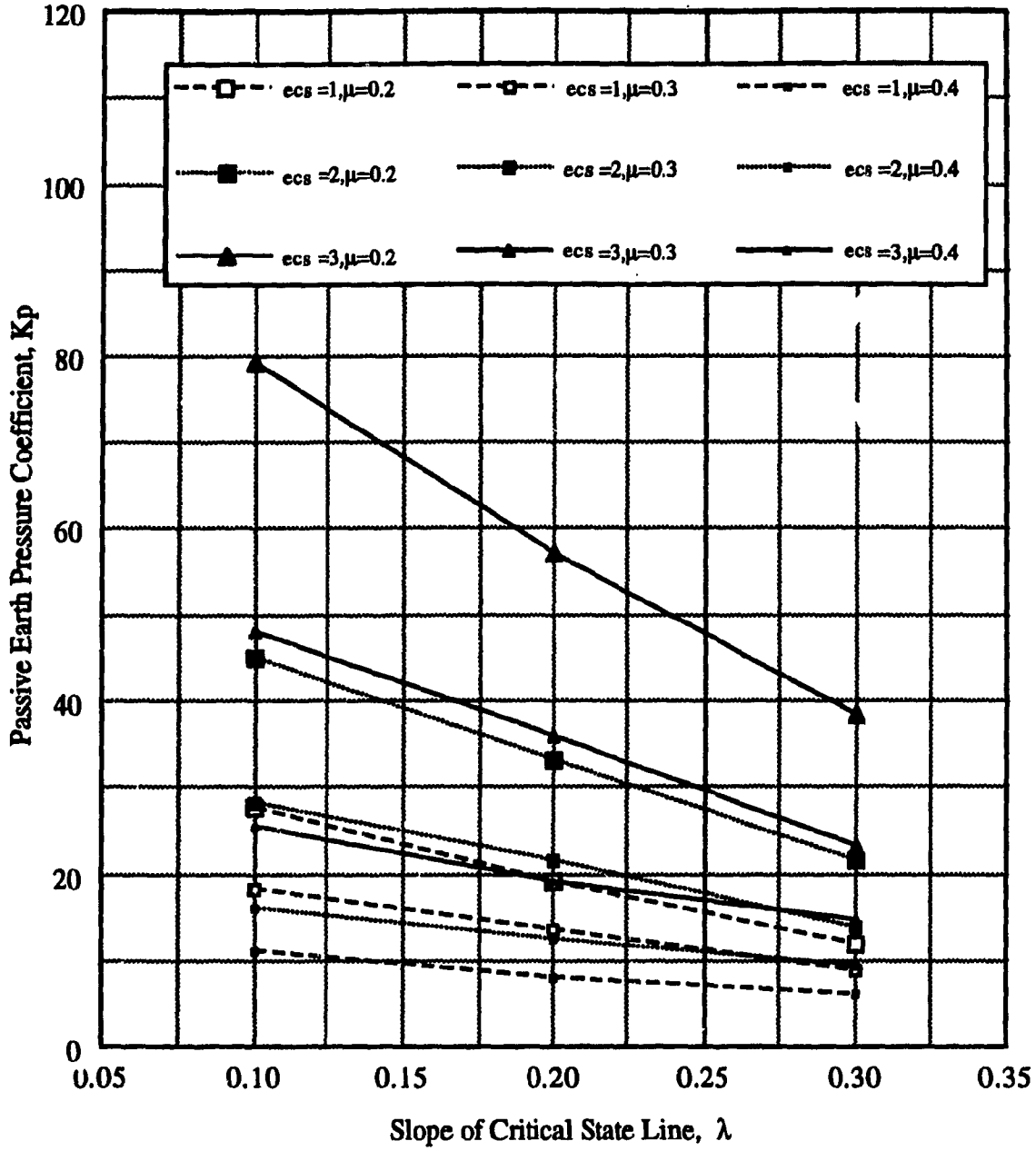

Figure (4-21): Kp versus λ for $\phi = 45^o$ and $\lambda/k = 80$

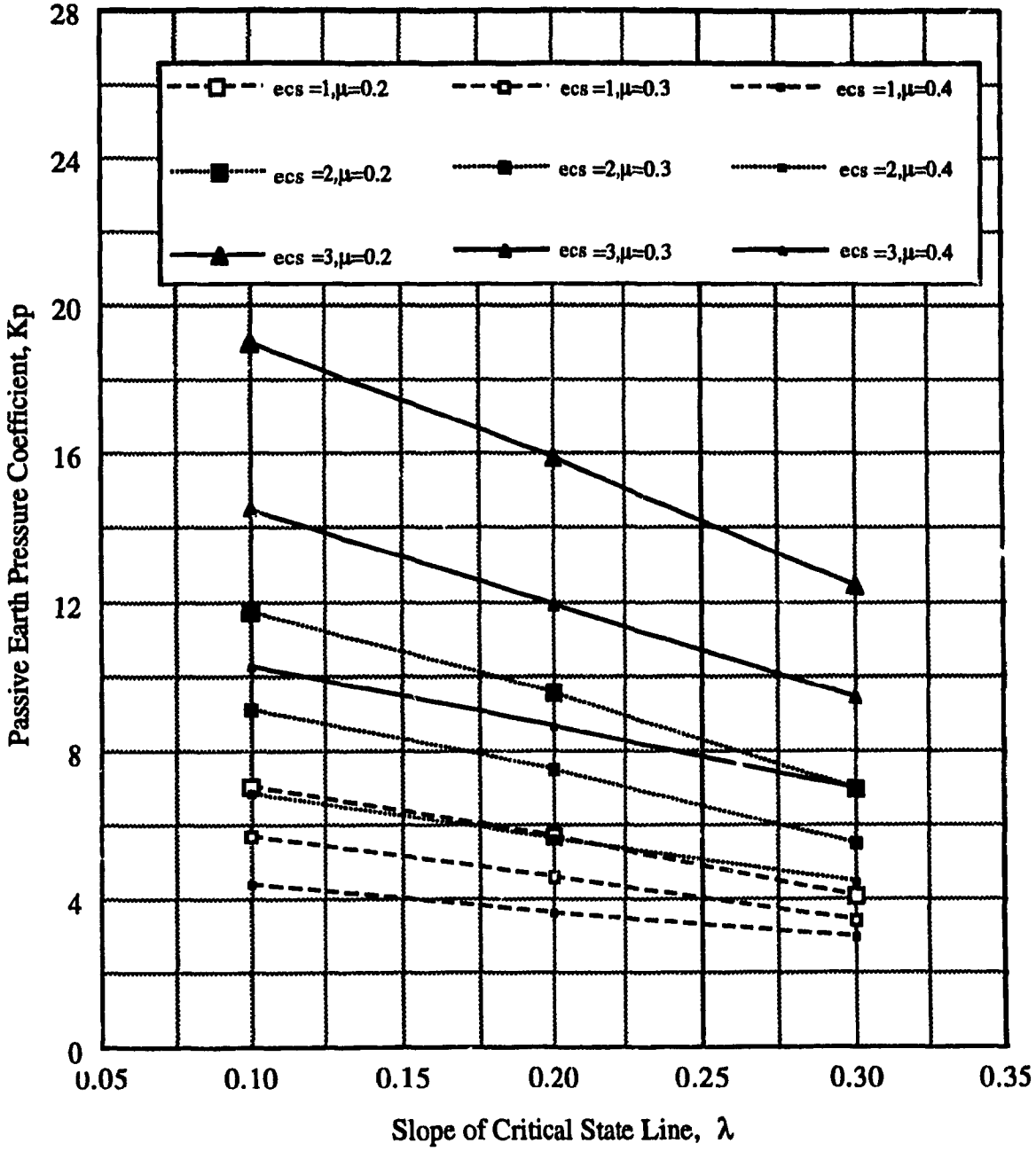

Figure (4-22): Kp versus λ for $\phi = 45^o$ and $\lambda/k = 30$

4.3.4 Effect of the angle of shearing resistance, ϕ

It is obvious that an increase of ϕ leads to an increase of Kp. Figures 4-7 to 4-14, also 4-15 to 4-22 show the influence of ϕ on the value of Kp in a Kp versus ecs and Kp versus λ plots respectively for each value of ϕ, after isolating λ, μ and λ/k. It is noticed from these graphs that the rate of change of Kp at a large value of ecs is bigger than that a. a small value of ecs, it can also be seen that Kp increases, when the ratio $\lambda/k = 80$, by an amount of 20 to 40% due to an increase of ϕ by an amount of 5^0 , however Kp increases, when $\lambda/k = 30$, by an amount of 10 to 30% for the same increase of ϕ.

4.4 Passive earth pressure for over consolidated sand

It is of interest to note that, in the analysis, the Over Consolidation Ratio (OCR) is defined as the ratio of maximum vertical effective stress over the actual vertical effective stress ($\sigma'_{vmax} / \sigma'_v$). Figure 4-23 presents a typical Kp versus OCR plot for different values of ϕ, λ, μ, ecs and k. This figure shows that as the OCR increases, the coefficient of passive earth pressure Kp increases. This is due to the fact that a proportion of the effective horizontal pressure at the at-rest state developed during initial loading being retained in the soil when the effective vertical stress is reduced resulting in a stiffer soil. Thus the stress needed to cause failure should be greater than that of normally consolidated soil resulting in a larger value of Kp.

It was noticed that the increase of Kp was at a constant rate and was related essentially to ϕ. So an empirical relationship is proposed to relate Kp to OCR as follows:

$$K_p = C.OCR^{\phi}.K_{pnc} \qquad (4\text{-}1)$$

C = 1 for Normally consolidated soil and

C = 1.14 for Over Consolidated soil.

Kpnc is the coefficient of passive earth pressure for normally consolidated soil for the same soil characteristics and ϕ is in radian.

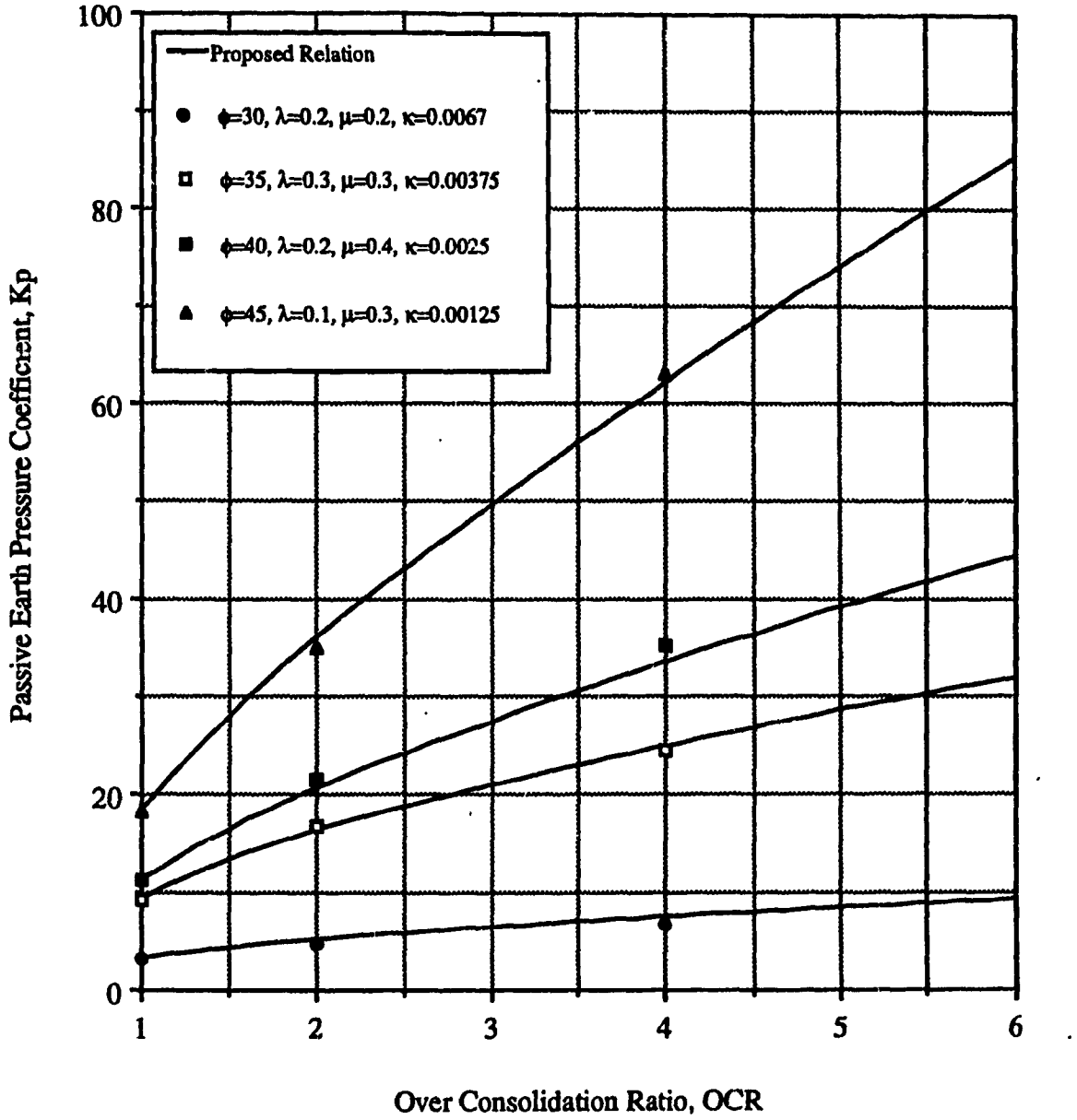

Figure (4-23): Typical Kp versus OCR plot

Figure 4-23 show a good agreement between the test results and this proposed relation.

The general remarks that can be done on this relation is that when μ=0.4, the test results show values a little higher than the ones of Kp obtained from the above relation, when μ=0.3, the test results agree well with the relation and finally when μ=0.2, the test results are a little smaller than Kp obtained from the relation.

In order to examine the validity of the above relation, the experimental results on over consolidated sand of Al-Khouri, I. (1994) were compared with equation 4-1. Al-Khouri studied experimentally the effect of OCR on Kp using different angle of shearing resistance, ϕ, different wall friction angle, δ and he varied OCR from a value of 1 to 4. His results concerning $\phi = 30^o, 35^o, 40^o$ and 45^o , and for $\delta = 2\phi/3$ are presented in table 4-11. Also, the coefficient of passive earth pressure Kp obtained by equation 4-1, considering the same value of Kp for normally consolidated sand (OCR = 1), are presented beside.

Table (4-11): Comparison between the experimental values of Kp obtained by Al-Khoury (1994) and the proposed relation

ϕ	OCR=1	OCR=2		OCR=3		OCR=4	
		experimental	theoretical	experimental	theoretical	experimental	theoretical
30^o	4.4	8.8	7.2	10.2	8.9	11.3	10.4
35^o	5.9	12.1	10.3	13.9	13.2	15.6	15.7
40^o	8.4	17.4	15.5	20.7	20.6	22.9	25.2
45^o	12.8	27.1	25.2	31.3	34.6	35.4	43.3

From table 4-11, it can be seen that the above proposed relation for over consolidated sand agree, generally, well with the experimental results of Al-Khouri, especially for OCR equal to 2 and 3.

4-5 Comparison between the critical state, Coulomb and Shields results for normally consolidated sand

Considering the range of critical state parameters for sand proposed by Atkinson ((table (3-1)), the minimum values of Kp were corresponding to: $\lambda = 0.3$, ecs = 1, $\mu = 0.4$ and $\lambda/k = 30$, and the maximum values were corresponding to: $\lambda = 0.1$, ecs = 3, $\mu = 0.2$ and $\lambda/k = 80$. These values are presented in table (4-12)

Table (4-12): minimum and maximum value of Kp

ϕ	λ=0.1, ecs=3, μ=0.2, λ/k=80	λ=0.3, ecs=1, μ=0.4, λ/k=30
30°	37.10	1.73
35°	48.60	2.15
40°	62.40	2.50
45°	79.20	2.93

It can be noticed from this table that the differences between the minimum and maximum values of Kp, for a given ϕ, is large which prove that the exact determination of the critical state parameters play a role of high importance in the estimation of passive earth pressure coefficient.

Table 4-13 and figure 4-24 represent the minimum and maximum values of Kp after fixing the elastic parameters of the soil to an average values: the ratio λ/k =50 and μ= 0.3. These are, probably, the elastic parameters of the majority of sand.

The value of Kp obtained by Coulomb and by Shields for the same ϕ are presented in the same table and plotted on the same figure for the purpose of comparison. These values were obtained from equation (2-2) and equation (2-5) given in chapter two. It is seen from the table that Shields values of Kp fit close to the low bound of the range of Kp

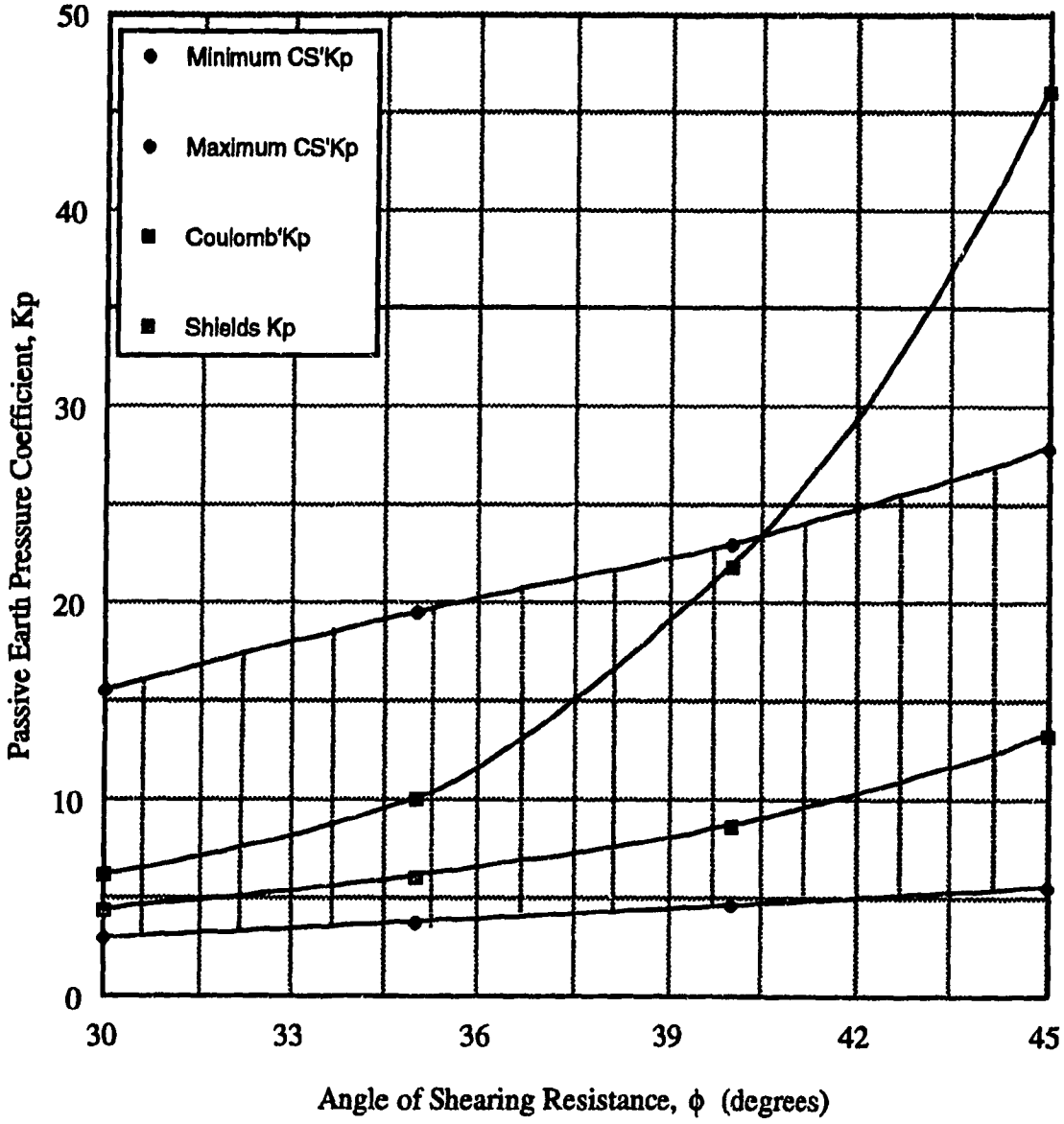

Figure (4-24): Comparison between critical state' Kp, when $\lambda/k = 50$ and $\mu = 0.3$, Coulomb' Kp and Shields Kp.

upper bound of the same range. This little difference with Coulomb' Kp is probably due to his assumption considering a plane failure surface.

Table (4-13): Comparison between critical state's Kp, when $\lambda/k = 50$ and $\mu = 0.3$, Coulomb's Kp and Shields Kp

ϕ	λ=0.1, ecs=3	λ=0.3, ecs=1	Coulomb's Kp	Shields Kp
30°	15.47	2.89	6.11	4.40
35°	19.46	3.73	9.96	6.08
40°	22.94	4.58	21.83	8.64
45°	27.86	5.52	46.08	13.26

4-6. Determination of passive earth pressure coefficient using design charts

In order to facilitate the use of the results of the present investigation, design charts, for normally consolidated sand, are developed in figures 4-25 to 4-30 as a Kp versus ecs plots. Several methods could be used in order evaluate Kp for a given critical state parameters. A proposed procedure of using the design charts is demonstrated in the following numerical example:

1- Determine the critical state soil mechanics parameters of the soil (ϕ, ecs, λ, k and μ) as explained in section 3-5-1-6 in chapter three. Also, determine the over consolidation ratio.

2- For example, if the soil parameters are: $\phi=40^o$, $\lambda=0.15$, ecs=1.75, $\mu=0.25$, $\lambda/k=60$ and OCR = 2, the following steps are proposed in order to determine Kp:

(a) From figure 4-25, find Kp for: $\phi=40^o$, $\lambda=0.1$, $\lambda/k=80$, ecs=1.75 and $\mu=0.25$. Similarly, from figure 4-27, find Kp for: $\phi=40^o$, $\lambda=0.2$, $\lambda/k=80$, ecs=1.75 and $\mu=0.25$ as shown in figure 4-31. These 2 values are: 26.7 and 19.8 respectively.

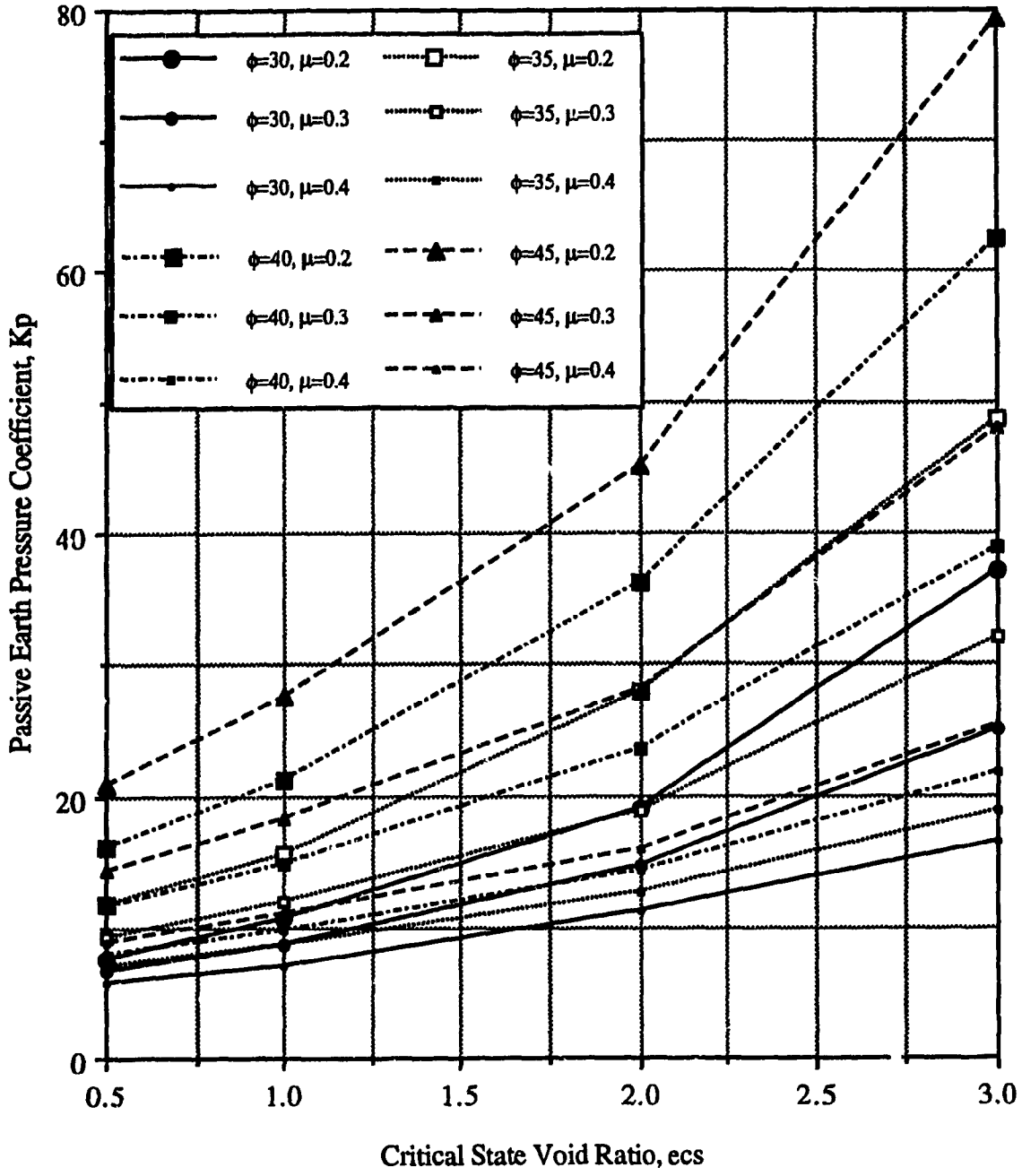

Figure (4-25): Design chart of passive earth pressure coefficients as a function of critical state soil mechanics parameters ($\lambda = 0.1$ and $\lambda/k = 80$)

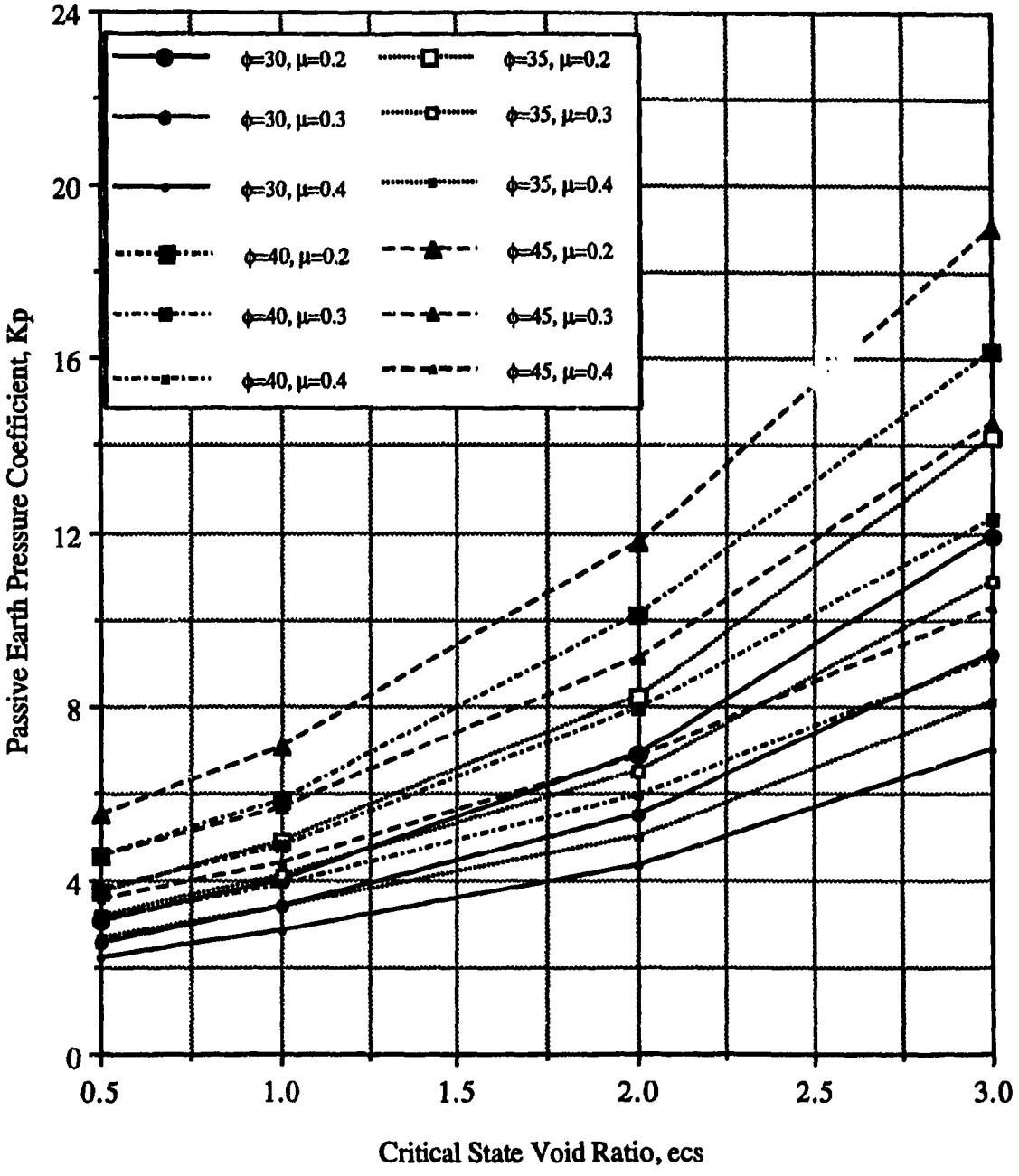

Figure (4-26): Design chart of passive earth pressure coefficients as a function of critical state soil mechanics parameters ($\lambda = 0.1$ and $\lambda/k = 30$)

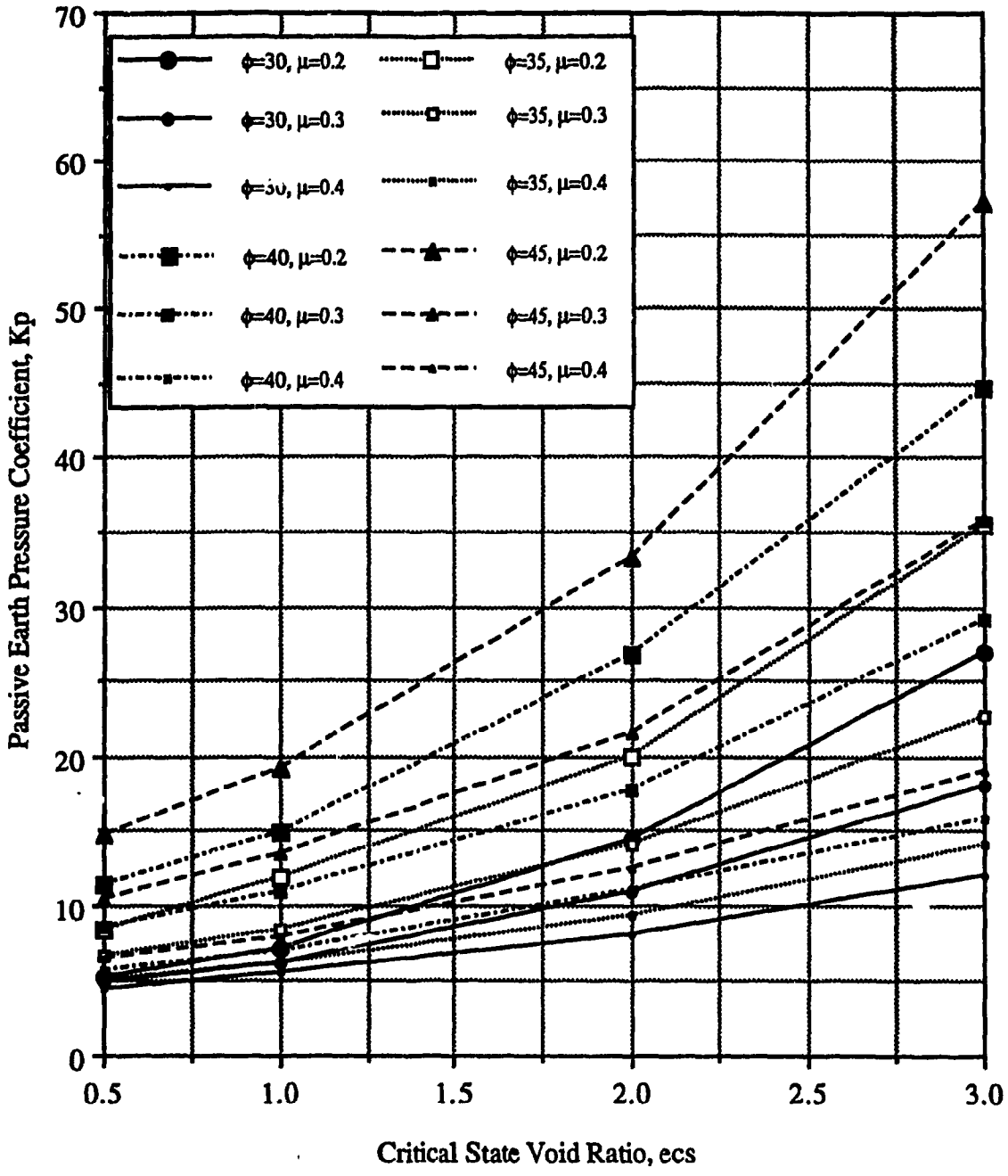

Figure (4-27): Design chart of passive earth pressure coefficients as a function of critical state soil mechanics parameters ($\lambda = 0.2$ and $\lambda/k = 80$)

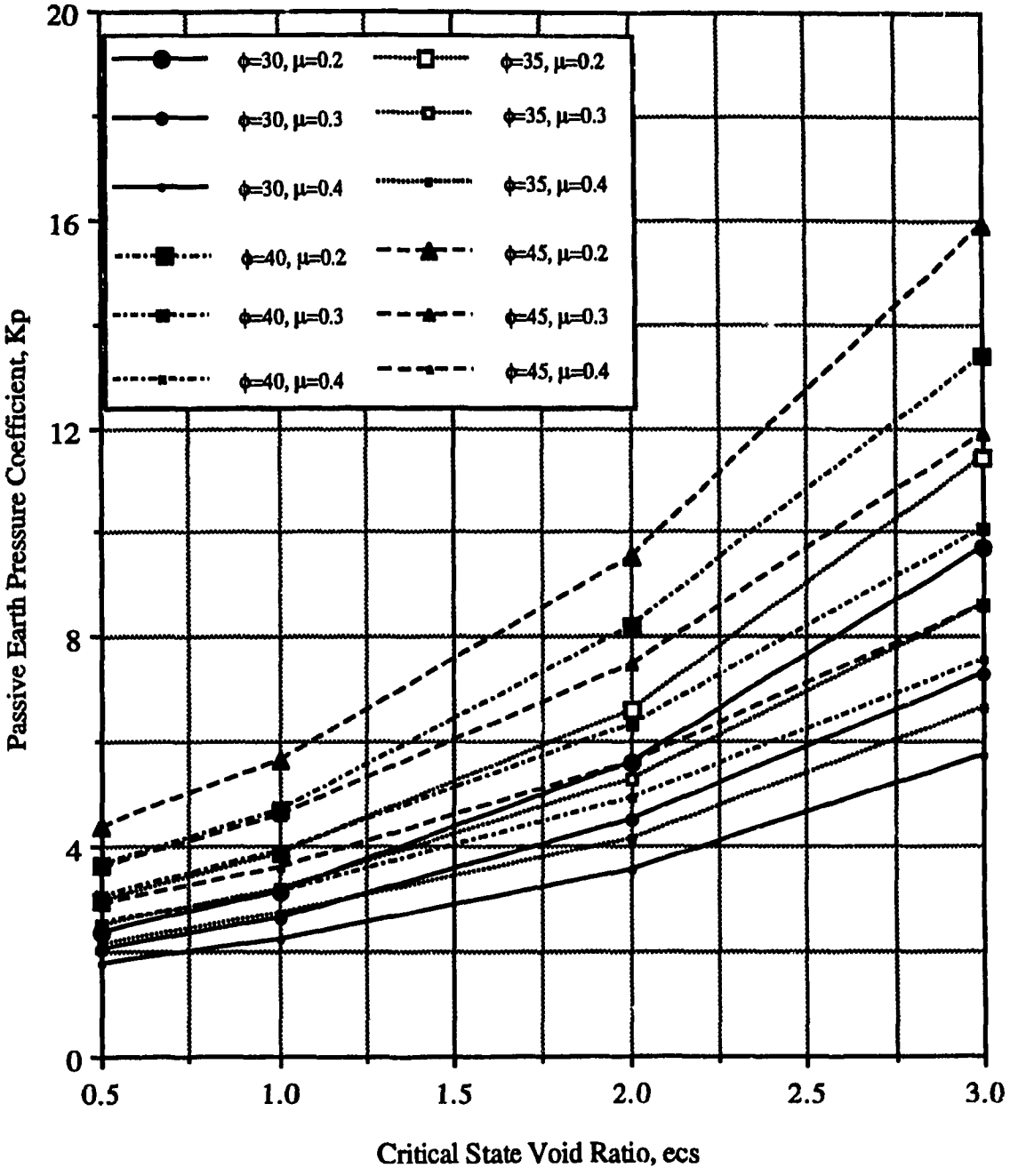

Figure (4-28): Design chart of passive earth pressure coefficients as a function of critical state soil mechanics parameters ($\lambda = 0.2$ and $\lambda/k = 30$)

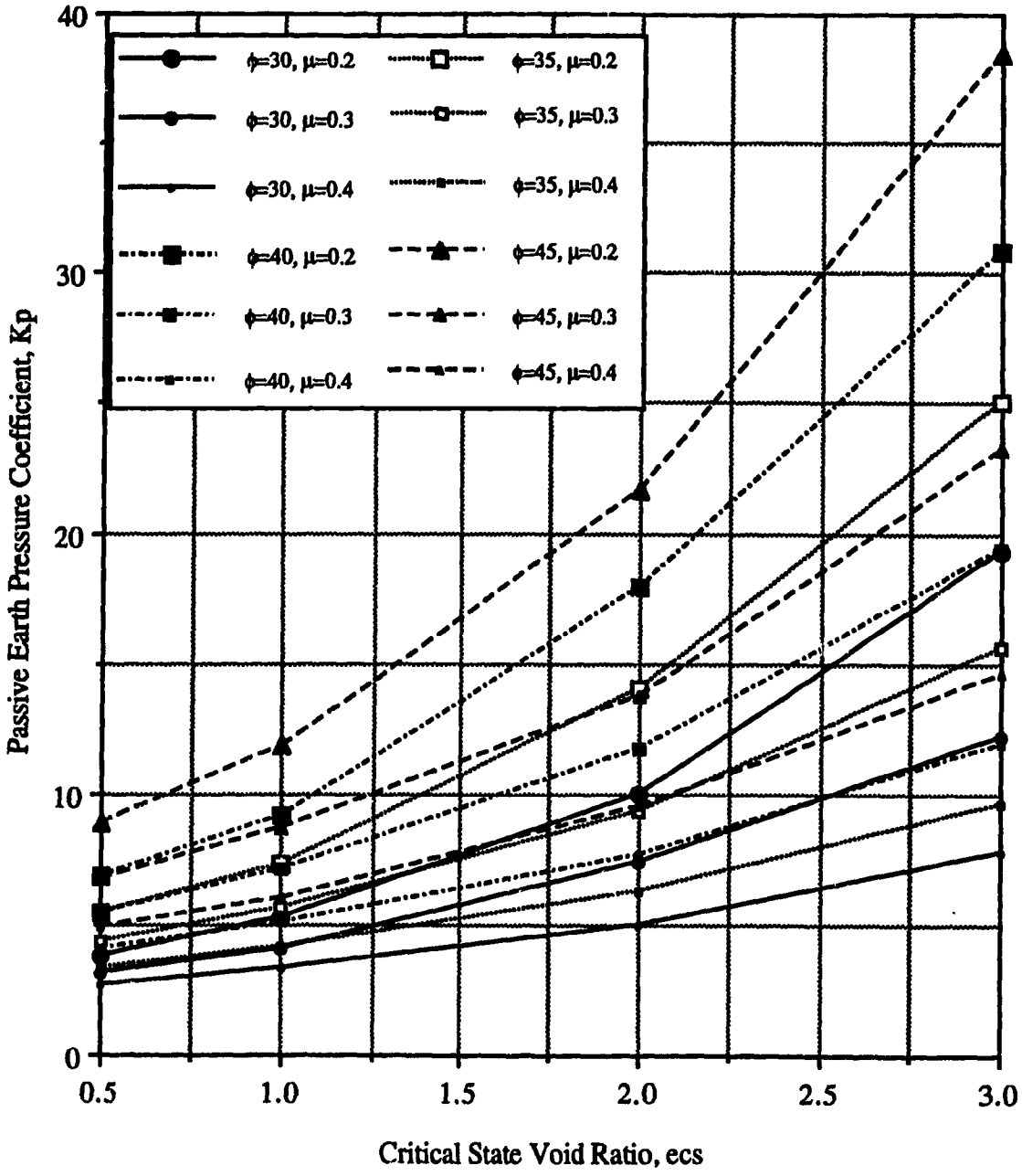

Figure (4-29): Design chart of passive earth pressure coefficients as a function of critical state soil mechanics parameters ($\lambda = 0.3$ and $\lambda/k = 80$)

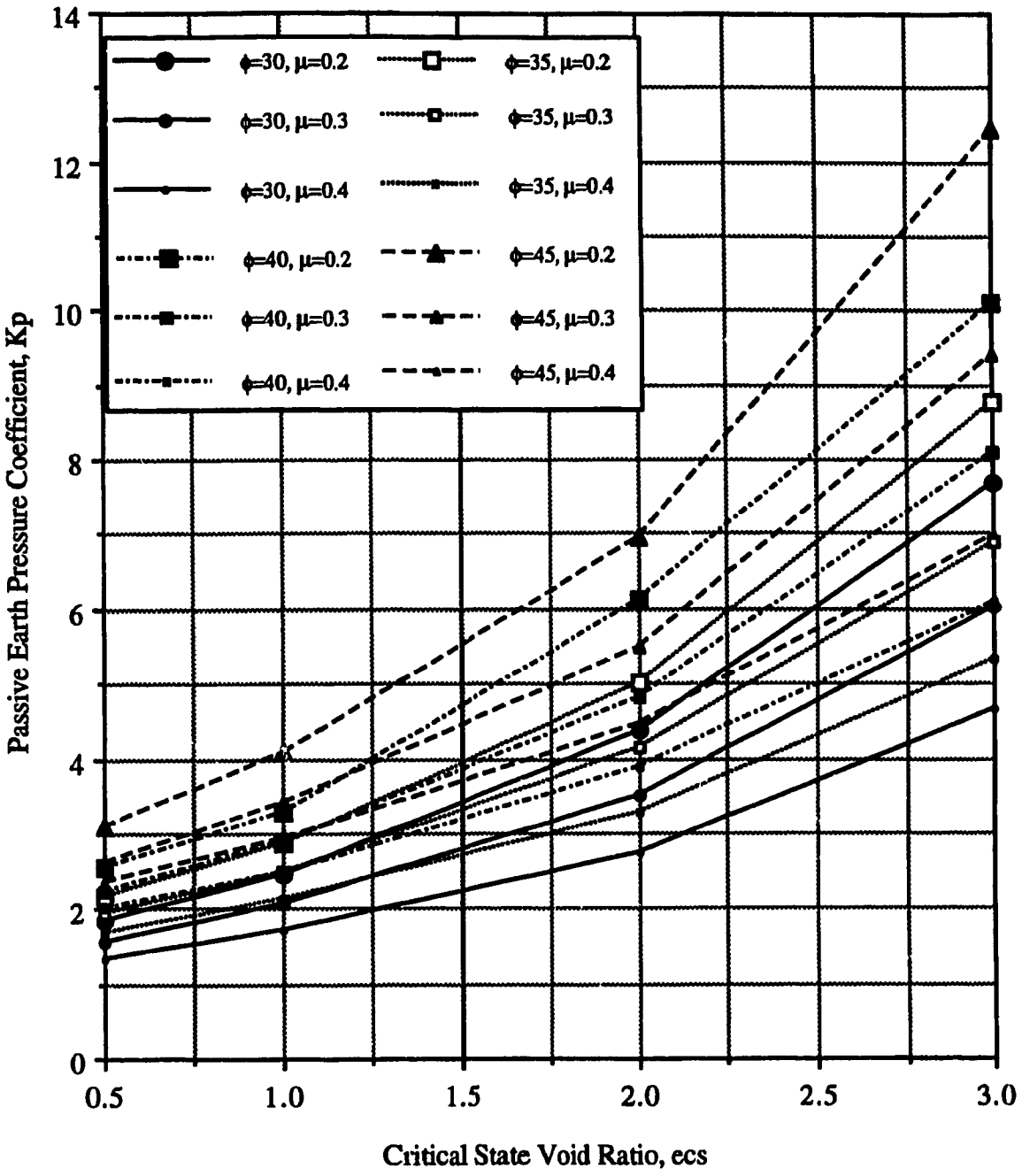

Figure (4-30): Design chart of passive earth pressure coefficients as a function of critical state soil mechanics parameters ($\lambda = 0.3$ and $\lambda/k = 30$)

(b) Find the value of Kp for: $\phi=40^{o}$, $\lambda=0.15$, $\lambda/k=80$, ecs=1.75 and $\mu=0.25$ by interpolating the 2 values obtained in step (a). This value is: 23.25.

(c) As in step (a), find Kp, from figures 4-26 and 4-28, for $\phi=40^{o}$, $\lambda=0.1$, $\lambda/k=30$, ecs=1.75 and $\mu=0.25$ and for $\phi=40^{o}$, $\lambda=0.2$, $\lambda/k=30$, ecs=1.75 and $\mu=0.25$ as illustrated in figure 4-31. These are: 8 and 6.5 respectively.

(d) Find Kp for $\phi=40^{o}$, $\lambda=0.15$, $\lambda/k=30$, ecs=1.75 and $\mu=0.25$ similarly to step (b). This average value is 7.25.

(e) By interpolating the 2 values of Kp found in steps (b) and (d) for $\lambda/k=60$, the coefficient of passive earth pressure for normally consolidated sand having the following critical state parameters: $\phi=40^{o}$, $\lambda=0.15$, $\lambda/k=60$, ecs=1.75 and $\mu=0.25$ will be 16.85.

(f) Finally, apply equation (4-1) to find Kp for an Over Consolidation Ratio equal to 2. The predicted value of Kp of this example will be 31.16.

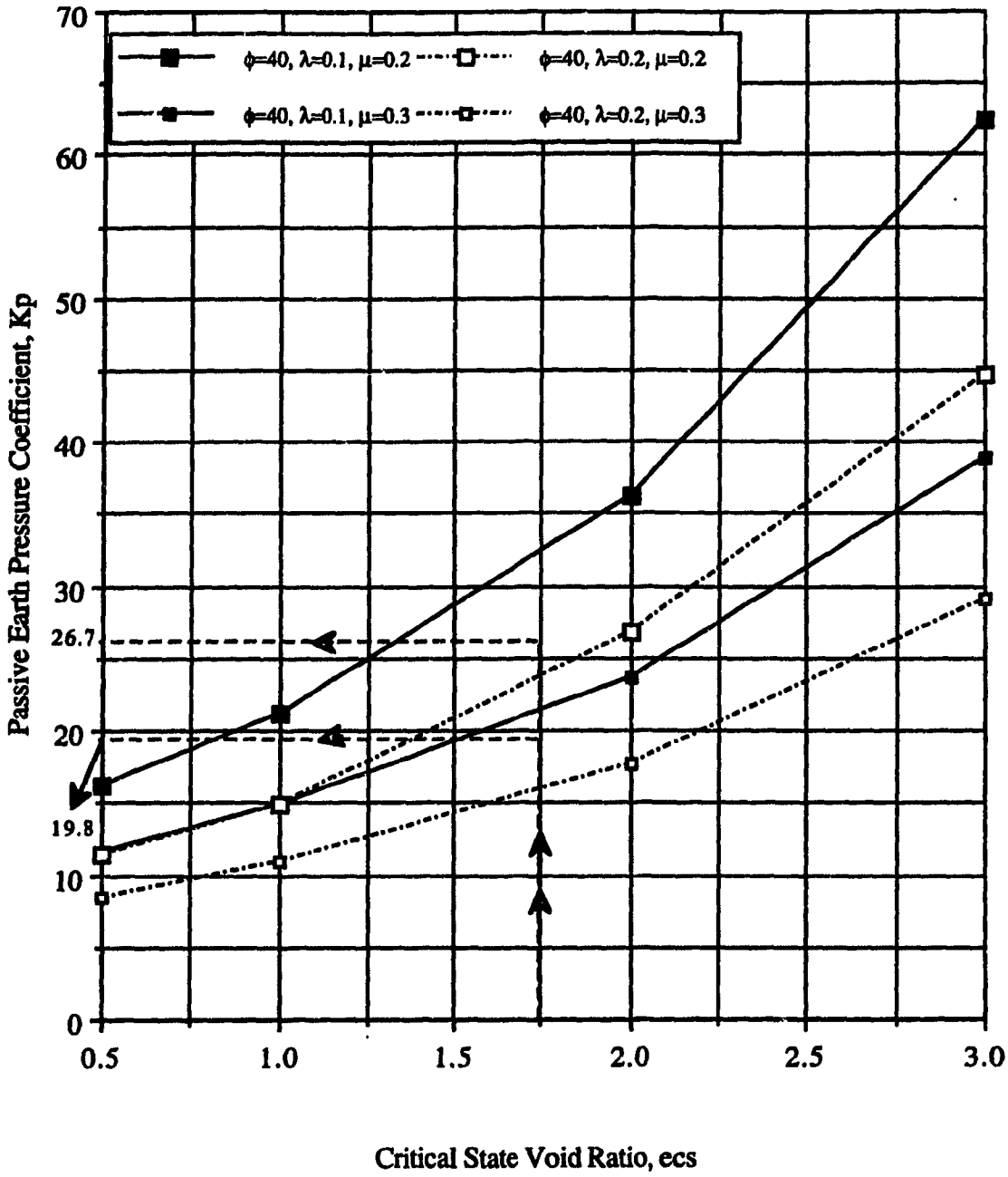

Figure (4-31): Example on the determination of Kp for $\phi = 40^{o}$, $\lambda = 0.15$, $\mu = 0.25$ and $\lambda/k = 80$

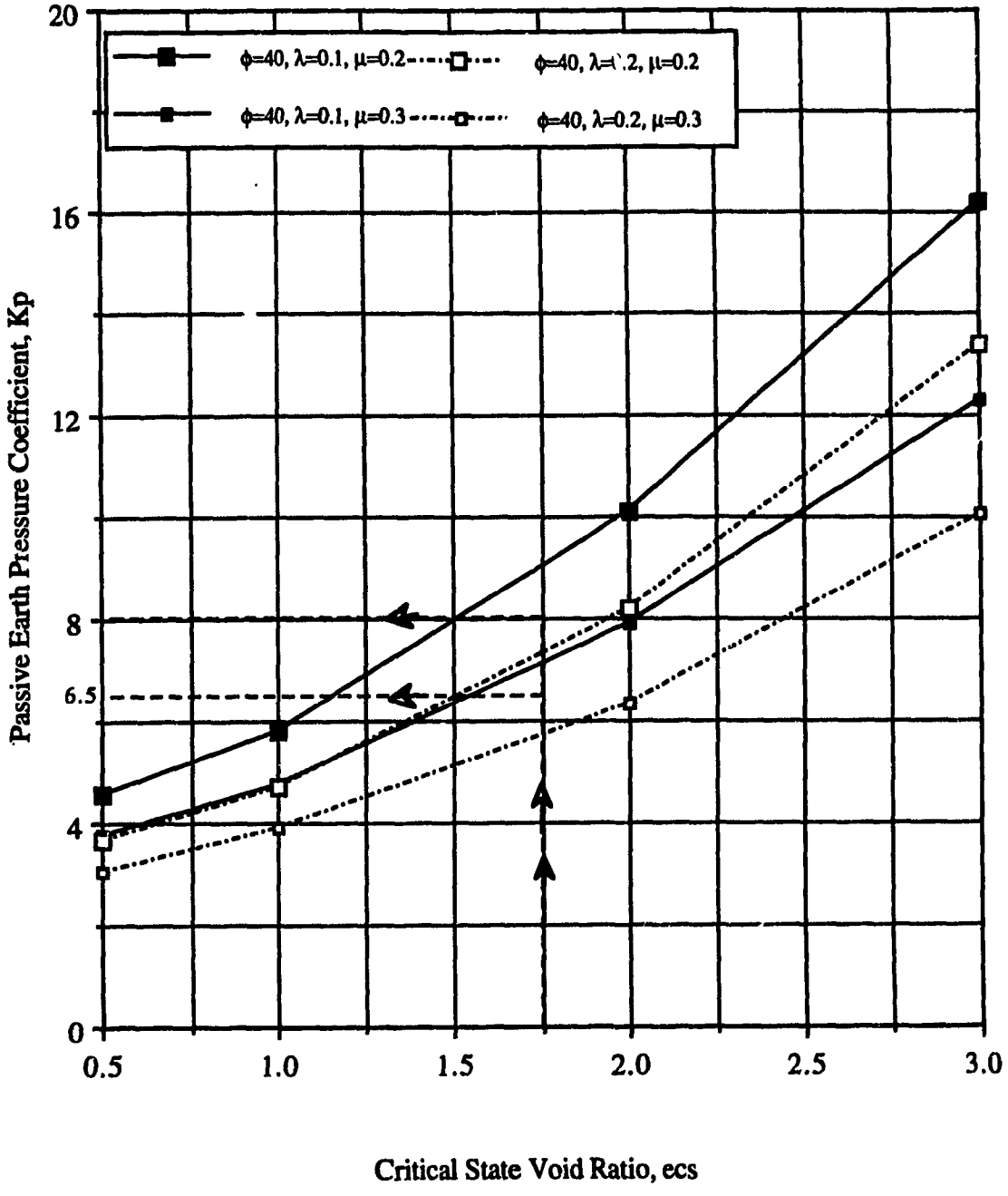

Figure (4-32): Example on the determination of Kp for $\phi = 40^o$, $\lambda = 0.15$, $\mu = 0.25$ and $\lambda/k = 30$

CHAPTER 5
CONCLUSIONS AND RECOMMENDATIONS

5.1 Conclusions

Parametric study, based on finite element analysis, on the determination of passive earth pressure developed behind a rigid vertical wall translating horizontally into a mass of normally consolidated and over consolidated sand was conducted, the following can be concluded:

1. Finite element technique is a powerful tool in solving retaining structure problems.

2. The distribution of passive earth pressure behind the wall is a triangular one at every stage of the wall displacement.

3. Soil failure occur at wall displacement equal to about 7.5% and 6.2% of the height of the wall in case of loose and dense sand respectively. The critical state soil parameters have a little effect on these values.

4. The rupture surface is curved, in all cases, starting from the toe of the wall, going down under the foundation level and then up to reach the sand surface.

5. The assumption used of representing the soil by modified cam clay model, where the equations of the critical state soil mechanics theory are assembled, is a reasonable assumption. This is based on the fact that the results of the normally consolidated sand, concerning the distribution of pressure behind the wall, the shape of the rupture surface and the amount of wall displacement at which failure occurs, were compared with the theoretical and experimental data available in literature, where agreement was achieved.

6. The critical state soil mechanics parameters have a significant influence on the value of passive earth pressure coefficient, Kp. This is based on the fact that for given angle of shearing resistance, ϕ, there is a range of values of Kp and the exact

determination of the critical state parameters is of high importance in the estimation of appropriate value of Kp.

7. The value of Kp increases due to an increase of critical state void ratio, ecs and a decrease of the slope of the critical state line, λ. Also Kp increases with a decrease of the elastic parameters of the soil: The slope of the swelling line, k and Poisson ratio, μ.

8. For over consolidated sand, Kp increases due to an increase of the Over Consolidation Ratio (OCR), this increase satisfy the following proposed relationship:

$$K_p = 1.14.OCR^{\phi}.K_{pnc}$$

9. Design charts are presented to assist the practicing engineers in determining the appropriate values of Kp according to the critical state soil mechanics parameters.

5.2 Recommendations for future work

1. The present investigation should be extended to deal with other type of wall movement as rotation of the wall about its top or bottom.

2. The results of the present research program should be examined against experimental data where critical state soil mechanics parameters will be measured and recorded. The comparison between finite element and laboratory results would be important.

3. Due to the fact that the failure surface starts from the toe of the wall and goes down under the foundation level, it would of interest to study the effect of the variation of the soil condition under the foundation level on the value of Kp.

4. All design chart presented in this research should be put forward in a simple formulas introduced in a computer program to be directly used by practicing engineers.

5. The present investigation should be extended to study the effect of the critical state soil mechanics parameters on the active earth pressure under different wall movements and for the case of earth pressure at-rest.

References

1. Al-Khouri, I., 1994, "*Passive Earth Pressure and Over Consolidation Ratio Relationship in Homogeneous and Layered Cohesionless Soil*". Unpublished Master of Engineering, Concordia University.

2. Atkinson, J., 1993, "*An introduction to the mechanics of soil and foundations through critical state soil mechanics*". McGraw-Hill International Series in civil engineering.

3. Atkinson, J. and Bransby, P. L., 1978, "*The mechanics of soils, an introduction to critical state soil mechanics*". McGraw Hill Book Company Limited

4. Bang, S. and Kim H. T. , 1987, "*Passive Lateral Earth Pressure Development Behind Rigid Walls*". Transportation Research Record 1129.

5. Belidore, B. F., 1729, "*La Science des Ingénieurs*". Navier, (1st edition 1813) Paris.

6. Belloti, R., Formigoni, G., and Jamiolkowski, M., 1976, "*Remarks on the effect of Over consolidation on Ko*". Proceeding, Istanbul Conference on Soil Mechanics and Foundations Nngineering, Istanbul, Turkey, vol. 1, pp. 17-25.

7. Britto A. M. and Gunn M. J., 1981, "*Program CRISP Cambridge University department of civil engineering*". Vol 1, 2, 3.

8. Britto A. M. and Gunn M. J., 1987, "*Critical state soil mechanics via finite elements*". Ellis Horwood Limited, England.

9. Brooker, E. W. and Ireland, H. O., 1965, "*Earth Pressure at rest Related to Stress History*". Canadian Geotechnical Journal, vol. 2, No. 1, pp. 1-15.

10. Caquot, A. and Kerisel, J., 1948, "*Tables de poussée et butée*". Gauthier-Vallars, Paris

11. Caquot, A. and Kerisel, J., 1956, "*Traité de méchanique des sols*". Gauthier-Vallars, Paris.

12. Clough, G.W. and Duncan, J.M., 1991, "*Finite element analysis of retaining wall behavior*". Journal of soil mechanics of foundations division, proceeding of the ASCE

13. Coulomb, C. A., 1776, "*Essai sur une application des règles des maximis et minimis à quelque problèmes de statique*". Mémoire Académie Royale des Sciences, 7, Paris.

14. Franzius, D., 1924, "Versuche mit passivem Druck". Bauingenicur.Ileft. 10. Berlin.

15. Gauthey, E. M., 1816, "*Oeuvres*". Traité de la Construction des Ponts, vol. 1, pp. 1809-1818. Paris.

16. Grahramani, A. and Sahzevari, A., 1974, "*A load displacement analysis for passive earth pressure problem*". Acta Technica .

17. Hansen, J.B., 1953, "*Earth pressure calculation*". The Danish Technical press, Institution of Danish Civil Engineers, Copenhagen.

18. Jaky, J., 1944, "*Pressure in Soil*". Proceeding, 2nd International Conference on Soil Mechanics and Foundations Engineering, vol. 1, pp. 103-107.

19. James, R.G. and Bransby, P. L., 1970, "*Experimental and theoretical investigations of a passive earth pressure problem*". Geotechnique, 18.

20. Mayniel, E., 1808, "*Traité expérimental, analytique et pratique de la poussée des terres de revêtement*". P.316, Paris.

21. Meyerhof, G. C, 1976, "*Bearing Capacity and Settlement of Piles Foundations*". Journal of Geotechnical Engineering Division, ASCE, vol. 102 (GT3), pp. 197-228.

22. Muller-Breslau, H., 1906, "*Erddruck auf Stuetzmauern*". pp. 159. Berlin.

23. Narain J., Saran S. and Nandakumaran, P., 1969, "*Model study of passive pressure in sand*". Journal of soil mechanics and foundations division proceeding of the ASCE.

24. Rankine, W. J. M., 1857, "*On the stability of loose earth*". Proc. of the Royal Society of London, London, vol 147.

25. Rowe, P.W. and Peaker, K., 1965, "*Passive earth pressure measurements.* Geotechnique". Vol. xv, No. 1

26. Schmidt, B., 1966, "*Discussion: Earth Pressures at rest Related to Stress History*". Canadian Geotechnical Journal, vol. 3, No. 4 pp. 239-242

27. Shields, D. H. and Tolunay, A. Z., 1972, "*Passive pressure coefficients for sand by the Terzaghi and Peck method*". Canadian geotechnical journal, vol. 9, no 4.

28. Shields, D. H. and Tolunay, A. Z., 1973, "*Passive Pressure coefficients by method of slices*". Journal of the soil mechanics and foundations division.

29. Terzaghi, K., 1920, "*Old earth pressure theories and new tests results*". Reprinted in from theory to practice (1960) Wiley, New York

30. Wood, D. M., 1990, "*Soil behavior and critical state soil mechanics*". Cambridge University Press.

31. Wroth, C. P. "*General theories of earth pressure and deformation*". Proceeding 5th European Conference on Soil Mechanics and Foundation Engineering, Madrid, vol. 2, pp. 33-52.

32. Wroth, C. P. ,1975, "*In-situ measurement of initial stresses and deformation characteristics*". Proceeding Specialty Conference on In-Situ Measurement of Soil Properties. ASCE, vol. 2, pp. 181-230